Volume 4, Number 2, 2004 ISSN 1562-8353

Nonlinear Dynamics and Systems Theory

An International Journal of Research and Surveys

Academic Periodical Press

Nonlinear Dynamics and Systems Theory

An International Journal of Research and Surveys

ISSN 1562-8353 Printed in Ukraine

NONLINEAR DYNAMICS AND SYSTEMS THEORY
An International Journal of Research and Surveys
Published since 2001

Volume 4 Number 2 2004

CONTENTS

Robust Control for a Class of Dynamical Systems with Uncertainties 125
Xinkai Chen and Guisheng Zhai

A Modified *LQ*-Optimal Control Problem for Causal Functional Differential Equations 139
C. Corduneanu

Adaptive Calculation of Lyapunov Exponents from Time Series Observations of Chaotic Time Varying Dynamical Systems 145
A. Khaki-Sedigh, M. Ataei, B. Lohmann and C. Lucas

A Nonlinear Model of Composite Delaminated Beam with Piezoelectric Actuator, with Account of Nonpenetration Constraint for the Delamination Crack Faces 161
V.Y. Perel and A.N. Palazotto

Robust Active Control for Structural Systems with Structured Uncertainties 195
Sheng-Guo Wang, H.Y. Yeh and P.N. Roschke

A Criterion for Stability of Nonlinear Time-Varying Dynamic System 217
Yongmao Wang, Yan Shi and Hirofumi Sasaki

Imaginary Axis Eigenvalues of a Delay System with Applications in Stability Analysis 231
Z. Zahreddine

CORRIGENDUM

Set Differential Equations and Monotone Flows 241
V. Lakshmikantham and A.S. Vatsala

Founded by A.A.Martynyuk in 2001.
Registered in Ukraine Number: KB №5267 / 04.07.2001.

NONLINEAR DYNAMICS AND SYSTEMS THEORY

An International Journal of Research and Surveys

Nonlinear Dynamics and Systems Theory (ISSN 1562-8353) is an international journal published under the auspices of the S.P.Timoshenko Institute of Mechanics of National Academy of Sciences of Ukraine and the Laboratory for Industrial and Aplied Mathematics (LIAM) at York University (Toronto, Canada). It is aimed at publishing high quality original scientific papers and surveys in area of nonlinear dynamics and systems theory and technical reports on solving practical problems. The scope of the journal is very broad covering:

SCOPE OF THE JOURNAL

Analysis of uncertain systems • Bifurcations and instability in dynamical behaviors • Celestial mechanics, variable mass processes, rockets • Control of chaotic systems • Controllability, observability, and structural properties • Deterministic and random vibrations • Differential games • Dynamical systems on manifolds • Dynamics of systems of particles • Hamilton and Lagrange equations • Hysteresis • Identification and adaptive control of stochastic systems • Modelling of real phenomena by ODE, FDE and PDE • Nonlinear boundary problems • Nonlinear control systems, guided systems • Nonlinear dynamics in biological systems • Nonlinear fluid dynamics • Nonlinear oscillations and waves • Nonlinear stability in continuum mechanics • Non-smooth dynamical systems with impacts or discontinuities • Numerical methods and simulation • Optimal control and applications • Qualitative analysis of systems with aftereffect • Robustness, sensitivity and disturbance rejection • Soft computing: artificial intelligence, neural networks, fuzzy logic, genetic algorithms, etc. • Stability of discrete systems • Stability of impulsive systems • Stability of large-scale power systems • Stability of linear and nonlinear control systems • Stochastic approximation and optimization • Symmetries and conservation laws

PUBLICATION AND SUBSCRIPTION INFORMATION

The Nonlinear Dynamics and Systems Theory (ISSN 1562-8353) is published three times per year in 2004.

Base list subscription price per volume: US$149.00. This price is available only to individuals whose library subscribes to the journal OR who warrant that the Journal is for their own use and provide a home address for mailing. Separate rates apply to academic and corporate/ government institutions. Our charge includes postage, packing, handling and airmail delivery of all issues. Mail order and inquires to: Department of Processes Stability, S.P.Timoshenko Institute of Mechanics NAS of Ukraine, Nesterov str.,3, 03057, Kiev-57, MSP 680, Ukraine, Tel: ++38-044-456-6140, Fax: ++38-044-456-1939, E-mail: anchern@stability.kiev.ua, http:\\www.sciencearea.com.ua

ABSTRACTING INFORMATION

Nonlinear Dynamics and Systems Theory is currently abstracted/indexed by Zentralblatt MATH and Mathematical Reviews.

Nonlinear Dynamics and Systems Theory, **4**(2) (2004) 125–137

Robust Control for a Class of Dynamical Systems with Uncertainties

Xinkai Chen[1] and Guisheng Zhai[2]

[1] *Department of Electronic & Information Systems, Faculty of Systems Engineering, Shibaura Institute of Technology, Minuma-ku, Saitama-city, Saitama 337-8570, Japan*
[2] *Graduate School of Engineering, Osaka Prefecture University, 1-1 Gakuen-Cho, Sakai, Osaka 599-8531, Japan*

Received: April 22, 2003; Revised: February 18, 2004

Abstract: In this paper, a new robust control is proposed for a class of dynamical systems with uncertainties. The considered dynamical systems may be nonminimum phase systems. The designed controller requires only input output measurement of the system. First, by using least square approximation technique, nonminimum phase systems are approximated by minimum phase systems. Then, the uncertainty is approximately estimated. Finally, based on the approximate minimum phase system and the estimate of the uncertainty, the robust control input is synthesized. Example and simulation results are presented to show the effectiveness of the proposed algorithm.

Keywords: *Robust control; nonminimum phase systems; uncertainties; approximate inverse systems; least square method.*

Mathematics Subject Classification (2000): 93C15, 93C80, 93D09, 93E10, 93E12.

1 Introduction

In recent years, the robust control for uncertain dynamical systems has been a topic of considerable interest. It is well known that all the practical control systems are subjected to uncertainties. Various robust design methodologies have been proposed for minimum phase dynamical systems until now [7, 10, 11]. For the systems with uncertainties, robust controllers are proposed in [3 − 5, 9, 13] recently. The overall systems can be ensured to be globally uniformly ultimately bounded (GUUB) which can be made arbitrarily close to exponential stability if the control energy permits. However, these approaches cannot be extended to the robust control for nonminimum phase dynamical systems with uncertainties.

It has long been known that the output tracking control of nonminimum phase plants is very difficult [8] even though the systems are perfectly known, and there is a fundamental limitation to the control performance, because the boundedness of all signals is not assured due to the unstable pole-zero cancellation. For discrete time nonminimum phase dynamical systems, one considerable method proposed by Clarke [6], in which the perfect output tracking is given up, is to minimize the control input and the difference between the plant output and the desired output. Chen and Fukuda [1] give a robust control for the continuous time systems with uncertainties by also minimizing the control input and the output error. The shortcoming of this kind of approach is that the difference between the plant output and the desired output still remains.

This paper tries to consider the robust control for a class of uncertain systems which may be nonminimum phase systems. By applying least square techniques, the class of nonminimum phase systems are approximated by minimum phase dynamical systems. Then, based on the approximated minimum phase system, the uncertainties are estimated. Finally, the robust control, which assures that the system input and output remain bounded in the closed-loop system, is synthesized. The output tracking error is controlled by the design parameters. This paper is organized as follows. Section 2 gives the problem formulation. In Section 3, approximate inverse system is introduced, the class of nonminimum phase systems are approximated by minimum phase systems. In Section 4, based on the approximated minimum phase systems, the uncertainties are estimated. In Section 5, the robust controller is synthesized. In Section 6, design example and simulations are presented to show the effectiveness of the proposed algorithm. Section 7 concludes this paper.

2 Problem Statement

Consider an uncertain system of the form

$$a(s)y(t) = b(s)u(t) + k(s)v(t), \tag{1}$$

where s denotes the differential operator; $u(t)$ and $y(t)$ are scalar input and output, respectively; $v(t)$ is an unknown signal composed of model uncertainties, nonlinearities and disturbances; $a(s)$ and $b(s)$ are described by

$$a(s) = s^n + a_1 s^{n-1} + \cdots + a_{n-1}s + a_n, \tag{2}$$

$$b(s) = b_r s^{n-r} + b_{r-1} s^{n-r+1} + \cdots + b_{n-1}s + b_n, \tag{3}$$

$$k(s) = k_m s^{n-m} + k_{m-1} s^{n-m+1} + \cdots + k_{n-1}s + k_n. \tag{4}$$

In this paper, we make the following assumptions:

(A1) The parameters in $a(s)$ and $b(s)$ are known; $b_r \neq 0$; $a(s)$ and $b(s)$ are coprime.

(A2) The real parts of the roots of $b(s)$ are smaller than 1.

This paper attempts to construct a robust controller to drive the system output to track a desired uniformly bounded signal $y_d(t)$ for the uncertain system, where $y_d(t)$ is differentiable to a necessary order and the derivatives are also uniformly bounded.

Even though assumption (A2) looks somewhat strict, it is meaningful to consider the output tracking problem for the formulated system because many practical control systems meet this assumption.

3 Approximate Inverse Systems

Express $b(s)$ as

$$b(s) = b_r\kappa_1(s)\kappa_2(s), \tag{5}$$

where $\kappa_1(s)$ is a υ-th order monic polynomial with no root lying in the left half plane, $\kappa_2(s)$ is an $(n-r-\upsilon)$-th order monic Hurwitz polynomial. Furthermore, we suppose

$$\kappa_1(s) = (s-\phi_1)\dots(s-\phi_\tau)(s-\alpha_1)(s-\bar{\alpha}_1)\dots(s-\alpha_\iota)(s-\bar{\alpha}_\iota), \tag{6}$$

where ϕ_i $(i=1,\dots,\tau)$ are real numbers satisfying $1>\phi_i\ge 0$; α_j $(j=1,\dots,\iota)$ are complex numbers satisfying $1>\operatorname{Re}(\alpha_j)\ge 0$; $\tau+2\iota=\upsilon$.

Now, we introduce the next polynomial

$$\xi(s) = \left\{\left\{\prod_{i=1}^{\tau}(s+\chi_i)\right\}\left\{\prod_{j=1}^{\iota}(s+\beta_j)(s+\bar{\beta}_j)\right\}\right\}^{p+1}, \tag{7}$$

where p is a positive integer, χ_i's are positive real numbers, β_j's are complex numbers, $j=1,\dots,\iota$. Let

$$\begin{aligned}(s+\chi_i)^{p+1} &= s^{p+1}+g_{i1}s^p+\dots+g_{ip}s+g_{i,p+1},\\ (s+\beta_j)^{p+1} &= s^{p+1}+l_{j1}s^p+\dots+l_{jp}s+l_{j,p+1}.\end{aligned} \tag{8}$$

Furthermore, we introduce the following polynomials

$$\begin{aligned}\theta_i(s) &= s^p+\theta_{i1}s^{p-1}+\dots+\theta_{i,p-1}s+\theta_{ip},\\ \vartheta_j(s) &= s^p+\vartheta_{j1}s^{p-1}+\dots+\vartheta_{j,p-1}s+\vartheta_{jp},\\ \bar{\vartheta}_j(s) &= s^p+\bar{\vartheta}_{j1}s^{p-1}+\dots+\bar{\vartheta}_{j,p-1}s+\bar{\vartheta}_{jp}.\end{aligned} \tag{9}$$

The coefficients of $\theta_i(s)$ and $\vartheta_j(s)$ are determined by

$$\theta_i = (N_i^TN_i)^{-1}N_i^Tg_i, \quad \vartheta_j = (K_j^*K_j)^{-1}K_j^*l_j, \tag{10}$$

where

$$N_i = \begin{bmatrix} 1 & 0 & \dots & 0\\ -\phi_i & 1 & \dots & \dots\\ 0 & -\phi_i & \dots & 0\\ \vdots & \vdots & \ddots & \vdots\\ 0 & 0 & \dots & 1\\ 0 & 0 & \dots & -\phi_i \end{bmatrix}, \quad \theta_i = \begin{bmatrix} 1\\ \theta_{i1}\\ \vdots\\ \theta_{ip}\end{bmatrix}, \quad g_i = \begin{bmatrix} 1\\ g_{i1}\\ \vdots\\ g_{i,p+1}\end{bmatrix}, \quad i=1,\dots,\tau, \tag{11}$$

$$K_j = \begin{bmatrix} 1 & 0 & \dots & 0\\ -\alpha_j & 1 & \dots & \dots\\ 0 & -\alpha_j & \dots & 0\\ \vdots & \vdots & \ddots & \vdots\\ 0 & 0 & \dots & 1\\ 0 & 0 & \dots & -\alpha_j \end{bmatrix}, \quad \vartheta_j = \begin{bmatrix} 1\\ \vartheta_{j1}\\ \vdots\\ \vartheta_{jp}\end{bmatrix}, \quad l_j = \begin{bmatrix} 1\\ l_{j1}\\ \vdots\\ l_{j,p+1}\end{bmatrix}, \quad j=1,\dots,\iota. \tag{12}$$

Define

$$\zeta(s)=\left\{\prod_{i=1}^{\tau}\theta_i(s)\right\}\left\{\prod_{j=1}^{\iota}\vartheta_j(s)\bar{\vartheta}_j(s)\right\}, \tag{13}$$

and

$$\bar{u}(t)=\frac{\kappa_1(s)\zeta(s)}{\xi(s)}\,u(t). \tag{14}$$

Remark 1 It should be pointed out that $\xi(s)$ is a monic $(p+1)\upsilon$-th order Hurwitz polynomial. $\kappa_1(s)\zeta(s)$ is a monic $(p+1)\upsilon$-th order polynomial.

Let

$$\Delta(s)=\xi(s)-\kappa_1(s)\zeta(s)=\psi_1 s^{(p+1)\upsilon-1}+\cdots+\psi_{(p+1)\upsilon-1}s+\psi_{(p+1)\upsilon}. \tag{15}$$

We have the next theorem to describe the coefficients of $\Delta(s)$.

Theorem 1 *If the parameters* $\chi_i,\ i=1,\ldots,\tau,$ *and* $\beta_j,\ j=1,\ldots,\iota,$ *are chosen such that* $1-\phi_i>\chi_i>0,\ 0<\mathrm{Re}(\beta_j)<1-\mathrm{Re}\,(\alpha_j),\ \mathrm{Im}\,(\beta_j)=-\,\mathrm{Im}\,(\alpha_j),$ *then*

$$(p+1)^2\upsilon^2\sum_{i=1}^{(p+1)\upsilon}|\psi_i|^2\to 0 \tag{16}$$

as $p\to\infty$.

Proof The proof is given in the Appendix.

Remark 2 In general, the parameter p should not be chosen to be very large, since a very large p may result in complicated computation, slow and long transients, etc.

Theorem 2 *For a uniformly bounded signal* $\sigma(t)$*, the next relation uniformly holds*

$$\sigma(t)-\frac{\kappa_1(s)\zeta(s)}{\xi(s)}\sigma(t)\to 0 \tag{17}$$

for all t *as* $p\to\infty$.

Proof Express $\sigma(t)-\frac{\kappa_1(s)\zeta(s)}{\xi(s)}\,\sigma(t)$ as

$$\begin{aligned}\sigma(t)-\frac{\kappa_1(s)\zeta(s)}{\xi(s)}\,\sigma(t)=\psi_1\frac{s^{(p+1)\upsilon-1}}{\xi(s)}\,\sigma(t)+\ldots+\psi_{(p+1)\upsilon-1}\frac{s}{\xi(s)}\,\sigma(t)\\ +\,\psi_{(p+1)\upsilon}\frac{1}{\xi(s)}\,\sigma(t).\end{aligned} \tag{18}$$

Since $\frac{s^i}{\xi(s)}\,\sigma(t)$ are bounded for $i=0,1,\ldots,(p+1)\upsilon-1,$ relation (17) can be easily concluded by using (18) and Theorem 1.

Remark 3 The difference $\sigma(t)-\frac{\kappa_1(s)\zeta(s)}{\xi(s)}\,\sigma(t)$ also depends on the frequency of the signal $\sigma(t)$.

Define

$$\bar{v}(t)=\frac{k(s)\zeta(s)}{b_r\kappa_2(s)\xi(s)}\,v(t). \tag{19}$$

Then, by employing the definition (14) and (19), (1) can be rewritten as

$$a(s)\zeta(s)y(t) = b_r\kappa_2(s)\xi(s)\left\{\bar{u}(t)+\bar{v}(t)\right\}, \tag{20}$$

where $a(s)\zeta(s)$ is a monic $(n+\upsilon p)$-th order polynomial, $\kappa_2(s)\xi(s)$ is a monic $(n+\upsilon p-r)$-th order Hurwitz polynomial with real coefficients.

For simplicity, the signal $\bar{v}(t)$ is called "disturbance" of the system in the following sections of this paper.

4 Disturbance Identifier Formulation

In this section, by estimating the filters of $\bar{v}(t)$, the signal $\bar{v}(t)$ is eventually estimated, based on our proposed formulation in [2]. For the disturbance $\bar{v}(t)$, we make the following assumption.

(A3) The disturbance $\bar{v}(t)$ and its first order derivative are bounded. However, the bounds are unknown.

Because $\bar{v}(t)$ is bounded, it is easy to see that its filters are also bounded, i.e.

$$\left|\frac{1}{(s+\lambda)^i}\,\bar{v}(t)\right| \le C_i \tag{21}$$

for $i \ge 0$, where λ is a positive constant, C_i's are unknown positive constants.

Now, we introduce a monic $(n+\upsilon p)$-th order Hurwitz polynomial

$$f(s) = \kappa_2(s)\xi(s)(s+\lambda)^r. \tag{22}$$

Then, (20) can be rewritten as

$$\dot{y}(t)+\lambda y(t) = \frac{f(s)-a(s)\zeta(s)}{\kappa_2(s)\xi(s)(s+\lambda)^{r-1}}\,y(t) + \frac{b_r}{(s+\lambda)^{r-1}}\,\bar{u}(t) + \frac{b_r}{(s+\lambda)^{r-1}}\,\bar{v}(t). \tag{23}$$

As $f(s)-a(s)\zeta(s)$ is an $(n+\upsilon p-1)$-th order polynomial, it is easy to know that $\dfrac{f(s)-a(s)\zeta(s)}{\kappa_2(s)\xi(s)(s+\lambda)^{r-1}}\,y(t)$ is a signal which can be calculated.

The next proposition gives an estimate of the signal $\bar{v}(t)$.

Proposition 1 For small positive constants $\delta_i > 0$ $(i = 1,\dots,r)$, construct the dynamical systems described by

$$\begin{gathered}\dot{\hat{y}}(t)+\lambda\hat{y}(t) = \frac{f(s)-a(s)\zeta(s)}{\kappa_2(s)\xi(s)(s+\lambda)^{r-1}}\,y(t) + \frac{b_r}{(s+\lambda)^{r-1}}\,\bar{u}(t) + b_r w_1(t),\\ \hat{y}(t_0) = y(t_0),\end{gathered} \tag{24}$$

$$\dot{\hat{w}}_{i-1}(t)+\lambda\hat{w}_{i-1}(t) = w_i(t)\,,\quad \hat{w}_{i-1}(t_0)=0,\quad i=2,\dots,r, \tag{25}$$

where $w_i(t),\ i=1,\dots,r$, are given as

$$w_1(t) = \frac{b_r\{y(t)-\hat{y}(t)\}\widehat{C}_{r-1}(t)}{|b_r\{y(t)-\hat{y}(t)\}|+\delta_1} \tag{26}$$

and

$$w_i(t) = \frac{\{w_{i-1}(t) - \hat{w}_{i-1}(t)\}\widehat{C}_{r-i}(t)}{|w_{i-1}(t) - \hat{w}_{i-1}(t)| + \delta_i}, \quad i = 2, \ldots, r, \tag{27}$$

respectively; $\widehat{C}_i(t)$'s are updated by the following adaptive algorithm

$$\dot{\widehat{C}}_{r-1}(t) = \begin{cases} o_{r-1}|y(t) - \hat{y}(t)| & \text{if } |b_r\{y(t) - \hat{y}(t)\}| > \delta_1, \\ 0 & \text{otherwise}, \end{cases} \tag{28}$$

$$\dot{\widehat{C}}_{r-i}(t) = \begin{cases} o_{r-i}|w_{i-1}(t) - \hat{w}_{i-1}(t)| & \text{if } |w_{i-1}(t) - \hat{w}_{i-1}(t)\}| > \delta_i, \\ 0 & \text{otherwise}, \end{cases} \tag{29}$$

$$(i = 2, \ldots, r)$$

where o_{r-i}'s are positive constants. It can be concluded that, when $\sum_{j=1}^{r} \delta_j$ is very small, $w_i(t)$'s are all bounded for $i = 1, \ldots, r$. Furthermore, $w_i(t)$'s are the corresponding approximate estimates of $\frac{1}{(s+\lambda)^{r-i}}\,\bar{v}(t)$, i.e. there exist $\epsilon_i(\delta_1, \ldots, \delta_i) > 0$ and $T_i > 0$ such that

$$\left|\frac{1}{(s+\lambda)^{r-i}}\bar{v}(t) - w_i(t)\right| \le \epsilon_i(\delta_1, \ldots, \delta_i) \tag{30}$$

as $t > T_i$, where $\epsilon_i(\delta_1, \ldots, \delta_i)$ has the property that $\epsilon_i(\delta_1, \ldots, \delta_i) \to 0$ as $\sum_{j=1}^{i}\delta_j \to 0$ for $i = 1, \ldots, r$.

Proof The proposition can be similarly proved by referring to [2].

Remark 4 The design parameter $\lambda > 0$ determines the estimating speed. The design parameters $\delta_i > 0$ $(i = 1, \ldots, r)$ determine the estimating precision.

5 The Robust Control Input

Now, we introduce monic Hurwitz polynomials $d(s)$ and $h(s)$ of orders $(n + \upsilon p)$ and r, respectively. Consider the following equation

$$d(s)h(s) = \eta(s)\{\zeta(s)a(s)\} + \mu(s), \tag{31}$$

where $\eta(s)$ is a monic r-th order polynomial, $\mu(s)$ is a $(n + \upsilon p - 1)$-th order polynomial. It is very clear that the solutions $\eta(s)$ and $\mu(s)$ exist uniquely. Multiplying (31) by $y(t)$ and applying (20) yields

$$d(s)h(s)y(t) = b_r\eta(s)\kappa_2(s)\xi(s)\{\bar{u}(t) + \bar{v}(t)\} + \mu(s)y(t) \tag{32}$$

i.e.

$$h(s)y(t) = b_r\{\bar{u}(t) + \bar{v}(t)\} + b_r\,\frac{\eta(s)\kappa_2(s)\xi(s) - d(s)}{d(s)}\,\{\bar{u}(t) + \bar{v}(t)\} + \frac{\mu(s)}{d(s)}\,y(t). \tag{33}$$

Based on the above preparation, we have the next theorem.

Theorem 3 *If $\bar{u}(t)$ is set as*

$$\bar{u}(t) = -w_r(t) - \frac{\eta(s)\kappa_2(s)\xi(s) - d(s)}{d(s)}\{\bar{u}(t) + w_r(t)\} + \frac{1}{b_r}\left\{-\frac{\mu(s)}{d(s)}y(t) + h(s)y_d(t)\right\}, \quad (34)$$

in which $w_r(t)$ is the estimate of $\bar{v}(t)$ obtained in Theorem 2, then there exist $T' > t_0$ and $\varepsilon'(t, \delta_1, \dots, \delta_r) > 0$ such that

$$|y(t) - y_d(t)| < \varepsilon'(t, \delta_1, \dots, \delta_r) \quad (35)$$

for all $t > T'$, where $\varepsilon'(t, \delta_1, \dots, \delta_r)$ has the property that $\varepsilon'(t, \delta_1, \dots, \delta_r) \to 0$ as $t \to \infty$ and $\sum_{i=1}^{r} \delta_i \to 0$.

Proof By combining (33) and (34), the result is obvious by applying Proposition 1.

By the definition of $\bar{u}(t)$, it can be seen that it is a filter of $u(t)$. Further, from Theorem 2, it can be known that the difference between $\bar{u}(t)$ and $u(t)$ is very small if $u(t)$ is uniformly bounded. Thus, we are inspired to choose the real control input $u(t)$ as

$$u(t) = -w_r(t) - \frac{\eta(s)\kappa_2(s)\xi(s) - d(s)}{d(s)}\{u(t) + w_r(t)\} + \frac{1}{b_r}\left\{-\frac{\mu(s)}{d(s)}y(t) + h(s)y_d(t)\right\}. \quad (36)$$

The next theorem is derived to describe the stability of the closed-loop system.

Theorem 4 *If the control $u(t)$ is chosen as (36), then all the signals in the loop remain uniformly bounded for a sufficiently large p. Furthermore, there exist $T > t_0$ and $\varepsilon(t, p, \delta_1, \dots, \delta_r) > 0$ such that*

$$|y(t) - y_d(t)| < \varepsilon(t, p, \delta_1, \dots, \delta_r) \quad (37)$$

for all $t > T$, where $\varepsilon(t, p, \delta_1, \dots, \delta_r)$ has the property that $\varepsilon(t, p, \delta_1, \dots, \delta_r) \to 0$ as $t \to \infty$, $p \to \infty$ and $\sum_{i=1}^{r} \delta_i \to 0$.

Proof By using (20) and the definition of $\bar{u}(t)$, system (1) can be rewritten as

$$a(s)\zeta(s)y(t) = b_r\kappa_2(s)\xi(s)\{u(t) + \bar{v}(t)\} - b_r\kappa_2(s)\Delta(s)u(t). \quad (38)$$

From (36) and (38), the closed-loop system can be expressed as

$$\begin{aligned} &\begin{bmatrix} a(s)\zeta(s) & -b_r\kappa_2(s)\{\xi(s) - \Delta(s)\} \\ [\mu(s) & b_r\eta(s)\kappa_2(s)\xi(s) \end{bmatrix} \begin{bmatrix} y(t) \\ u(t) \end{bmatrix} \\ &\quad = \begin{bmatrix} b_r\kappa_2(s)\xi(s) \\ 0 \end{bmatrix} \bar{v}(t) - \begin{bmatrix} 0 \\ b_r\eta(s)\kappa_2(s)\xi(s) \end{bmatrix} w_r(t) + \begin{bmatrix} 0 \\ h(s) \end{bmatrix} y_d(t). \end{aligned} \quad (39)$$

Since

$$\det \begin{bmatrix} a(s)\zeta(s) & -b_r\kappa_2(s)\xi(s) \\ \mu(s) & b_r\eta(s)\kappa_2(s)\xi(s) \end{bmatrix} = b_r\kappa_2(s)\xi(s)d(s)h(s) \quad (40)$$

is a Hurwitz polynomial and the order of $\Delta(s)$ is lower than that of $\xi(s)$, by Theorem 1, it can be concluded that

$$\det\begin{bmatrix} a(s)\zeta(s) & -b_r\kappa_2(s)\{\xi(s)-\Delta(s)\} \\ \mu(s) & b_r\eta(s)\kappa_2(s)\xi(s) \end{bmatrix} = b_r\kappa_2(s)\left(\xi(s)d(s)h(s)-\mu(s)\Delta(s)\right) \tag{41}$$

is also a Hurwitz polynomial if p is chosen to be large enough. Therefore, based on (39), it can be seen that all the signals in the closed-loop remain uniformly bounded for a sufficiently large p.

By the definition of $\bar{u}(t)$, (32) can be rewritten as

$$\begin{aligned} d(s)h(s)y(t) = {} & b_r\eta(s)\kappa_2(s)\xi(s)\{u(t)+\bar{v}(t)\} \\ & + \mu(s)y(t) - b_r\kappa_2(s)\eta(s)(\xi(s)-\kappa_1(s)\zeta(s))u(t). \end{aligned} \tag{42}$$

Substituting (36) into (42) gives

$$\begin{aligned} h(s)(y(t)-y_d(t)) = {} & \frac{b_r\eta(s)\kappa_2(s)\xi(s)}{d(s)}\{\bar{v}(t)-w_r(t)\} \\ & - \frac{b_r\eta(s)\kappa_2(s)\xi(s)}{d(s)}\left\{u(t)-\frac{\kappa_1(s)\zeta(s)}{\xi(s)}u(t)\right\}. \end{aligned} \tag{43}$$

Since $\dfrac{b_r\eta(s)\kappa_2(s)\xi(s)}{d(s)}$ is proper, by Theorem 2 and the above discussions, it can be seen that $\dfrac{b_r\eta(s)\kappa_2(s)\xi(s)}{d(s)}\left\{u(t)-\dfrac{\kappa_1(s)\zeta(s)}{\xi(s)}u(t)\right\}$ approaches zero as $p\to\infty$. Furthermore, by using the fact that $w_r(t)$ is the approximate estimate of $\bar{v}(t)$, (37) can be proved based on (43). Thus, the theorem is proved.

Remark 5 As p increases, the computation may become complicated. On the other hand, as p is large enough, $u(t)$ is uniformly bounded and good tracking performance may be obtained. Therefore, the choice of the parameter p depends on the requirement of the considered system.

6 Design Example and Simulation Results

In this section, a nonminimum phase system will be presented to show the design procedure of the proposed output tracking algorithm. Consider the system described by

$$(s-1)^3y(t) = (4s-0.5)\,u(t) + (2s-1)\,v(t), \tag{44}$$

where $y(t)$ is the output; $u(t)$ is the input; $v(t)$ is the unknown disturbance governed by

$$v(t) = \cos(5t)\left(\frac{\{\dot{y}(t)+u(t)\}}{|\dot{y}(t)+u(t)|+0.5}\right)\left(\frac{y(t)}{|y(t)|+1}\right).$$

The purpose of the control is to drive the output to follow the signal $y_d(t) = 2\sin(t)$.

As $b(s) = 4(s-0.125)$ is a first order polynomial, for simplicity, we use the inverse system proposed for $s-\alpha$ in (58)–(63). The parameter β is chosen as $\beta = 0.3$. The accuracy of the approximate inverse system depends on the choice of the parameter p. However, when p is chosen too large, the computation may become complicated. In the presented example, p is chosen as $p = 7$. Under the above choice, the value of J is $J = 1.1153 \times 10^{-6}$. The least square approximate solution c of (63) is obtained as $c_1 = 2.5250$, $c_2 = 2.8356$, $c_3 = 1.8665$, $c_4 = 0.8003$, $c_5 = 0.2369$, $c_6 = 0.0499$, $c_7 = 0.0079$.

Corresponding to (20), system (44) can be rewritten as

$$(s-1)^3 c(s) y(t) = 4(s+0.3)^8 \{\bar{u}(t) + \bar{v}(t)\}, \tag{45}$$

where

$$\bar{u}(t) = \frac{(s-0.125)c(s)}{(s+1)^8}\, u(t), \qquad \bar{v}(t) = \frac{(2s-1)c(s)}{4(s+0.3)^8}\, v(t). \tag{46}$$

Choose the Hurwitz polynomial $f(s)$ in (22) as $f(s) = (s+0.3)^8(s+2)^2$, where λ is chosen as $\lambda = 2$. Corresponding to (23), we have

$$\dot{y}(t) + 2y(t) = \frac{f(s) - (s-1)^3 c(s)}{(s+0.3)^8 (s+2)}\, y(t) + \frac{4}{s+2}\, \bar{u}(t) + \frac{4}{s+2} \bar{v}(t). \tag{47}$$

From Proposition 1, we construct the following dynamical systems

$$\dot{\hat{y}}(t) + 2\hat{y}(t) = \frac{f(s) - (s-1)^3 c(s)}{(s+0.3)^8 (s+2)} y(t) + \frac{4}{s+2} \bar{u}(t) + 4w_1(t), \qquad \hat{y}(0) = 0, \tag{48}$$

$$\dot{\hat{w}}_1(t) + 2\hat{w}_1(t) = w_2(t), \quad \hat{w}_1(0) = 0, \tag{49}$$

where $w_1(t)$ and $w_2(t)$ are respectively determined by

$$w_1(t) = \frac{4\{y(t) - \hat{y}(t)\}\hat{C}_1(t)}{4|y(t) - \hat{y}(t)| + \delta_1}, \tag{50}$$

$$w_2(t) = \frac{\{w_1(t) - \hat{w}_1(t)\}\hat{C}_0(t)}{|w_1(t) - \hat{w}_1(t)| + \delta_2}, \tag{51}$$

and $\widehat{C}_1(t)$, $\widehat{C}_0(t)$ are respectively determined as

$$\dot{\widehat{C}}_1(t) = \begin{cases} o_1|y(t) - \hat{y}(t)| & \text{if } \ 4|y(t) - \hat{y}(t)| > \delta_1, \\ 0 & \text{otherwise}, \end{cases} \qquad \widehat{C}_1(0) = 0.1, \tag{52}$$

$$\dot{\widehat{C}}_0(t) = \begin{cases} o_0|w_1(t) - \hat{w}_1(t)| & \text{if } \ |w_1(t) - \hat{w}_1(t)\}| > \delta_2, \\ 0 & \text{otherwise}, \end{cases} \qquad \widehat{C}_0(0) = 0.1. \tag{53}$$

Therefore, $w_2(t)$ can be regarded as the approximate estimate of the disturbance $\bar{v}(t)$.

Choose the polynomials $h(s)$ and $d(s)$ as

$$h(s) = (s+1)^2, \quad d(s) = (s+1)^{10}. \tag{54}$$

Solving (31) yields

$$\eta(s) = s^2 + 12.4750s + 73.6650, \tag{55}$$

$$\begin{aligned} \mu(s) = {} & 276.7552s^9 + 622.7649s^8 + 781.4575s^7 + 829.5264s^6 + 749.6166s^5 \\ & + 507.3089s^4 + 238.4558s^3 + 74.5042s^2 + 14.0286s + 1.5820. \end{aligned} \tag{56}$$

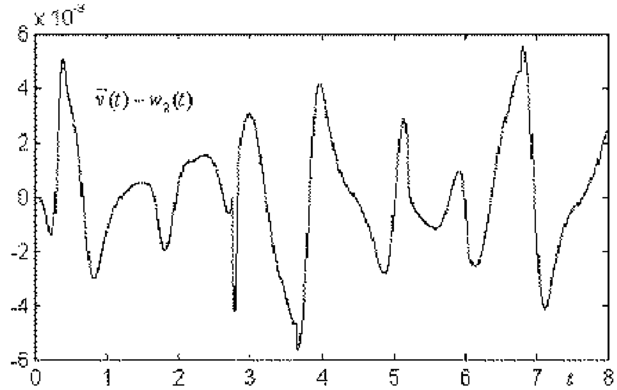

Figure 6.1. The difference between $\bar{v}(t)$ and its estimate $w_2(t)$.

Therefore, the control should be chosen as

$$\begin{aligned} u(t) = & -w_2(t) - \frac{\eta(s)(s+0.3)^8 - d(s)}{d(s)}\{u(t) + w_2(t)\} \\ & + \frac{1}{4}\left\{-\frac{\mu(s)}{d(s)}y(t) + 2(s+1)^2\sin(t)\right\}. \end{aligned} \tag{57}$$

In the simulation process, the sampling period is chosen as 1×10^{-4} second. The parameters are chosen as $\delta_1 = \delta_2 = 2 \times 10^{-4}$, $o_1 = o_0 = 0.5$. The starting time is $t_0 = 0$. Figure 6.1 shows the difference $\bar{v}(t) - w_2(t)$. Figure 6.2 shows the output tracking control input. It can be seen the control input remains uniformly bounded. Figure 6.3 shows the difference between the output and the desired output. It can be seen that the proposed control works very well. If the parameters δ_2 and δ_2 are chosen to be much smaller, and the parameter p is chosen to be much larger, the output tracking performance may become much better.

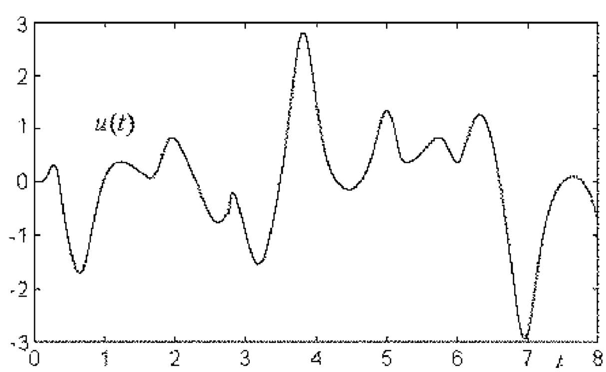

Figure 6.2. The output tracking control input $u(t)$.

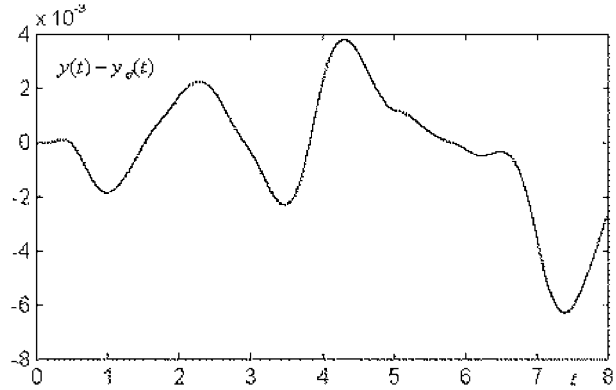

Figure 6.3. The difference between the output and the desired output.

7 Conclusions

In this paper, a new robust controller is formulated for a class of uncertain systems by using only the input output information. The disturbance, which is composed of the nonlinearities, the model uncertainties, etc., is assumed bounded with unknown bound. First, based on the least square approximate inverse systems method, the class of non-minimum phase systems is approximated by minimum phase systems. The approximate error can be made to be as small as necessary by choosing large p. Then, the disturbance is estimated. Finally, the robust controller is formulated based on the approximated minimum phase systems and the disturbance error. The output tracking error is controlled by the design parameters. Simulation results of the robust control for a nonminimum phase system show the effectiveness of the proposed method.

Appendix: Proof of Theorem 1

First, we consider the approximate inverse system of $s-\alpha$, where $\alpha \in C$ (C denotes the set of complex numbers), $\mathrm{Re}(\alpha) \geq 0$. Consider the equation

$$(s-\alpha)c(s) = (s+\beta)^{p+1}, \tag{58}$$

$$\begin{aligned} c(s) &= s^p + c_1 s^{p-1} + \cdots + c_{p-1}s + c_p, \\ (s+\beta)^{p+1} &= s^{p+1} + l_1 s^p + \cdots + l_p s + l_{p+1}, \end{aligned} \tag{59}$$

where $\mathrm{Re}(\beta) > 0$, $\beta \in C$ can be assigned in advance; p is a positive integer. The problem is finding $c(s)$ such that (58) holds. The parameter p is introduced so that the accuracy of the approximate inverse system becomes better.

It is easy to see that solving (58) is equivalent to solving the following equation

$$Kc = l, \tag{60}$$

where

$$K = \begin{bmatrix} 1 & 0 & \dots & 0 \\ -\alpha & 1 & \dots & \dots \\ 0 & -\alpha & \dots & 0 \\ \vdots & \vdots & \ddots & \vdots \\ 0 & 0 & \dots & 1 \\ 0 & 0 & \dots & -\alpha \end{bmatrix}_{(p+2)\times(p+1)}, \quad c = \begin{bmatrix} 1 \\ c_1 \\ \vdots \\ c_p \end{bmatrix}, \quad l = \begin{bmatrix} 1 \\ l_1 \\ \vdots \\ l_{p+1} \end{bmatrix}. \tag{61}$$

Since (60) cannot be satisfied exactly, the solution of c which may minimize the following criterion

$$J = (Kc - l)^*(Kc - l) \tag{62}$$

will be derived, where A^* denotes the complex conjugate of the transpose of A. It is well known that the least square approximate solution is given by [12]

$$c = (K^*K)^{-1}K^*l. \tag{63}$$

Lemma A.1 *If β is chosen such that $0 < \mathrm{Re}(\beta) < 1 - \mathrm{Re}(\alpha)$ and $\mathrm{Im}(\beta) = -\mathrm{Im}(\alpha)$, then*

$$(p+1)^2 J \to 0 \tag{64}$$

as $p \to \infty$.

Proof It is well-known that there exists a unitary matrix $U \in C^{(p+2)\times(p+2)}$ such that

$$U^*K = \begin{bmatrix} Q \\ 0 \end{bmatrix}, \quad \text{i.e.,} \quad K = U \begin{bmatrix} Q \\ 0 \end{bmatrix}, \tag{65}$$

where $Q \in C^{(p+1)\times(p+1)}$ is an upper triangular matrix. Thus, combining (62), (63) and (65) yields

$$J = l^*U \begin{bmatrix} 0_{(p+1)\times(p+1)} & 0 \\ 0 & 1 \end{bmatrix} U^*l. \tag{66}$$

Now, express U^* and K as

$$U^* = \begin{bmatrix} U_{11} & U_{12} \\ U_{21} & U_{22} \end{bmatrix}, \quad , K = \begin{bmatrix} K_1 \\ K_2 \end{bmatrix}, \tag{67}$$

where

$$U_{11} \in C^{(p+1)\times(p+1)}, \quad U_{12} \in C^{1\times(p+1)}, \quad K_1 \in C^{(p+1)\times(p+1)},$$
$$U_{21} \in C^{(p+1)\times 1}, \quad U_{22} \in C, \quad K_2 \in C^{1\times(p+1)}.$$

From (65) and (67), we can also get $U_{21}K_1 + U_{22}K_2 = 0$, i.e.,

$$\begin{aligned} U_{21} = -U_{22}K_2K_1^{-1} &= -U_{22}\begin{bmatrix} 0 & \dots & 0 & -\alpha \end{bmatrix} \begin{bmatrix} 1 & 0 & 0 & \dots & 0 \\ \alpha & 1 & 0 & \dots & 0 \\ \alpha^2 & \alpha & 1 & \dots & 0 \\ \vdots & \vdots & \vdots & \vdots & \vdots \\ \alpha^p & \alpha^{p-1} & \alpha^{p-2} & \dots & 1 \end{bmatrix} \\ &= \alpha U_{22}\begin{bmatrix} \alpha^p & \dots & \alpha & 1 \end{bmatrix}. \end{aligned} \tag{68}$$

Thus, from (66), (68) and (59), it gives

$$J = |[U_{21} \;\; U_{22}]l|^2 = |U_{22}(\alpha^{p+1} + l_1\alpha^p + \cdots + l_p\alpha + l_{p+1})|^2 = |U_{22}|^2|\alpha + \beta|^{2(p+1)}. \quad (69)$$

It should be pointed out that $0 < |U_{22}| \le 1$. Since $\mathrm{Re}(\beta) > 0$, it can be seen that a necessary condition to make J to be very small is that $\mathrm{Re}(\alpha) < 1$. This is why we make the assumption that the real parts of the unstable zeros of $b(s)$ are smaller than 1. Under this assumption, it is very clear that $(p+1)^2 J \to 0$ if $p \to \infty$ and β is chosen such that $0 < \mathrm{Re}(\beta) < 1 - \mathrm{Re}(\alpha)$ and $\mathrm{Im}(\beta) = -\mathrm{Im}(\alpha)$.

Now, define $\bar{c}(s) = [s^p, \ldots, s, 1]\bar{c}$, a similar result about the coefficients of $(s+\bar{\beta})^{p+1} - (s - \bar{\alpha})\bar{c}(s)$ can be derived as in Lemma A.1. Let

$$\begin{aligned} &\left\{(s+\beta)(s+\bar{\beta})\right\}^{p+1} - (s-\alpha)(s-\bar{\alpha})c(s)\bar{c}(s) \\ &\qquad = \varpi_1 s^{2(p+1)-1} + \cdots + \varpi_{2(p+1)-1}s + \varpi_{2(p+1)}. \end{aligned} \quad (70)$$

It can be easily proved that $4(p+1)^2 \sum_{i=1}^{2(p+1)} |\varpi_i|^2 \to 0$ as $p \to \infty$.

Therefore, the theorem can be proved by considering all the factors of $\kappa_1(s)$.

References

[1] Chen, X. and Fukuda, T. Model reference robust control for nonminimum phase systems with disturbances. *Int. J. Contr.* **72**(2) (1999) 123–132.

[2] Chen, X., Fukuda, T. and Young, K.D. A new nonlinear robust disturbance observer. *Systems & Control Letters* **41**(2) (2000) 189–199.

[3] Chen, X. and Su, C. Robust output tracking control for the systems with uncertainties. *Int. J. Syst. Sci.* **33**(4) (2002) 247–257.

[4] Chen, X. and Su, C. Design and analysis of nonlinear control for uncertain linear systems. *IEEE Trans. Circuits & Systems I: Fundamental Theory and Appl.* **5**(2) (2003) 307–314.

[5] Chen, Y.H. Optimal design of robust control for uncertain systems: a Fuzzy approach. *Nonlinear Dynamics and Systems Theory* **1**(2) (2001) 133–144.

[6] Clarke, D.W. Self-tuning control of nonminimum-phase systems. *Automatica* **2**(5) (1984) 501–517.

[7] Galperin, E.A. Some generalization of Lyapunov's approach to stability and control. *Nonlinear Dynamics and Systems Theory* **2**(1) (2002) 1–24.

[8] Hashtrudi-Zaad, K. and Khorasani, K. An integral manifold approach to tracking control for a class of nonminimum phase linear systems using output feedback. *Automatica* **32**(11) (1996) 1533–1552.

[9] Qu, Z. and Dawson, D.M. Model reference robust control of linear systems. *Proc. Amer. Control Conf.* (Chicago, USA, 1992) P.1182–1186.

[10] Sastry, S. and Bodson, M. *Adaptive Control: Stability, Convergence, and Robustness.* Prentice Hall, Englewood Cliffs, NJ, 1989.

[11] Slotine, J.J. and Li, W. *Applied Nonlinear Control.* Prentice Hall, Englewood Cliffs, NJ, 1991.

[12] Watkins, D.S. *Fundamentals of Matrix Computations.* John Wiley & Sons, New York, 1991.

[13] Zhu, J.Y., Martindale, S.C. and Dawson, D.M. A new design for model reference robust control using state-space techniques. *Int. J. Contr.* **62**(5) (1995) 1061–1084.

Nonlinear Dynamics and Systems Theory, 4(2) (2004) 139–144

A Modified LQ-Optimal Control Problem for Causal Functional Differential Equations

C. Corduneanu

The University of Texas at Arlington,
Box 19408 UTA, Arlington TX 760197, USA

Received: October 10, 2003; Revised: June 9, 2004

Abstract: This paper continues some ideas from a preceding paper of the author, in which only point-wise initial data are considered. Here, the constraints on state variables and control involve functional initial data, leading to a modified control problem.

Keywords: *LQ-optimal control; modified problem; causal operators/equations.*

Mathematics Subject Classification (2000): 49J10, 49J15.

1 Introduction

The following problem will be considered in this paper.

Given the functional differential equations, with causal operators A and B

$$\frac{dx}{dt} = (Ax)(t) + (Bu)(t), \quad t \in [t_0, T], \tag{1}$$

with $x\colon [t_0,T] \to R^n$, $u\colon [t_0,T] \to R^m$, $A\colon L^2([0,T], R^n) \to L^2([t_0,T], R^n)$ and $B\colon L^2([t_0,T], R^m) \to L^2([t_0,T], R^n)$, one attaches the initial value condition

$$x(t) = \varphi(t), \quad t \in [0, t_0), \quad x(t_0) = \theta, \tag{2}$$

and considers the minimization of the cost functional

$$C(x;\varphi,u) = \int_0^{t_0} \langle (P\varphi)(t), \varphi(t)\rangle\, dt + \int_{t_0}^{T} \big(\langle (Qx)(t), x(t)\rangle \;+\; \langle (Ru)(t), u(t)\rangle\big) dt, \tag{3}$$

under certain conditions to be specified below. Our main interest will be in proving the existence of an optimal triplet $(\bar{x};\bar{\varphi},\bar{u})$, such that

$$C(\bar{x};\bar{\varphi},\bar{u}) = \min C(x;\varphi,u), \tag{4}$$

the minimum being taken with respect to $\varphi \in \Phi \subset L^2([0,t_0], R^n)$ and $u \in U \subset L^2([t_0,T[, R^m)$, where Φ and U are the admissible sets for φ and u, respectively.

Remark 1 The case of the point data initial value problem has been discussed in our preceding paper [1], as well as in our book [2]. In that case, the first integral in the right-hand side of (3) is missing, since the only initial condition was $x(t_0) = \theta$. This particular case of the initial value is not restrictive. Indeed, if we substitute to $x(t_0) = \theta$ the more general condition $x(t_0) = x^0 \in R^n$, then letting $y(t) = x(t) - \bar{x}(t)$, one finds instead of (1) the equation

$$\frac{dy}{dt} = (Ay)(t) + (Bu)(t),$$

if $\bar{x}(t)$ is the (unique) solution of the homogeneous equation $dx/dt = (Ax)(t)$, such that $\bar{x}(t_0) = x^0$. Obviously, $y(t_0) = \theta$ is the null element of R^n, which agrees with the second condition in (2).

Remark 2 The nature of the functional (3) suggests the following interpretation of the control problem formulated above.

Namely, once we obtain the optimal triplet $(\bar{x}; \bar{\varphi}, \bar{u})$, then imposing on the dynamical system described by (1) the dynamics resulting from (2), and then applying the control u on $[t_0,T]$, we will obtain the optimal trajectory on $[t_0,T]$.

This feature of the problem illustrates the possibility of achieving a certain objective by acting on the initial interval $[0,t_0]$, first in accordance with (2), and then implementing the control u as resulting from the optimal problem.

Remark 3 It is possible to formulate a more general problem than the one described above, by considering nonlinear equations instead of (1), such as

$$\frac{dx}{dt} = (Fx)(t) + (Gu)(t), \tag{5}$$

under some initial data (2), and with a nonlinear cost functional of the general form

$$C(x; \varphi, u) = \int_0^{t_0} (K\varphi)(t)\, dt + \int_{t_0}^{T} L(x; u)(t)\, dt. \tag{6}$$

We shall not attempt to deal with problems of this type, in which F, G, K and L stand for some nonlinear operators, with adequate properties.

Remark 4 Once proven the existence of the optimal triplet $(\bar{x}; \bar{\varphi}, \bar{u})$, the next important problem consists in achieving the synthesis of the control problem. In other words, to express the variable u in terms of φ and x. Or, maybe it is more adequate to express both φ and u in terms of the (desired) trajectory x, if at all possible. Of course, these feedback relations should also contain causal operators. A paper by A.J. Pritchard and Yuncheng You [3], in which only classical Volterra operator are considered, seems to be promising in this regard.

2 The Main Result

We shall now formulate a set of sufficient conditions assuring the existence of the optimal triplet $(\bar{x}; \bar{\varphi}, \bar{u})$.

This will be achieved by reducing the problem to an elementary result in the theory of Hilbert spaces. Namely, *in a Hilbert space, every closed convex set contains a unique element of minimal norm.* We have applied this result in [1, 2], when only the case of point-wise data was considered, which meant that only the second integral appeared in the right-hand side of (3).

We shall take as underlying space the Hilbert space

$$H = L^2([0, t_0], R^n) \times L^2([t_0, T],\, R^m), \tag{7}$$

in which the scalar product is given by the sum of the scalar products in the factor spaces. This implies the fact that the norm in H is the square root of the sum of squares of norms in the factor spaces.

Let us now state the basic conditions under which we shall be able to prove the existence and uniqueness of the optimal triplet $(\bar{x}; \bar{\varphi}, \bar{u})$.

(1) The operators A and B appearing in the equation (1) are linear, continuous and causal on the space $L^2([0, T],\, R^n)$, resp. from $L^2([t_0, T],\, R^m)$ into $L^2([t_0, T],\, R^n)$.

(2) The linear operators P, Q and R appearing in the cost functional (2) are bounded and self-adjoint; moreover, P and R are positive definite, while Q is nonnegative definite.

(3) The initial set $\Phi \subset L^2([0, t_0],\, R^n)$, and the control set $U \subset L^2([t_0, T], R^m)$ are convex closed sets.

The following result can be stated.

Theorem *Consider the modified LQ-optimal control problem of minimizing the cost functional $C(x; \varphi, u)$ given by* (3)*, under the constraints (1), (2) and $\varphi \in \Phi$, $u \in U$. If conditions (1), (2) and (3) formulated above are satisfied, then there exists a unique optimal triplet $(\bar{x}; \bar{\varphi}, \bar{u})$, i.e., such that (4) takes place.*

Proof First of all, it is necessary to show that the cost functional $C(x; \varphi, u)$, given by (3), has a meaning for any $\varphi \in \Phi$ and $u \in U$. In other words, we need to prove that $x(t)$ from (1), under initial condition (2), is defined on the whole interval $[t_0, T]$.

We notice that (1) has the form

$$\frac{dx}{dt} = (Ax)(t) + f(t), \qquad t \in [t_0, T], \tag{8}$$

with $f \in L^2([t_0, T],\, R^n)$, because $Bu \in L^2([t_0, T],\, R^n)$ when $u \in U$. Hence, the solution of (8) under condition (2), can be represented by the variation of parameter formula

$$x(t) = \int_{t_0}^{t} X(t, s) f(s)\, ds + \int_{0}^{t_0} \widetilde{X}(t, s; t_0)\varphi(s)\, ds, \qquad t \in [t_0, T], \tag{9}$$

with $X(t, s)$ the Cauchy matrix attached to the homogeneous system $dx/dt = (Ax)(t)$ on the interval $[t_0, T]$, and $\widetilde{X}(t, s; t_0)$ a matrix whose definition and significance are given in [2]. The last integral in (9) represents the solution of the homogenous system, with initial condition (2).

Returning to the equation (1), and taking (8) into account, the solution of (1), for given $u \in U$, under initial condition (2), is given by

$$x(t) = \int_{t_0}^{t} X(t, s)(Bu)(s)\, ds + \int_{0}^{t_0} \widetilde{X}(t, s; t_0)\varphi(s)\, ds, \tag{10}$$

on $[t_0, T]$. The formula (10) shows that the solution $x(t)$ of (1), (2) is defined on $[t_0, T]$. It is absolutely continuous on that interval. The integrals in (3) obviously make sense.

Following the same lines as in $[1, 2]$ and taking into account the fact that the new scalar product in H is given by

$$\langle\langle(x;\varphi,u),(y;\psi,v)\rangle\rangle = \int_0^{t_0} \langle(P\varphi)(t),\psi(t)\rangle\, dt + \int_{t_0}^{T} (\langle(Qx)(t),y(t)\rangle + \langle(Ru)(t),v(t)\rangle)\, dt, \quad (11)$$

one can easily see that the cost functional $C(x;\varphi,u)$, given by (3), can be represented in the form

$$C(x;\varphi,u) = \langle\langle(x;\varphi,u),(x;\varphi,u)\rangle\rangle = |||(x;\varphi,u)|||^2. \quad (12)$$

In (12), the triple bar stands for the new norm in H. Therefore, the problem of minimizing the cost functional $C(x;\varphi,u)$ in (3), has been reduced to the problem of minimum norm in the Hilbert space H.

Since the product $\Phi\times U$ is a convex set in H, we need to show that it is also closed in the topology of H, induced by the norm $|||\cdot|||$, derived from the scalar product defined by (11). Using estimates established in [2], as well as a similar one for $x(t)$ given by (10),

$$\int_{t_0}^{T} |x(t)|^2\, dt \le C_1 \int_{t_0}^{T} |u(t)|^2\, dt + C_2 \int_0^{t_0} |\varphi(t)|^2\, dt,$$

one obtains for some positive constants λ, $\Lambda > 0$,

$$\lambda\left(\int_0^{t_0} |\varphi(t)|^2\, dt + \int_{t_0}^{T} |u(t)|^2\, dt\right) \le |||(x;\varphi,u)|||^2 \le \Lambda\left(\int_0^{t_0} |\varphi(t)|^2\, dt + \int_{t_0}^{T} |u(t)|^2\, dt\right), \quad (13)$$

which proves the equivalence of the two topologies on H; that induced by the L^2–norms in the factor spaces and the new norm $|||\cdot|||$.

Consequently, by applying the minimum norm property of Hilbert spaces quoted above, we derive the existence and uniqueness of an element $(\overline{\varphi},\overline{u}) \in \Phi\times U$, such that the triplet $(\bar{x};\overline{\varphi},\overline{u})$, with $\bar{x}$ determined from (1), (2) when $u=\overline{u}$, $\varphi=\overline{\varphi}$, is the unique optimal triplet for the problem considered above.

This ends the proof of the theorem stated in this section.

Remark 1 Some properties of the matrices $X(t,s)$ and $\widetilde{X}(t,s;t_0)$ are mentioned in [2]. For instance, noticing that the integral

$$\int_0^{t_0} \widetilde{X}(t,s;t_0)\varphi(s)\, ds$$

represents an absolutely continuous function of $t\in[t_0,T]$, with values in R^n, for each $\varphi\in L^2([0,t_0],R^n)$, enables us to derive estimates appearing in (13).

Remark 2 The relationship between the elements of the optimal triplet is given by the formula (10), i.e.,

$$\bar{x}(t) = \int_{t_0}^{t} X(t,s)(B\overline{u})(s)\,ds + \int_{0}^{t_0} \widetilde{X}(t,s;t_0)\,\overline{\varphi}(s)\,ds. \tag{14}$$

It is useful to notice that the first integral in the right-hand side of (14) can be expressed in the form

$$\int_{t_0}^{t} X(t,s)(Bu)(s)\,ds = \int_{t_0}^{t} X_1(t,s)u(s)\,ds, \tag{15}$$

where $X_1(t,s)$, $t_0 \le s \le t \le T$, is completely determined by $X(t,s)$ and the operator B. The existence of $X_1(t,s)$, which is a matrix of type n by m, follows from the fact that the first term in (15) represents a continuous operator from $L^2([t_0,T],\, R^m)$ into $L^2([t_0,T],\, R^n)$ (actually, each $u \in L^2$ is taken into an absolutely continuous function).

Therefore, (14) can be rewritten as

$$\bar{x}(t) = \int_{t_0}^{t} X_1(t,s)\overline{u}(s)\,ds + \int_{0}^{t_0} \widetilde{X}(t,s;t_0)\,\overline{\varphi}(s)\,ds \tag{16}$$

which shows that in order to determine the feedback equation, one has to solve (16) with respect to $\overline{u}(t)$. When this is possible, the feedback equation will be of the form $\overline{u}(t) = F(\bar{x},\overline{\varphi})(t)$. Equation (16) is a first kind Volterra integral equation not always solvable.

3 Feedback Control

It is always important to establish the feedback relationship in any control problem. This will allow to apply the control in such a manner that the desired trajectory, and finally the target, are obtained.

Let us notice that the equation (16) has the form

$$y(t) = f(t) + \int_{t_0}^{t} K(t,s)u(s)\,ds, \qquad t_0 \le t \le T, \tag{17}$$

which expresses the input–output relation. Identifying (16) and (17) is an elementary operation. For instance, $K(t,s)$ is given by

$$K(t,s) = X_1(t,s), \tag{18}$$

with $X_1(t,s)$ resulting from (15). It is determined by $X(t,s)$ and the operator B, but we do not have a constructive way to obtain $X_1(t,s)$, $t_0 \le s \le t \le T$.

In regard to the equation (17), the study of A.J. Pritchard and Yuncheng You [3], in which R^n or R^m are substituted by arbitrary Hilbert spaces, brings substantial contributions when the cost functional is chosen of the form

$$J(u,f) = \langle (Gy)(T), y(T)\rangle + \int_{t_0}^{T} (\langle\langle (Qy)(t), y(t)\rangle + \langle (Ry)(t), y(t)\rangle) dt. \tag{19}$$

While (19) is similar to (3), there is a difference because of the modified form of the optimal control problem we have dealt with in preceding sections of this paper.

It would be interesting to see if the modified problem can be treated by the method developed in [3]. The existence of the optimal control can be proven using a similar scheme as above.

A more general input-output equation than (17) is also considered in [3]. Namely,

$$y(t) = f(t) + \int_{t_0}^{t} \Lambda(t,s)y(s)\,ds + \int_{t_0}^{t} N(t,s)u(s)\,ds$$

is reduced to the form (17), the same way our modified control problem is reduced to the form (17).

Extending the treatment of the problem, from the case when the cost functional (19) is replaced by the functional (3), constitutes, we believe, a new type of problem in LQ-optimal control.

As a byproduct of the solution of the above formulated problem, will be the causal character of the feedback relation. This property is examined in detail in [3], where a truncation procedure is exposed and connection with some Fredholm integral equations is emphasized.

We are not attempting here to get in more detail in respect to the above mentioned problems and the procedures of their solution.

References

[1] Corduneanu, C. LQ-optimal control problems for systems with abstract Volterra operators. *Tekhn. Kibernetika* **1** (1993) 132–136.

[2] Corduneanu, C. *Functional Equations with Causal Operators.* Taylor and Francis, London, 2002.

[3] Pritchard, A.J. and Yuncheng You. Causal feedback optimal control for Volterra integral equations. *SIAM J. Control and Optimization* **34** (1996) 1874–1890.

Nonlinear Dynamics and Systems Theory, **4**(2) (2004) 145–159

Adaptive Calculation of Lyapunov Exponents from Time Series Observations of Chaotic Time Varying Dynamical Systems

A. Khaki-Sedigh[1], M. Ataei[2], B. Lohmann[2] and C. Lucas[3]

[1] *Department of Electrical Engineering, K. N. Toosi University of Technology, Sayyed Khandan Bridge, P.O. Box 16315-1355, Tehran, Iran*
[2] *Institute of Automation, University of Bremen, Universität Bremen, Otto-Hahn-Allee./ NW1, D-28359, Bremen, Germany*
[3] *Faculty of Engineering, Department of Electrical Engineering, University of Tehran, North Kargar Avenue, Tehran, Iran*

Received: May 5, 2003; Revised: May 16, 2004

Abstract: This paper considers the adaptive computation of Lyapunov Exponents (LEs) from time series observations based on the Jacobian approach. It is shown that the LEs can be calculated adaptively in the face of parameter variations of the dynamical system. This is achieved by formulating the regression vector properly and adaptively updating the parameter vector using the Recursive Least-Squares principles. In cases where the structure of the dynamical system is unknown, a general non-linear regression vector for local model fitting based on a locally adaptive algorithm is presented. In this case, the Recursive Least-Squares method is used to fit a suitable local model, then by state space realization in canonical form, the Jacobian matrices are computed which are used in the QR factorization method to calculate the LEs. This method essentially relies on recursive model estimation based on output data. Hence, this on-line dynamical modeling of the process will circumvent the computations typically required in the reconstructed state space. Therefore, difficulties such as the problem of large number of data and high computational effort and time are avoided. Finally, simulation results are presented for some well-known and practical chaotic systems with time varying parameters to show the effectiveness of the proposed adaptive methodology.

Keywords: *Time series; Lyapunov exponents; chaos; time varying chaotic systems; Jacobian matrices; QR factorization; non-linear regressive.*

Mathematics Subject Classification (2000): 37M10, 37L30, 37M25, 93C40.

1 Introduction

Chaos is defined based on its various characteristics [5], however, the Lyapunov exponents are conceptually the most basic and useful dynamical diagnostic for deterministic chaotic systems. The calculation of LEs for systems whose dynamical equations with constant parameters are known is straightforward. However, these methods cannot be applied directly to a set of measurement data. Two general approaches for computing the LEs from output time series are the *geometrical* and *Jacobian approaches.* In geometrical approaches, the long term evolution of an infinitesimal sphere of initial conditions is considered. [33] is one of the basic works on this approach whose idea has been modified for calculating the largest LE from short noisy data [27], and [19]. The extension of this approach for multiple time series has also been reported in [4]. On the other hand, in the Jacobian approach, local Jacobian matrices are estimated and the long term product of matrices is computed. This is presented in [29] and [15] and its idea has been extended in several references, e.g. [7], [11], and [25]. In this approach, the Jacobians are found by *locally linear mapping* the neighborhoods near the reference trajectory to neighborhoods at a subsequent time [8]. In [29] and [15], the linearized flow map from the neighbor data set into m step ahead of this set is considered as an approximation for the tangent map. In [7], it is shown that using the local neighborhood-to-neighborhood mappings with higher order Taylor series, can lead to superior results. But, all of these methods involve a state space reconstruction of the process and then finding the proper neighbors. In order to reconstruct the state space properly, the determination of embedding dimension and lag time is vital. To deal with these issues the *False Neighbor* [20] and *Singular Value Decomposition* [6] approaches are proposed which are modified and extended to multivariate time series cases [1], [2], and [24]. In addition, another problem associated with the methods based on the neighborhood approach is its high computational effort and time consuming procedures, which can be partially resolved by an adaptive reconstruction of the chaotic attractors from a single trajectory as presented in [34]. Four other methods for estimating the Jacobian have been referred to in [22], including the local thin-plate splines, radial basis functions, projection pursuit and neural nets. In [25], the Jacobians are estimated over boxes of the state space to speed up the algorithm of LEs computation.

However, in all the previous work associated with LE computation, it is generally assumed that the dynamical system under study has fixed parameters and is time invariant. But, in real applications, as it will be explained in Section 3, this is not always the case. Hence, in this paper, calculation of the LEs by an adaptive method is considered. Since the geometric approach is based on the evolution of neighbor trajectories in the reconstructed state space, it cannot be used adaptively for on-line calculation of LEs in the case of systems with time varying parameters. Therefore, the procedure adopted in this paper falls into the Jacobian approach category, which is shown to have the capability of on-line calculations. It is shown that in the proposed methodology, the LEs of an uncertain or time varying chaotic dynamical systems are computed adaptively. The important step in this approach is to estimate the Jacobian matrices. Since the LEs are derived from the eigenvalues of the Jacobians, any small error in the computation of Jacobians can cause major error in the LE computation. Some general perturbation results and error analysis in QR algorithms for computing LEs can be found in [14], [13]. In this paper, two main objectives are followed. The first goal is to use a known non-linear structure for the chaotic dynamical equations and recursively estimating the unknown parameters of the model, the procedure of the Jacobian estimation is performed on-line to overcome the problem of time variation and also uncertainty in the parameters of the dynamical system. Therefore, any variations in the unknown physical parameters of the system will appear on-line on the LEs, i.e., the LEs of the system for the current parameters is available. The advantages of on-line availability of LEs are discussed in Section 3. The second objective of the paper is to consider a general non-linear structure for the completely unknown chaotic dynamical system. This is a local model that is fitted to the system by using the Recursive Least-Squares method. Then by realizing the derived difference equation in state space canonical form, the Jacobians are estimated in each point of the trajectory. These Jacobians are then used to calculate the LEs in the QR algorithm. In this method, a general time varying non-linear model is proposed for the unknown dynamical system.

This paper is organized as follows. The background materials are given in Section 2. Some practical time varying chaotic systems and the problems associated with the LE computations for such systems are outlined in Section 3. An adaptive algorithm for calculation of the LEs is presented in Section 4. In Section 5, by considering the general non-linear regression vector, a locally adaptive algorithm for calculating the LEs is presented. Finally, simulation results are provided to show the effectiveness of the proposed methodology in well known and practical chaotic dynamical systems in Section 6.

2 Background Materials

To present the adaptive LE estimation based on the Jacobian approach, some basic definitions and algorithms are provided as follows. Consider the autonomous discrete-time dynamical system described in the following form:

$$X_{k+1} = F(X_k), \quad k = 0, 1, \dots \tag{1}$$

where X_k is the state vector in the R^m space and $F(\cdot)$ is a continuously differentiable non-linear function. Linearization of the system for a small range around the operational trajectory in the phase space can be written as:

$$\delta X_{k+1} \cong J_k \, \delta X_k, \quad k = 0, 1, \dots \tag{2}$$

where $J_k = \dfrac{\partial F}{\partial X} \,|_{X_k} \in R^{m\times m}$ is the Jacobian matrix in point k. The LEs are defined as [14].

Definition 1 Let $Y^k = J_{k-1}J_{k-2}\cdots J_0$, then the following symmetric positive definite $m \times m$ matrix exists:

$$\Lambda = \lim_{k\to\infty} \left((Y^k)^{\mathrm{T}} Y^k \right)^{\frac{1}{2k}} \tag{3}$$

and the logarithms of their eigenvalues are called the *Lyapunov Exponents.*

However, computation of the LEs by using this definition has some problems. The first problem is that for large value of k, the fundamental solution Y^k may take very large values and the calculation of Λ is therefore not feasible. Further, the computation of Y^k should be such that the linear independence of the columns is maintained. Otherwise, this computation leads only to the largest LE. To deal with these problems, the QR factorization algorithm is used for approximation of LEs [15], [7], [11], [25], [14], and [13]. The steps involved in this method can be summarized as follows [14]:

1. Consider the orthogonal $m \times m$ matrix Q_0 such that $Q_0^{\mathrm{T}} Q_0 = I_{m\times m}$.
2. Solve $Z_{k+1} = J_k Q_k, \; k = 0, 1, \ldots,$ and obtain the decomposition: $Z_{k+1} = Q_{k+1} R_{k+1}$ where Q_{k+1} is an orthogonal $m \times m$ matrix and R_{k+1} is an upper triangular $m \times m$ matrix with positive diagonal elements.
3. $\lambda_i = \lim\limits_{k\to\infty} \dfrac{1}{k} \log((R_-\{k\})_{ii} \cdots (R_-\{1\})_{ii}) = \lim\limits_{k\to\infty} \dfrac{1}{k} \sum\limits_{j=1}^{k} \log((R_-\{j\})_{ii}),$
   $i = 1, \ldots, m.$

3 Practical Motivations

Analysing the chaotic motion has become an active field of research, due to its wide applications and chaos theory has been successfully applied to many engineering systems such as pulse combustors, internal combustion engines and power plant pulverized coal burners.

The evolutionary motion of each system is described by its dynamical equations. In practical cases, some of the parameters in the system model may not be completely known or may vary in time. In the following, two practical time varying chaotic systems are provided

3.1 Power electronics circuits

Power electronic is a discipline spawned by real life applications in industrial, commercial, residential and aerospace environments. Much of the developments of the field of the power electronics evolve around some immediate needs for solving specific power conversion problems. Power electronics circuits can be described as piecewise switched circuits, which assume different topologies at different times. The result is a *non-linear time varying* operation, which naturally demands the use of non-linear methods for analysis and design. On the other hand, most power supply engineers would have experienced chaos in switching regulators when some parameters like input voltage and feedback gain are varied [31]. Also, in [9], the bifurcation behaviour under variation of a range of circuit parameters including storage inductance, load resistance, output capacitance is examined. Further attempts to derive the related maps for power electronics circuits and the demonstration of the occurrence of chaos under variation of parameters can be found in [12] and references therein.

3.2 Plasma-dust grain system

Researchers on plasma-dust grain systems are developing new research fields in plasma physics. In [28] a plasma-dust grain system, which is spatially one dimensional and has no external electric and magnetic field is considered. The charge of each dust grain, q, is a time dependent variable and continuously changes with time. It is assumed that the density fluctuation depends only on time and the dust charge varies temporally as:

$$q = q_0(\delta - \varepsilon \cos(\omega t))^{1/2}, \tag{4}$$

where q_0, δ, ε, and ω are determined as the fixed parameters. Equation of motion in this case is as follows:

$$\ddot{x} - (\alpha - \beta x^2)\dot{x} + x\omega_0^2(\delta - \varepsilon\cos(\omega t)) = 0, \tag{5}$$

where x is the average velocity of the dust grains. The coefficients α, β, and ω_0 correspond to production rate, loss rate, and the plasma frequency of the dust grains, respectively. The second term of the left-hand side of (5) is similar to that of the van der Pol equation, and the third term to the Mathieu one. Henceforth, this equation is called *van der Pol–Mathieu* equation.

In practice, the parameters α and β are time varying which causes large fluctuations in the behaviour of the system for different values. Two typical behaviour of the system are considered as follows. It should be noted that the values of the other parameters are assumed fixed.

Case I. The limit cycle-like behaviour For the fixed value of β, by examining the shape of the attractor for different values of α, it is seen that for some values the attractor is similar to a limit cycle. The LEs of the system for $\beta = 100$ and $\alpha = 0.78, 20$ have been computed which are summarized in Table 3.1. It is seen that there is no positive LE which confirms the non-chaotic behaviour.

Table 3.1 The calculated LEs of plasma dust-grain system for different parameters.

Parameters		Lyapunov exponents	
$\alpha = 0.78$	$\beta = 100$	$\lambda_1 = -0.1711$	$\lambda_2 = -0.7781$
$\alpha = 20$	$\beta = 100$	$\lambda_1 = -0.0491$	$\lambda_2 = -35.3375$
$\alpha = 1$	$\beta = 10$	$\lambda_1 = 0.0164$	$\lambda_2 = -1.0857$

Case II. The chaotic behaviour In this case the parameters are selected as $\alpha = 1$, $\beta = 10$. The computed LEs are provided in Table 3.1. It is seen that one of the LEs is positive which corresponds to the case of chaos.

The time varying nature of the parameters of a chaotic system can be observed in many other applications. For example, in [23], the chaotic instability behaviour of a spacecraft for a range of forcing amplitudes and frequencies when a sinusoidally varying torque is applied to the spacecraft is found. Such a torque may arise in practice from an unbalanced rotor or from vibrations in appendages. In [10], two-axis rate gyro with feedback control mounted on a space vehicle is considered and chaos is detected in the non-autonomous case in which there is an sinusoidal angular velocity about the spin of gyro. These results are of importance to spacecraft designers as any instabilities in the attitude dynamics of spacecraft could have disastrous effects on its normal operation. For example, chaotic motion in the attitude motion of communication satellite would be seriously detrimental to the high pointing accuracies required by antennae providing the desired coverage on the earth's surface. It is thus prudent for designers to avoid the region of chaotic instability via parameter design [23]. In the power electronics circuits which was explained in Section 3.1, the usual reaction is to avoid the occurrence of chaos by adjusting the component values and parameters. Thus, knowing how and when chaos occurs will be of prime importance [31]. In addition, control of chaos is the other important related subject in the field of chaotic systems [16], [26], and [32]. In mechanical systems which chaos may lead to irregular motions, it has to be reduced or suppressed. In this case, a feedback constant control torque with the assistance of the LEs calculations is used to bring the system from a chaotic regime to a regular one [10].

Therefore, the adaptive computation of quantitative LEs in parametric space as a common tool to determine chaos onset and different operational regions can be of vital importance in many engineering applications.

4 Adaptive Calculation of LEs

This section presents the adaptive calculation of the LEs. It is supposed that the output data of the dynamical system is available as a univariate time series. The dynamical behaviour of system is described by the following non-linear difference equation:

$$y(k+1) = f(X(k)), \tag{6}$$

where $f(\cdot)$ is a continuously differentiable function and $X(k)$ is a delayed vector as:

$$X(k) = [y(k-m+1),\, y(k-m+2),\, \dots\, y(k)]. \tag{7}$$

In this section, it is supposed that the dynamical structure of the system is known. Hence, m also has a definite value. However, it is assumed that the parameters of the dynamical equations are not known or they have variations with time. Here, a definite structure for the non-linear autoregressive function (6) is assumed as follows, which is linear in the unknown parameters:

$$y(k+1) = \sum_i \theta_i \phi_i(X(k)), \tag{8}$$

where ϕ_i are definite basis functions and θ_i are unknown and time varying parameters.

By considering $X(k)$ in (7) as the state vector, a canonical state space representation of the system is obtained as follows:

$$X(k) = \begin{bmatrix} x_1(k) \\ x_2(k) \\ \vdots \\ x_m(k) \end{bmatrix} = \begin{bmatrix} y(k-m+1) \\ y(k-m+2) \\ \vdots \\ y(k) \end{bmatrix} \Longrightarrow X(k+1) = \begin{bmatrix} x_2(k) \\ x_3(k) \\ \vdots \\ f(X(k)) \end{bmatrix}. \tag{9}$$

The Jacobian $m \times m$ matrix J_k in each point k of the typical trajectory for this canonical representation is as:

$$J_k = \begin{bmatrix} 0 & 1 & \dots & 0 & 0 \\ 0 & 0 & 1 & \dots & 0 \\ \vdots & \vdots & \vdots & \ddots & \vdots \\ Df_1 & Df_2 & \dots & Df_{m-1} & Df_m \end{bmatrix}, \tag{10}$$

where $Df_i = \dfrac{\partial f}{\partial x_i}$.

Assuming the structure given by equation (8), the Df_i, $i = 1, \dots, m$, are known expressions in terms of the parameters of the model. Therefore, to have the Jacobians in each point of the trajectory, only the recursive estimation of unknown parameters in equation (8) is required. To achieve this, the Recursive Least-Squares algorithm is used. By defining the regression vector as:

$$\phi(k) = [\phi_1(k), \phi_2(k), \dots, \phi_q(k)]^{\mathrm{T}}, \tag{11}$$

where q is number of basis functions and by considering the parameter vector θ, Recursive Least-Squares method is used to estimate the vector θ as follows [21]:

$$\hat{\theta}(k+1) = \hat{\theta}(k) + F(k+1)\phi(k)\varepsilon^0(k+1), \tag{12}$$

where:

$$\begin{aligned} F(k+1) &= F(k) - \frac{F(k)\phi(k)\phi^{\mathrm{T}}(k)F(k)}{1+\phi^{\mathrm{T}}(k)F(k)\phi(k)}, \\ \varepsilon^0(k+1) &= y(k+1) - \hat{\theta}^{\mathrm{T}}(k)\phi(k). \end{aligned} \tag{13}$$

Now, by using the estimated parameters, the QR method for calculation of the LEs can be modified as an *adaptive algorithm* for the computation of the LEs as follows:

Algorithm 1:

1. In step k using the relation (12), the unknown parameters are estimated. Therefore, the function $f(\cdot)$ according to the difference equation (8) is known.
2. The Jacobian $m \times m$ matrix J_k is computed and the decomposition $J_k Q_k = Q_{k+1} R_{k+1}$ is obtained where Q_k is an orthogonal $m \times m$ matrix and R_{k+1} is an upper triangular matrix with positive diagonal elements.
3. The LEs are calculated adaptively as:

$$\lambda_i(k+1) = \frac{1}{k+1}\Big(k\lambda_i(k) + \log\big((R_-\{k+1\})_{ii}\big)\Big), \quad i = 1, \dots, m, \tag{14}$$

for $k \ge M$, where M is large enough.

In the face of system parameter variations, the LEs of the system will change and the proposed adaptive algorithm shall identify the new LEs. Therefore, calculating the LEs adaptively makes it possible to have the estimated value in each time step.

5 Adaptive Calculation of LEs for Systems with Unknown Structure

In Section 4, it was assumed that the model for the evolutionary motion of the time varying dynamical system is known. However, in some practical applications the structure of the underlying dynamical system, which generates the data is unknown. The process output signal $y(t)$ of a causal non-linear process, whose dynamic behaviour is described by the differential equation of the form

$$L(D)\{y(t)\} + F\{y(t), \dot{y}(t), \dots\} = L(D)\{u(t)\} \tag{15}$$

can be calculated by the Volterra (functional) series of infinite order. In equation (15), $L(D)$ are differential operators with $D = \dfrac{d}{dt}$, $u(t)$ is the input signal, and $F(\cdot)$ is called a multinomial in $y(t)$. The discrete Volterra series is approximated by a parametric non-linear model. By the use of the discrete parametric Volterra model, the static and dynamic input/output behaviour of all non-linear processes whose differential equations belong to the class of non-linear systems given by equation (15) can be described. Therefore, a non-linear process model with a finite number of parameters and linear in the unknown parameters will be derived from the discrete Volterra series for the use in the adaptive computation loop. For each non-linear differential equation of the form given by equation (15), a static and dynamically equivalent input/output relation difference equation model can be derived. This difference equation can be formulated in a general expression as follows [18]:

$$\begin{aligned} y(k+1) &+ \sum_{i=0}^{m-1} \theta_{1i} y(k-i) + \sum_{\beta=0}^{h} \sum_{i=0}^{m-1} \theta_{2\beta i} y(k-i) y(k-i-\beta) + \dots \\ &+ \sum_{\beta_1=0}^{h} \sum_{\beta_2=\beta_1}^{h} \dots \sum_{\beta_{p-1}=\beta_{p-2}}^{h} \sum_{i=0}^{m-1} \theta_{p\beta_1 \dots \beta_{p-1} i} y(k-i) y(k-1-\beta_1) \dots y(k-1-\beta_{p-1}) \\ &= \sum_{i=0}^{m-1} \varphi_i u(k-i) + \theta_0, \end{aligned} \tag{16}$$

where p is the degree of non-linearity of the difference equation, m is the dynamic order, and h is an integer time-shift operator.

Since the solutions of the non-linear differential equations of the chaotic systems are strongly depend on the parameters and initial conditions, the idea of using the general expression (16) for locally modeling the systems is considered. As, only the output time series is assumed available, $u = 0$ is supposed. To present the adaptive calculation of the LEs, consider the following time series:

$$y(t_0),\, y(t_0 + t_s),\, y(t_0 + 2t_s),\, \dots,\, y(t_0 + (N-1)t_s) \equiv y_1,\, y_2,\, \dots,\, y_N, \tag{17}$$

where t_s is the sampling time, t_0 is the starting point of observation and N is the total number of data. The proposed algorithm, which we call it a *Locally Adaptive Algorithm* can be summarized as follows:

Algorithm 2:

1. Consider the points with indices $j = d, 2d, 3d, \dots, \left(\left[\frac{N}{d}\right] - 1\right)d$, where d is an integer value. Note that, the Jacobians will be computed in these points.
2. For each value of j, consider the last r data as $Y_j = (y_{j-r+1}, \dots, y_j)$, where r is an integer value and $r \le d$.
3. Employ the Recursive Least-Squares algorithm to estimate the unknown parameters of the general non-linear autoregressive model.
4. Compute the Jacobian $m \times m$ matrix J_j from equation (10) and the decomposition $J_j Q_j = Q_{j+d} R_{j+d}$ is obtained where Q_j is an orthogonal $m \times m$ matrix, and R_{j+d} is an upper triangular $m \times m$ matrix with positive diagonal elements.
5. The LEs are calculated adaptively as:

$$\lambda_i(j+d) = \frac{1}{\left(\frac{j}{d}\right) + 1} \left(\left(\frac{j}{d}\right) \lambda_i(j) + \log((R_-\{j+d\})_{ii}) \right), \quad i = 1, \dots, m. \tag{18}$$

In the implementation of algorithm (2), the following remarks should be taken into account:

Remark 1 In this case the number of elements in the delay vector (7), which is also the order of polynomial model, is generally not known a priori. In fact, these delay vectors construct the embedding vector space of the original state space of the chaotic system. Therefore, the embedding dimension and the order of the polynomial model, have the same role. For different values of model order, various polynomials are achieved which lead to different LEs. It is therefore important to have an appropriate criteria for model order selection, if it is not known in a practical problem. A criterion for choosing the suitable model order or embedding dimension by using polynomial modelling has been presented in [3]. In addition, since this is a relevant problem in computing the LEs, many other methods are available which provide the minimum embedding dimension, as stated in the introduction.

Remark 2 Here, the term “local” is used in the sense of time, i.e., the points which are used for the parameter estimation in each index j, are neighbors in time not in the position in the reconstructed state space. Therefore, computing the Jacobians do not rely on finding the local map between neighbors of any reference point in the reconstructed state space and their subsequences as is done in [29] and [15]. This requires much computational efforts and a large number of data and is time consuming. Note that all these have been avoided in this adaptive methodology. In addition, the local map concept in the previous work can not be followed in an adaptive methodology, since many points of the attractor are required to find the local neighbors and after any parameter change the new attractor must be found.

Remark 3 It is assumed that, the system dynamics is observable through the available time series (17). This is a generic property, which is assumed for state space reconstruction from time series [30]. In [2], it is shown that the determination of optimum embedding dimension, sometimes fails for some time series and multiple time series are required in this case. This may occur due to lack of observability condition from a single time series. This problem can also occur for the estimation of Jacobians.

Remark 4 Selection of r is based on the convergence of model parameters and the initial vector of the unknown parameter and significantly effects the rate of convergence. The choice of estimated parameter in j is a good initial vector for stage $j + d$ in the Recursive Least-Squares algorithm.

Remark 5 If the number of samples in the Y_j, are not enough for the parameter convergence, by using the re-sampling method, the number of data in this group can be increased. And, convergence of the parameters can be achieved during sufficient values of iterations.

6 Simulation Results

To show the effectiveness of the proposed adaptive calculation of LEs, the algorithms are applied to some well-known chaotic systems. The dissipative systems, which can be described either by flows or maps are considered. The flows and maps denote to a set of autonomous first-order differential and difference equations, respectively.

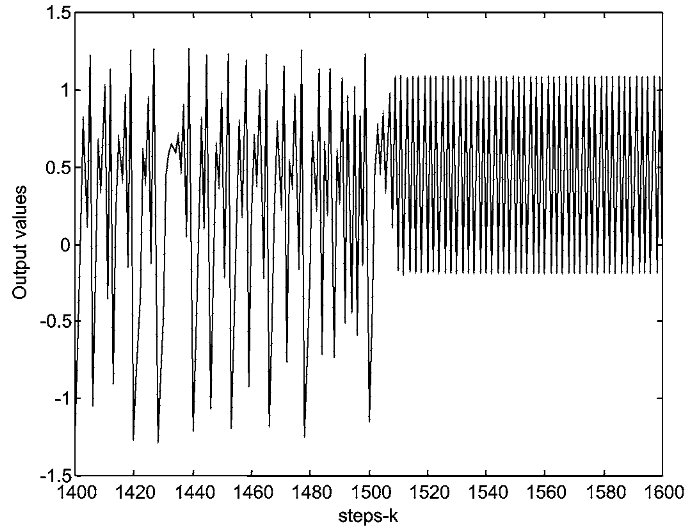

Figure 6.1. Data of Henon map with changes in parameters in step $k = 1500$.

6.1 Henon map

To illustrate the application of the Algorithm 1, first the Henon map is considered. This map can be considered as a two dimensional extension of the logistic map. It is described by the following equation:

$$y(k+1) = 1 - ay^2(k) + by(k-1), \tag{19}$$

where a and $|b| \leq 1$ are unknown time varying parameters. Suppose that the nominal parameters are $a = 1.4,\ b = 0.3$ which after some steps, change to the new values as $a = 1,\ b = 0.1$. Figure 6.1 shows the graph of the output data around the region that the nominal parameters have been changed to their new values. In practical systems, this kind of changes in nominal parameters is a common phenomenon, which occurs due to time dependent variations in the physical quantities of the system and causes variations in the LEs of the system. To see the effect of these variations, the algorithm (1) is applied to this data. In this example, the regression vector is a polynomial of order 2 and degree of non-linearity 2, which is the same as the structure of system which is known. The calculated LEs are shown in Figures 6.2a and 6.2b. It is seen that in the first stage of simulation, after a few iterations the LEs have converged to the true values, which are $\lambda_1 = 0.42,\ \lambda_2 = -1.62$. In $k = 1500$, which the parameters change to the new values $a = 1,\ b = 0.1,$ the calculated LEs converge to the correct LEs for these parameters. It is shown that, the estimated LEs converge to the true values given by, $\lambda_1 = -0.306$, $\lambda_2 = -1.99$.

6.2 Plasma-dust grain system

In this part, the plasma-dust grain system, which was explained in Section 3.2, is considered. We rewrite the equation (5) as a set of two first-order ordinary differential

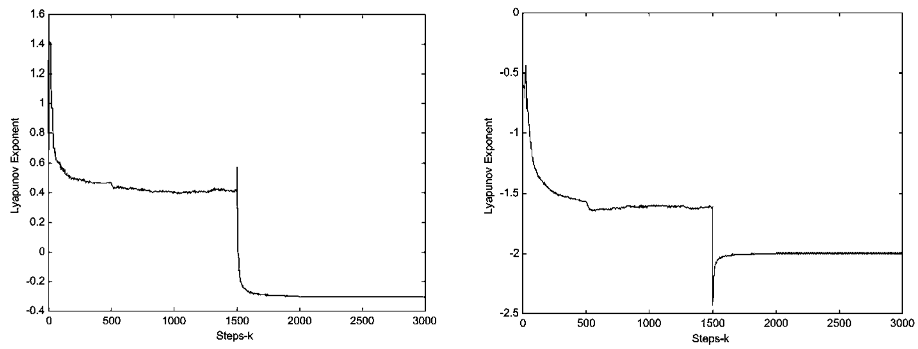

a) b)

Figure 6.2. The calculated LEs of Henon map for the data with changes in parameters in $k = 1500$. a) First LE; b) Second LE.

equations:

$$\begin{aligned} \frac{dx}{dt} &= y, \\ \frac{dy}{dt} &= (\alpha - \beta x^2)y - \omega_0^2 x(\delta - \varepsilon\cos(\omega t)), \end{aligned} \tag{20}$$

where in the simulations the parameters δ, ε, ω_0 and ω are assumed fixed but, α and β are time variant. In the first stage, the values of parameters are considered as $\alpha = 1$ and $\beta = 10$. Then after 500 sec., they change to the new values given by $\alpha = 0.78$ and $\beta = 100$. The corresponding LEs of these two regions have been calculated by using equation (5), which is shown in Table 3.1. As it was discussed in Section 3.2, chaotic and limit cycle-like behaviours are expected for these two operational regions, respectively. Now, let the time series observations of the variable x with a sampling time of 0.05 sec be available. By considering a second order polynomial model with degree of non-linearity equal to 3, the algorithm (1) is applied to calculate the LEs. As it is shown in Figures 6.3a and 6.3b, after a number of iterations the LEs have converged near true values, which are $\lambda_1 = 0.0161$, $\lambda_2 = -0.9089$.

In $k = 10000$, after a change in the parameters, the calculated LEs converge to the new LEs, which after 10000 iterations are $\lambda_1 = -0.0104$, $\lambda_2 = -0.7907$.

6.3 Ikeda map

In order to show the effectiveness of the proposed *Locally Adaptive Algorithm*, the Algorithm 2 is applied to the laser ring cavity problem. In quantum optics, the behaviour of the laser ring cavity is described by the following equation

$$z_{t+1} = \alpha e^{i\rho} z_t + \beta, \tag{21}$$

which is known as the Ikeda map. In this equation, the complex variable $z_t = x_t + iy_t$ represents the electric field at the beginning of the t^{th} passage around the ring, α is the coefficient of reflectivity of the partially reflecting output mirror, while β is related to

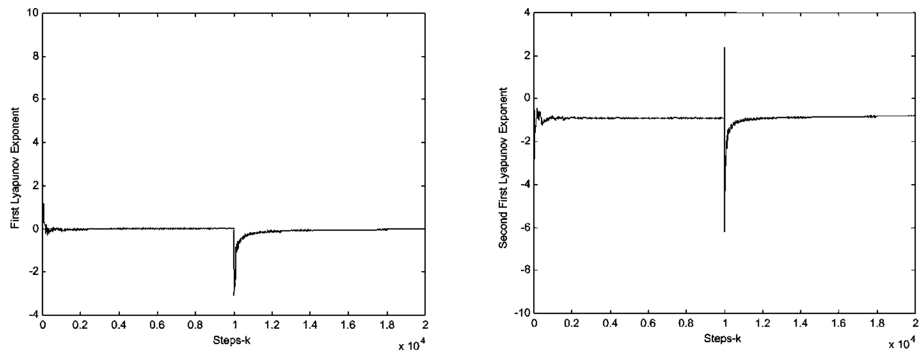

a) b)

Figure 6.3. The calculated LEs of plasma-dust grain flow for the data with changes in parameters in $k = 10000$. a) First LE; b) Second LE.

the laser input amplitude. The quantity ρ is a relatively complicated functional of the laser field inside the cavity and can be considered as

$$\rho = \Delta - \frac{\delta}{1 + |z_t|^2}, \tag{22}$$

where without any loss of generality it is assumed that, $\delta = 6$, and $\Delta = 0.4$ [17]. By selecting the definite values $\alpha = 0.9$ and $\beta = 1$, the Ikeda map can be rewritten as follows:

$$\begin{aligned} \rho &= 0.4 - \frac{6}{(1 + x^2(k) + y^2(k))}, \\ x(k+1) &= 1 + 0.9(x(k)\cos(\rho) - y(k)\sin(\rho)), \\ y(k+1) &= 0.9(x(k)\sin(\rho) + y(k)\cos(\rho)), \end{aligned} \tag{23}$$

where, the corresponding LEs are $\lambda_1 = 0.505,\ \lambda_2 = -0.715$ [19].

It is assumed that the system difference equations are not available. Therefore, the *Locally Adaptive Algorithm* is used to calculate the LEs. For this, the total number of $N = 5000$ data of the Ikeda map was considered in a time series. A second order polynomial model with a degree of non-linearity equal to 2, is considered as the non-linear autoregressive model. Then, by selecting $d = 5$, for computing the Jacobian matrix in each step, and by considering $r = 5$, all the available data in the interval $Y_j = (y_{j-r+1}, \ldots, y_j)$ were used for the Recursive Least-Squares algorithm to estimate the unknown parameters of the model. Then, by continuing the Algorithm 2 the LEs were calculated which are shown in Figures 6.4a and 6.4b. It is clearly shown that, the estimated LEs converge to $\lambda_1 = 0.5196,\ \lambda_2 = -0.6615$.

In the second test, the parameter α was considered to change from 0.9 to 0.55. The calculated LEs by using the differential equations in the second region are $\lambda_1 = 0.0921$, $\lambda_2 = -0.9537$. The *Locally Adaptive Algorithm* is then applied to the time series data of x variable, by using a polynomial model with order 2 and degree of non-linearity equal 2 and $r = d = 10$. As it is shown in Figures 6.5a and 6.5b, after a change in the parameters, the calculated LEs converge to the new LEs $\lambda_1 = 0.0933,\ \lambda_2 = -1.6205$.

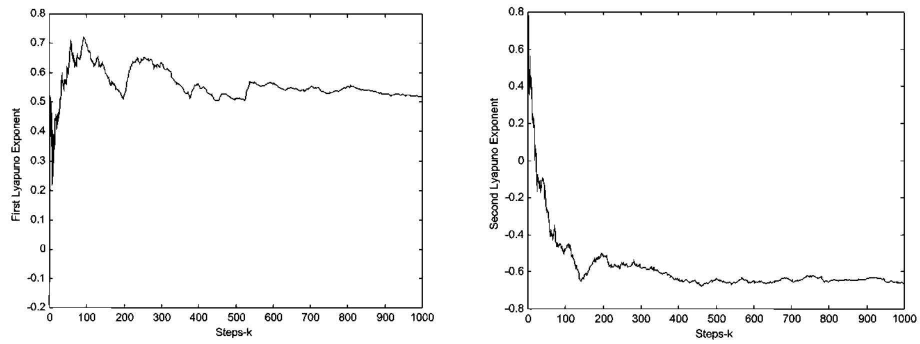

a) b)

Figure 6.4. The calculated LEs of Ikeda map by using Locally Adaptive Algorithm. a) First LE; b) Second LE.

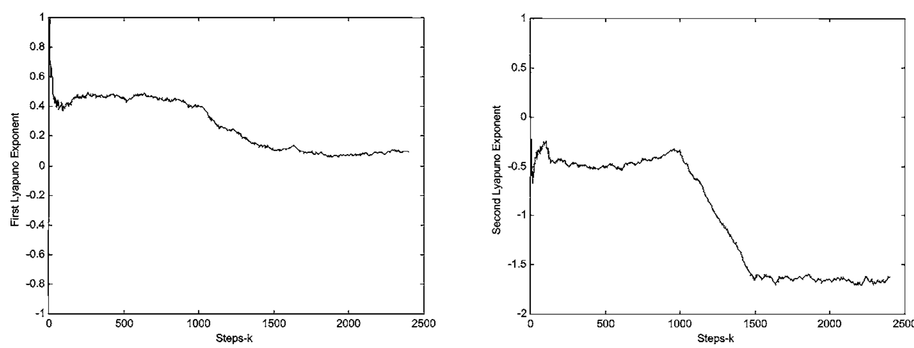

a) b)

Figure 6.5. The calculated LEs of Ikeda map for the data with changes in parameters in $k = 1000$. a) First LE; b) Second LE.

7 Conclusions

In this paper, an adaptive approach for the calculation of LEs is proposed. This ensures the effective calculation of LEs in the face of system parameter variations. The adaptive methodology is based on a non-linear regression vector and the Recursive Least-Squares algorithm for the on line parameter update. This requires a prior knowledge of the structure of the system. However, in some practical applications this structure is unknown and therefore by using a general non-linear regression vector for the local model fitting, a locally adaptive algorithm is also presented. The adaptive methodology not only solves the problem of LEs calculation for time varying and unknown chaotic dynamical systems, but also circumvents the requirement for computations in the reconstructed state space and the problem of large data number for finding the neighbours in the local mapping procedure for LE computation. Finally, to show the effectiveness of the proposed adaptive methodology, it is applied to the well-known Henon and Ikeda chaotic systems, and also the plasma dust-grain system. Simulation results are provided to present the main points of the paper.

Acknowledgements

We would like to thank the DAAD (German Academic Exchange Service) for financial assistance to make this research possible.

References

[1] Ataei, M., Khaki-Sedigh, A., Lohmann, B. and Lucas, C. Determining embedding dimension from output time series of dynamical systems- Scalar and multiple output cases. *Second Int. Conf. on System Identification and Control Problems*, SICPRO 03. January 29 – 31, 2003, P.1004–1013.

[2] Ataei, M., Khaki-Sedigh, A., Lohmann, B. and Lucas, C. Determination of embedding dimension using multiple time series based on singular value decomposition. 4^{th} *Int. Simp. on Math. Modeling.* February 5 – 7, 2003, P.190–196.

[3] Ataei, M., Khaki-Sedigh, A. and Lohmann, B. Estimating the Lyapunov exponents of chaotic time series based on polynomial modelling. *13th IFAC Symp. on System Identification.* 2003, P.174–179.

[4] Atay, F.M. and Yurtsever, E. Phase-space reconstruction in Hamiltonian systems through multiple time series. *Chem. Phys. Let.* **276** (1997) 282–288.

[5] Aulbach, B. and Kreninger, B. On three definitions of chaos. *Nonlinear Dynamics and Systems Theory* **1**(1) (2001) 23–38.

[6] Broomhead, D.S. and King, G.P. Extracting qualitative dynamics from experimental data. *Physica D* **20** (1986) 217–236.

[7] Brown, R., Bryant, P. and Abarbanel, H.D.I. Computing the Lyapunov spectrum of a dynamical system from an observed time series. *Phys. Rev. A* **43**(6) (1991) 2787–2806.

[8] Bryant, P., Brown, R. and Abarbanel, H.D.I. Lyapunov exponents from observed time series. *Phys. Rev. Let.* **65**(13) (1990) 1523–1526.

[9] Chakrabarty, K., Podder, G. and Banerjee, S. Bifurcation behaviour of buck converter. *IEEE Trans. on Power Electronics* **11**(3) (1995) 439–447.

[10] Chen, H.H. Chaotic and non-linear dynamic analysis of a two-axis rate gyro with feedback control mounted on a space vehicle. *J. of Sound and Vibr.* **259**(3) (2003) 541–557.

[11] Darbyshire, A.G. Calculating Liapunov exponents from a time series. *IEE Digest* **13**(5) (1994) 2/1–2/6.

[12] di Bernardo M. and Tse, C.K. *Chaos in Power Electronics: An Overview.* (Eds.: G. Chen and T. Ueta). World Scientific, New York, 2002.

[13] Dieci, L., Russell, R.D. and Van Vleck, E.S. On the computation of Lyapunov exponents from continuous dynamical systems. *SIAM J. Numer. Anal.* **34**(1) (1997) 402–423.

[14] Dieci, L. and Van Vleck, E.S. Computation of few Lyapunov exponents for continous and discrete dynamical systems. *Appl. Numer. Math.* **17** (1995) 275–291.

[15] Eckmann, J.P., Kamphorst, S.O., Ruelle, D. and Ciliberto, S. Liapunov exponents from time series. *Phys. Rev. A* **34**(6) (1986) 4971–4979.

[16] Fradkov, A.L. *Chaos Control Bibliography (1997 – 2000). Russian Systems and Control Archive (RUSYCON)*, www.rusycon.ru/chaos-control.html.

[17] Gallas, J.A., Grebogi, C. and Yorke, J.A. Metrices in parameter space: double crises which destroy chaotic attractors. *Phys. Rev. Lett.* **71**(9) (1993) 1359–1362.

[18] Isermann, R., Lachmann, K.H. and Matko, D. *Adaptive Control Systems.* Prentice Hall, 1992.

[19] Kantz, H. A robust method to estimate the maximum Lyapunov exponent of a time series. *Phys. Lett. A* **185** (1994) 77–87.

[20] Kennel, M.B., Brown, R. and Abarbanel, H.D.I. Determining embedding dimension for phase space reconstruction using a geometrical construction. *Phys. Rev. A* **45**(6) (1992) 3403–3411.

[21] Landau, I.D., Lozano, R. and M'Saad, M. *Adaptive Control*. Springer-Verlag, 1998.

[22] McCaffrey, D.F., Ellner, S., Gallant, A.R. and Nychka, D.W. Estimating the Lyapunov exponent of a chaotic system with nonparametric regression. *J. of the Amer. Statistical Association* **87**(419) (1992) 682–695.

[23] Meehan P.A. and Asokanthan, S.F. Control of chaotic instabilities in a spinning spacecraft with dissipation using Lyapunov's method. *Chaos, Solitons and Fractals* **13** (2002) 1857–1869.

[24] Mees, A.I., Rapp, P.E. and Jenning, L.S. Singular value decomposition and embedding dimension. *Phys. Rev. A* **36**(1) (1987) 340–346.

[25] Oiwa, N.N. and Fiedler-Ferrara, N. A fast algorithm for estimating Lyapunov exponents from time series. *Phys. Lett. A* **246** (1998) 117–121.

[26] Ott, E., Grebogi, C. and Yorke, A. Controlling Chaos. *Phys. Rev. Lett.* **64**(11) (1990) 1196–1199.

[27] Rosenstein, M.T., Collins, J.J. and De Luca, C.J. A practical method for calculating largest exponents from small data set. *Physica D* **65** (1993) 117–134.

[28] Saitou, Y. and Honzawa, T. Chaotic behaviour of charge varying dust grains in plasma. *ICPP and 25th EPS Conf. On Contr. Fusion and Plasma Physics*, ECA(22c), 1998, 2521–2524.

[29] Sano, M. and Sawada, Y. Measurement of the Lyapunov spectrum from a chaotic time series. *Phys. Rev. Let.* **55**(10) (1985) 1082–1085.

[30] Takens, F. Detecting strange attractors in turbulence. *Lecture Notes in Mathematics.* (Eds.: D.A. Rand and L.S. Young). Berlin, Springer, **898**, 1981, P.366–381.

[31] Tse, C.K. Recent development in the study of non-linear phenomena in power electronics circuits. *IEEE Circuits and Systems Soc. Newsletter* **March Issue** (2000) 14–48.

[32] Vincent, T.L. Chaotic control systems. *Nonlinear Dynamics and Systems Theory* **1**(2) (2001) 205–218.

[33] Wolf, A., Swift, J.B., Swinney, H.L. and Vastano, J.A. Determining Lyapunov exponents from a time series. *Physica D* **16** (1985) 285–317.

[34] Zoltowski, M. An adaptive reconstruction of chaotic attractors out of their single trajectories. *Signal Processing* **80** (2000) 1099–1113.

Nonlinear Dynamics and Systems Theory, **4**(2) (2004) 161–194

A Nonlinear Model of Composite Delaminated Beam with Piezoelectric Actuator, with Account of Nonpenetration Constraint for the Delamination Crack Faces

V.Y. Perel and A.N. Palazotto

Department of Aeronautics and Astronautics,
Air Force Institute of Technology, 2950 Hobson Way,
Wright Patterson Air Force Base, Ohio 45433-7765, USA

Received: January 22, 2004; Revised: May 7, 2004

Abstract: In this work, a new approach is developed for dynamic analysis of a composite beam with an inter-ply crack, in which a physically impossible interpenetration of the crack faces is prevented by imposing a special constraint, leading to nonlinearity of the formulated boundary value problem and to taking account of a contact interaction of the crack faces. A variational formulation of the problem and partial differential equations of motion with boundary conditions are developed, and solutions of example problems for a piezo-actuated cantilever beam are presented in a form of series in terms of eigenfunctions of the associated non-self-adjoint eigenvalue problem. A noticeable difference of forced vibrations of the delaminated and undelaminated beams due to the contact interaction of the crack faces is predicted by the developed model.

Keywords: *Composite beam; delamination; nonpenetration constraint for the crack faces; nonlinear dynamics; series solution; modal analysis.*

Mathematics Subject Classification (2000): 74A40, 74F15, 74S99.

1 Introduction

In this work, a new variational formulation and differential equations of motion with boundary conditions for a beam with through-width delamination are developed, in which a constraint is introduced that does not allow opposite faces of the crack to penetrate each other, leading to a nonlinear formulation of the problem and to taking account of contact interaction of the crack faces. An equation, which expresses this constraint, is written with the use of the Heaviside function in one of its analytical forms, and the constraint is imposed by the penalty function method. The longitudinal force resultants in the delaminated parts of the beam are taken into account, which are another source of the nonlinearity.

Besides, a variational formulation and a differential equation of motion with boundary conditions were developed for a beam without delamination and with a piezoelectric patch (actuator) on its upper surface. The two kinds of developed formulations, for the beam with the delamination and for the beam with the actuator, are combined to form a variational formulation and a system of differential equations with boundary conditions for a cantilever beam with the actuator and the delamination.

A solution for a transverse displacement as a function of time for the cantilever beam with the actuator and the delamination crack is found in a form of series of eigenfunctions of the differential eigenvalue problem, associated with the linearized differential equations of motion with boundary conditions. The series solution is found for both linearized and nonlinear formulations. The comparison of the two solutions is presented to emphasize the importance of using the nonlinear formulation to prevent the physically impossible interpenetration of the crack's faces. However, under small amplitudes of vibration, such interpenetration, as predicted by the solution based on the linearized formulation (without account of the nonpenetration constraint), is shown to be small in the example problem for the cantilever beam, excited by the piezoelectric actuator.

The rotary inertia terms in the differential equations of motion are taken into account (to produce more accurate results for frequencies), leading to non-self-adjoint differential operators for the linearized problem in case of clamped-free boundary conditions. The partial differential equations with the non-self-adjoint differential operators are solved by the Ritz method, with the use of the variational formulation of the problem. The solution for the transverse displacement is sought in the form of series of eigenfunctions of these non-self-adjoint differential operators, leading to the series solution of the linearized problem, which satisfies exactly both essential (displacement) and natural (force) boundary conditions, and a series solution of the nonlinearly formulated problem, which satisfies essential boundary conditions exactly and natural boundary conditions approximately.

In the example problems for the beam with the crack, excited by the piezoelectric actuator, with a voltage distributed uniformly along the length of the actuator, the time-dependent concentrated bending moment appears between the zones with the actuator and without the actuator, leading to nonhomogeneous time-dependent boundary condition between these two zones. The difficulty of solving the partial differential equations of motion with the time-dependent boundary condition is resolved by presenting the time-dependent bending moment in terms of the second spacial derivative of the Heaviside function and by including the bending moment into the equations of motion, as a forcing function, rather than into the boundary conditions.

Several types of models of delaminated beams have been proposed in the literature. In some models, for example, [1] and [2], the contact force between the delaminated parts is not taken into account, and the physically impossible mutual penetration of the delaminated parts is allowed. In other models, for example, [3], the delaminated parts are constrained to have the same transverse displacement, excluding the possibility of the delamination crack opening during the vibration. In the reference [4], the interaction between the delaminated parts is modeled with the use of a nonlinear (piecewise-linear) spring between the surfaces of the delaminated parts. Stiffness of the spring depends on the difference of displacements of the lower and upper delaminated parts. If the delamination crack is open, the stiffness of the spring is set equal to zero, making the distributed contact force equal to zero. When the delamination crack is closed, the stiffness of the spring is set either to infinity, or to some finite constant value. The authors set the spring stiffness equal to a constant (either zero, or 0.1, or infinity) before solving the problem, thus assuming that the crack remains either open or closed all the time during the vibration. So, the possibility for the crack to be open in some time intervals and closed in other time intervals during the vibration is not foreseen in this model.

In the paper [5], the contact force between the delaminated sublaminates is introduced as a function of the relative transverse displacement of the sublaminates, in such a way that the contact force automatically turns out to be zero, when the delamination crack is open, and takes on a non-zero value, if the crack is closed. So, this model does not require to specify in advance if the crack is open or closed, and allows for contact and separation of the crack faces during the vibration. However, the physically impossible interpenetration of the crack faces is not always prevented in this model. The interpenetration occurs because a constraint, preventing this phenomenon, is not introduced.

In the model of the delaminated composite beam, presented below, the constraint, preventing the mutual penetration (interpenetration, overlapping) of the delaminated sublaminates (of the crack's faces), is introduced with the use of the Heaviside function and the penalty function method, which is the main novelty of the presented approach to solving dynamic problems for beams with cracks. The longitudinal force resultants in the delaminated sublaminates and rotary inertia terms are taken into account also. The use of the constraint, which prevents the interpenetration of the crack faces, and taking account of the longitudinal force resultants lead to nonlinear partial differential equations of motion. Only thin beams are considered in this work, making it possible to develop a beam theory, based on assumption of negligibly small shear strains.

2 Model of Composite Beam with Delamination

2.1 Assumptions and notations

The x-coordinates of the delamination crack tips are denoted as α and β $(\alpha \le \beta)$, and z-coordinates of both crack tips are denoted as γ (Figure 2.1).

The transverse displacement of this beam is assumed to have the form

$$w(x,z,t) = W_0(x,t) + D_\beta^\alpha(x) H_\gamma(z)[W_1(x,t) - W_0(x,t)], \tag{1}$$

where $D_\beta^\alpha(x)$ is a double-sided unit step-function, defined by the formula

$$D_\beta^\alpha(x) \equiv \begin{cases} 1 & \text{for} \quad \alpha < x < \beta, \\ 0 & \text{for} \quad 0 \le x \le \alpha \quad \text{and} \quad \beta \le x \le L, \end{cases} \tag{2}$$

and $H_\gamma(z)$ is a Heaviside function (unit step-function), defined by the formula

$$H_\gamma(z) \equiv \begin{cases} 0 & \text{for} \quad -h/2 \le z \le \gamma, \\ 1 & \text{for} \quad \gamma < z \le h/2, \end{cases} \tag{3}$$

$W_0(x,t)$ is a transverse displacement at the beam's axis (at $z = 0$), and $W_1(x,t)$ is a transverse displacement of the upper sublaminate in the delaminated region $\alpha < x < \beta$. Equation (1) implies that the transverse displacement $w(x,z,t)$

(i) is equal to W_0 in the undelaminated regions, i.e. in the region $0 \le x \le \alpha$ (where it will be denoted as w_1) and in the region $\beta \le x \le L$ (where it will be denoted as w_4);

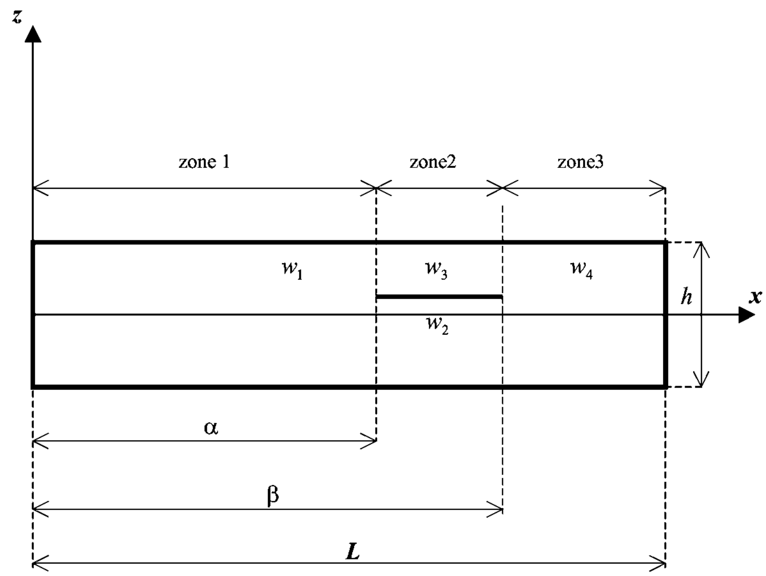

Figure 2.1. Beam with delamination.

α is x-coordinate of the left crack tip; β is x-coordinate of the right crack tip; γ is z-coordinate of the crack (distance from x-axis to crack); w_1 is transverse displacement of zone 1; w_2 is transverse displacement of lower part of zone 2 (under the crack); w_3 is transverse displacement of upper part of zone 2 (above the crack); w_4 is transverse displacement of zone 3.

(ii) is equal to W_0 in the lower sublaminate of the delaminated region (under the crack) i.e. in the region $\alpha < x < \beta$ and $-h/2 \le z \le \gamma$ (where it will be denoted as w_2);

(iii) is equal to W_1 in the upper sublaminate of the delaminated region, i.e. in the region $\alpha < x < \beta$ and $\gamma < z \le h/2$ (where it will be denoted as w_3).

With the use of these notation, equation (1) can be written as follows (Figure 2.1):

$$w(x,z,t) = \begin{cases} w_1(x,t) & \text{in} \quad 0 \le x \le \alpha, \\ w_2(x,t) & \text{in} \quad \alpha < x < \beta \quad \text{and} \quad -h/2 \le z \le \gamma, \\ w_3(x,t) & \text{in} \quad \alpha \le x \le \beta \quad \text{and} \quad \gamma < z \le h/2, \\ w_4(x,t) & \text{in} \quad \beta < x \le L. \end{cases} \tag{4}$$

In the simplest beam theory, based on Euler-Bernoulli assumptions and with no longitudinal displacement at the middle surface $z = 0$, the longitudinal displacement (in the x-direction) can be assumed to have the form

$$u(x,z,t) = -\frac{\partial w}{\partial x} z = -\left[\frac{\partial W_0}{\partial x} + \left(\frac{\partial W_1}{\partial x} - \frac{\partial W_0}{\partial x}\right) DH\right] z. \tag{5}$$

From here on, the functions $D_\beta^\alpha(x)$ and $H_\gamma(z)$ are denoted as D and H, for brevity. Primes will denote differentiation with respect to the x-coordinate, and dots — differentiation with respect to time.

We have the following constraints at locations of the tips of the delamination crack (at $x = \alpha$ and at $x = \beta$):

$$\begin{aligned} &w_1(\alpha) = w_2(\alpha), \quad w_1(\alpha) = w_3(\alpha), \quad w_1'(\alpha) = w_2'(\alpha), \quad w_1'(\alpha) = w_3'(\alpha), \\ &w_4(\beta) = w_2(\beta), \quad w_4(\beta) = w_3(\beta), \quad w_4'(\beta) = w_2'(\beta), \quad w_4'(\beta) = w_3'(\beta). \end{aligned} \tag{6}$$

These constraints allow one to introduce the following notations:

$$\begin{aligned} &w(\alpha) \equiv w_1(\alpha) = w_2(\alpha) = w_3(\alpha), \quad w(\beta) \equiv w_2(\beta) = w_3(\beta) = w_4(\beta), \\ &w'(\alpha) \equiv w_1'(\alpha) = w_2'(\alpha) = w_3'(\alpha), \quad w'(\beta) \equiv w_2'(\beta) = w_3'(\beta) = w_4'(\beta). \end{aligned} \tag{7}$$

The constitutive equation for the stress σ_{xx} in a layer of the composite beam can be taken in the form [6]

$$\sigma_{xx} = \frac{1}{\overline{S}_{11}}\, \varepsilon_{xx}, \tag{8}$$

where

$$\overline{S}_{11} = \frac{1}{E_1}\cos^4\theta + \frac{1}{E_2}\sin^4\theta + \left(\frac{1}{G_{12}} - 2\frac{\nu_{12}}{E_1}\right)\sin^2\theta\cos^2\theta, \tag{9}$$

and θ is an angle between the fiber direction and the x-axis, measured counterclockwise, and E_1, E_2, G_{12} and ν_{12} are engineering elastic constants in the principal material coordinate system.

During the vibration of the delaminated beam, the upper and lower delaminated parts touch each other, and the force of their interaction needs to be taken into account. This force enters into the differential equations of motion as a reaction of constraint, which prevents overlapping of the upper and lower delaminated parts. A constraint of this nature can be expressed by a relationship between w_2 and w_3 (i.e. displacements of the lower and upper delaminated parts) that prevents the difference $w_3 - w_2$ to take on negative values:

$$f(w_2, w_3) \equiv (w_3 - w_2)[1 - H_0(w_3 - w_2)] = 0. \tag{10a}$$

If delaminated sublaminates "attempt" to overlap during the vibration (if $w_3 - w_2 < 0$), or if the crack is closed $(w_3 - w_2 = 0)$, then $H_0(w_3 - w_2) = 0$, and, therefore, due to equation (10a), the difference $w_3 - w_2$ is set equal to zero. If the crack is open $(w_3 - w_2 > 0)$, then $H_0(w_3 - w_2) = 1$, and no constraints are imposed on the difference $w_3 - w_2$. With the use of the analytical representation of the Heaviside function (Appendix A, equation (A-5)), the nonpenetration constraint, expressed by equation (10a), can be written as follows:

$$f(w_2, w_3) \equiv (w_3 - w_2)\left(\frac{1}{2} - \frac{1}{\pi}\arctan\frac{w_3 - w_2}{\epsilon}\right) = 0, \tag{10b}$$

where ϵ is some small number.

2.2 Differential equations of motion for delaminated beam

It is implied that the beam is under external distributed load q (force per unit length), applied on the upper surface of the beam, and the load does not depend on displacements. To derive differential equations of motion with boundary conditions, we use the Hamilton's principle:

$$\delta \int_{t_1}^{t_2} J(t)\, dt = 0, \tag{11}$$

where $J(t)$ is a modified Lagrangian function of the system, in which the nonpenetration constraint $f(w_2, w_3) = 0$, defined by equation (10b), is taken into account with the use of the method of Lagrange multipliers:

$$\begin{aligned} J(t) &= \iiint\limits_{(V)} (\widehat{U} - \widehat{T}) dV - \int_0^L \lambda(x,t) f(w_2, w_3)\, dx - \int_0^L qw\big|_{z=h/2}\, dx \\ &= b\int_0^\alpha \int_{-h/2}^{h/2} (\widehat{U} - \widehat{T})\, dz dx - \int_0^\alpha qw_1\, dx + b\int_\alpha^\beta \int_{-h/2}^{\gamma} (\widehat{U} - \widehat{T})\, dz \\ &\quad + b\int_\alpha^\beta \int_\gamma^{h/2} (\widehat{U} - \widehat{T})\, dz dx - \int_\alpha^\beta qw_3\, dx - \int_\alpha^\beta \lambda(x,t) f(w_2, w_3)\, dx \\ &\quad + b\int_\beta^L \int_{-h/2}^{h/2} (\widehat{U} - \widehat{T})\, dz dx - \int_\beta^L qw_4\, dx. \end{aligned} \tag{12}$$

In equation (12), $\widehat{U}$ is strain energy density, $\widehat{T}$ is kinetic energy density and $\lambda(x,t)$ is the Lagrange multiplier. Expressions for the kinetic energy density and strain energy density in terms of displacements are

$$\widehat{T} = \frac{1}{2}\rho(\dot{u}^2 + \dot{w}^2), \tag{13}$$

$$\widehat{U} = \frac{1}{2}\sigma_{xx}\varepsilon_{xx} = \frac{1}{2}\sigma_{xx}\left[u' + \frac{1}{2}(w')^2\right]. \tag{14}$$

In the last equation, the nonlinear term $\frac{1}{2}(w')^2$ is included in the strain-displacement relation for the strain ε_{xx} to take account of longitudinal force resultants in the delaminated lower and upper sublaminates,

$$N_x^{(2)} = b\int_{-h/2}^{\gamma} \sigma_{xx}^{(2)} dz, \qquad N_x^{(3)} = b\int_{\gamma}^{h/2} \sigma_{xx}^{(3)} dz, \tag{15}$$

which may not be negligibly small even if there are no external longitudinal forces applied to the beam. If external longitudinal forces are not applied to the beam, the term $\frac{1}{2}\sigma_{xx}(w')^2$ need not be included into expression for strain energy density of the zones without delamination, $0 \le x \le \alpha$ and $\beta \le x \le L$. With the use of the assumed displacements (equations (1) and (5)), constitutive equation (8) and notations (4), the kinetic energy and the strain energy can be expressed in terms of the unknown functions $w_1(x,t)$, $w_2(x,t)$, $w_3(x,t)$ and $w_4(x,t)$, leading to the following expression for the Lagrangian function of the system:

$$J(t) = \int_0^\alpha \widetilde{J}_1(x,t)\, dx + \int_\alpha^\beta [\widetilde{J}_2(x,t) + \widetilde{J}_3(x,t)] dx + \int_\beta^L \widetilde{J}_4(x,t)\, dx, \tag{16}$$

where quantities $\widetilde{J}_1$, $\widetilde{J}_2$, $\widetilde{J}_3$ and $\widetilde{J}_4$ are linear densities of the Lagrangian in the corresponding parts of the beam,

$$\widetilde{J}_1(x,t) = \frac{1}{2}\,A_1(w_1'')^2 - \frac{1}{2}\,B_1(\dot{w}_1)^2 - \frac{1}{2}\,C_1(\dot{w}_1')^2 - q_1 w_1, \tag{17}$$

$$\widetilde{J}_2(x,t) = \frac{1}{2}\,A_2(w_2'')^2 - \frac{1}{2}\,B_2(\dot{w}_2)^2 - \frac{1}{2}\,C_2(\dot{w}_2')^2 + \frac{1}{4}\,N_x^{(2)}(w_2')^2 - \lambda(x,t)f(w_2,w_3), \tag{18}$$

$$\widetilde{J}_3(x,t) = \frac{1}{2}\,A_3(w_3'')^2 - \frac{1}{2}\,B_2(\dot{w}_3)^2 - \frac{1}{2}\,C_3(\dot{w}_3')^2 + \frac{1}{4}\,N_x^{(3)}(w_3')^2 - q_3 w_3, \tag{19}$$

$$\widetilde{J}_4(x,t) = \frac{1}{2}\,A_4(w_4'')^2 - \frac{1}{2}\,B_4(\dot{w}_4)^2\frac{1}{2}\,C_4(\dot{w}_4')^2 - q_4 w_4, \tag{20}$$

where q_1, q_3 and q_4 are external loads on the upper surface of the beam, acting on part 1 $(0 \le x \le \alpha)$, part 3 $\left(\alpha \le x \le \beta,\ \gamma < x \le \frac{h}{2}\right)$ and part 4 $(\beta \le x \le L)$ of the beam. Constants A_k, B_k, C_k $(k = 1,2,3,4)$ in equations (17)–(20) are defined as follows:

$$\begin{aligned}
&A_1 = b\int\limits_{-h/2}^{h/2} \frac{1}{\overline{S}_{11}^{(1)}}\,z^2\,dz, &&B_1 = b\int\limits_{-h/2}^{h/2} \rho^{(1)}dz, &&C_1 = b\int\limits_{-h/2}^{h/2} \rho^{(1)}z^2\,dz,\\
&A_2 = b\int\limits_{-h/2}^{\gamma} \frac{1}{\overline{S}_{11}^{(2)}}\,z^2\,dz, &&B_2 = b\int\limits_{-h/2}^{\gamma} \rho^{(2)}dz, &&C_2 = b\int\limits_{-h/2}^{\gamma} \rho^{(2)}z^2\,dz,\\
&A_3 = b\int\limits_{\gamma}^{h/2} \frac{1}{\overline{S}_{11}^{(3)}}\,z^2\,dz, &&B_3 = b\int\limits_{\gamma}^{h/2} \rho^{(3)}dz, &&C_3 = b\int\limits_{\gamma}^{h/2} \rho^{(3)}z^2\,dz,\\
&A_4 = b\int\limits_{-h/2}^{h/2} \frac{1}{\overline{S}_{11}^{(4)}}\,z^2\,dz, &&B_4 = b\int\limits_{-h/2}^{h/2} \rho^{(4)}dz, &&C_4 = b\int\limits_{-h/2}^{h/2} \rho^{(4)}z^2\,dz.
\end{aligned} \tag{21}$$

Upper index k in the notations $\overline{S}_{11}^{(k)}$ and $\rho^{(k)}$ $(k = 1,2,3,4)$ denotes that the material property is associated with the k-th part of the beam. Further we will consider beams for which $\overline{S}_{11}^{(1)} = \overline{S}_{11}^{(2)} = \overline{S}_{11}^{(3)} = \overline{S}_{11}^{(4)}$, $\rho^{(1)} = \rho^{(2)} = \rho^{(3)} = \rho^{(4)}$, and, therefore, $A_1 = A_4$, $B_1 = B_4$ and $C_1 = C_4$. But distinguishing between these last quantities will still be made to keep consistent index notations that allow for brief representation of subsequent equations.

In equations (18) and (19), the longitudinal force resultants are expressed in terms of displacements as follows:

$$N_x^{(2)} = b\int\limits_{-h/2}^{\gamma} \sigma_{xx}^{(2)}\,dz = b\int\limits_{-h/2}^{\gamma} \frac{1}{\overline{S}_{11}^{(2)}(z)}\,\varepsilon_{xx}^{(2)}\,dz = -H_2 w_2'' + \frac{1}{2}Q_2(w_2')^2, \tag{22a}$$

$$N_x^{(3)} = b\int\limits_{\gamma}^{h/2} \sigma_{xx}^{(3)}\,dz = b\int\limits_{\gamma}^{h/2} \frac{1}{\overline{S}_{11}^{(3)}(z)}\,\varepsilon_{xx}^{(3)}\,dz = -H_3 w_3'' + \frac{1}{2}\,Q_3(w_3')^2, \tag{22b}$$

where H_2, Q_2, H_3 and Q_3 are constants, defined as

$$\begin{aligned} H_2 &= b\int_{-h/2}^{\gamma} \frac{1}{\overline{S}_{11}^{(2)}(z)}\, z\,dz, &\qquad Q_2 &= b\int_{-h/2}^{\gamma} \frac{1}{\overline{S}_{11}^{(2)}(z)}\, dz,\\ H_3 &= b\int_{\gamma}^{h/2} \frac{1}{\overline{S}_{11}^{(3)}(z)}\, z\,dz, &\qquad Q_3 &= b\int_{\gamma}^{h/2} \frac{1}{\overline{S}_{11}^{(3)}(z)}\, dz. \end{aligned} \tag{23}$$

From the Hamilton's principle (11) with constraints (7), with account of expressions (16)–(20) and (22), and with the use of standard methods of calculus of variations, one can obtain the following differential equations, equation of constraint and boundary conditions.

Differential equations:

$$A_1 w_1'''' + B_1 \ddot{w}_1 - C_1 \ddot{w}_1'' = q_1 \quad \text{in} \quad 0 \le x \le \alpha, \tag{24}$$

$$\begin{gathered} A_2 w_2'''' + B_2 \ddot{w}_2 - C_2 \ddot{w}_2'' - 3Q_2 (w_2')^2 w_2'' \\ = \lambda(x,t)\left(\frac{1}{\pi}\arctan\frac{w_3 - w_2}{\epsilon} - \frac{1}{2}\right) \quad \text{in} \quad \alpha \le x \le \beta, \quad -h/2 \le z \le \gamma, \end{gathered} \tag{25}$$

$$\begin{gathered} A_3 w_3'''' + B_3 \ddot{w}_3 - C_3 \ddot{w}_3'' - 3Q_3 (w_3')^2 w_3'' \\ = q_3 - \lambda(x,t)\left(\frac{1}{\pi}\arctan\frac{w_3 - w_2}{\epsilon} - \frac{1}{2}\right) \quad \text{in} \quad \alpha \le x \le \beta, \quad \gamma < z \le h/2, \end{gathered} \tag{26}$$

$$A_4 w_4'''' + B_4 \ddot{w}_4 - C_4 \ddot{w}_4'' = q_3 \quad \text{in} \quad \beta \le x \le L. \tag{27}$$

Equation of constraint:

$$(w_3 - w_2)\left(\frac{1}{2} - \frac{1}{\pi}\arctan\frac{w_3 - w_2}{\epsilon}\right) = 0 \tag{28}$$

(equation (28) is the same as equation (10b)).

Boundary conditions:
At $x = 0$:

$$\text{either} \quad A_1 w_1''' - C_1 \ddot{w}_1' = 0 \quad \text{or} \quad w_1 \ \text{is constrained;} \tag{29a}$$

$$\text{either} \quad w_1'' = 0 \quad \text{or} \quad w_1' \ \text{is constrained.} \tag{29b}$$

At $x = \alpha$:

$$\begin{aligned} \text{either} \quad & \left(A_2 w_2''' - C_2 \ddot{w}_2' - Q_2 (w_2')^3\right) + \left(A_3 w_3''' - C_3 \ddot{w}_3' - Q_3 (w_3')^3\right) \\ & - (A_1 w_1''' - C_1 \ddot{w}_1') = 0 \quad \text{or } w \text{ is constrained;} \end{aligned} \tag{30a}$$

$$\begin{aligned} \text{either} \quad & A_1 w_1'' - \left(A_2 w_2'' - \frac{1}{2} H_2 (w_2')^2\right) - \left(A_3 w_3'' - \frac{1}{2} H_3 (w_3')^2\right) = 0 \\ & \text{or } w' \text{ is constrained.} \end{aligned} \tag{30b}$$

At $x = \beta$:

$$\text{either}\quad \left(A_2 w_2''' - C_2 \ddot{w}_2' - Q_2 (w_2')^3\right) + \left(A_3 w_3''' - C_3 \ddot{w}_3' - Q_3 (w_3')^3\right) - \left(A_4 w_4''' - C_4 \ddot{w}_4'\right) = 0 \quad \text{or } w \text{ is constrained;} \tag{31a}$$

$$\text{either}\quad \left(A_2 w_2'' - \frac{1}{2} H_2 (w_2')^2\right) + \left(A_3 w_3'' - \frac{1}{2} H_3 (w_3')^2\right) - A_4 w_4'' = 0 \quad \text{or } w' \text{ is constrained.} \tag{31b}$$

At $x = L$:

$$\text{either}\quad A_4 w_4''' - C_4 \ddot{w}_4' = 0 \quad \text{or } w \text{ is constrained,} \tag{32a}$$

$$\text{either}\quad w_4'' = 0 \quad \text{or } w' \text{ is constrained.} \tag{32b}$$

So, we obtained four differential equations (24) – (27) and one equation of constraint (28) for five unknown functions $w_1(x,t)$, $w_2(x,t)$, $w_3(x,t)$, $w_4(x,t)$ and $\lambda(x,t)$. The total order of these equations is 16. The number of boundary conditions is also 16. These boundary conditions are represented by equations (29) – (32) and (6).

3 Model of Composite Beam with Piezoelectric Actuator and Without Delamination

3.1 Assumptions and notations

In experiments and in structural health monitoring, it is convenient to excite and control vibrations of beams with the use of piezoelectric actuators, attached to them. Modeling such beams requires development of a differential equation of motion with boundary conditions for the beam's segment, covered with the piezoelectric actuator. This is the subject of the present paragraph. For simplicity, it is considered here that such a segment does not contain delaminations.

So, let us consider a *thin beam without delamination and with a piezoelectric layer*, attached to the beam's upper surface (Figure 3.1). In the subsequent text, the superscript (0) will denote quantities associated with the beam's composite layers without piezoelectric properties, and the superscript (p) will denote quantities associated with the piezoelectric patch (actuator). The distributed transverse load (force per unit length) on the surface of the beam, covered with the actuator, will be denoted as q_0.

The transverse and longitudinal displacements will be assumed to have the form of the Euler-Bernoulli theory:

$$w(x,z,t) = w_0(x,t), \tag{33}$$

$$u(x,z,t) = -\frac{\partial w_0(x,t)}{\partial x}\, z. \tag{34}$$

In equation (34), the axial longitudinal displacement $u\big|_{z=0}$ is assumed to be negligibly small, because we consider the case of no longitudinal external forces, applied to the beam, and small amplitudes of vibration. It is assumed that an electric field is applied to

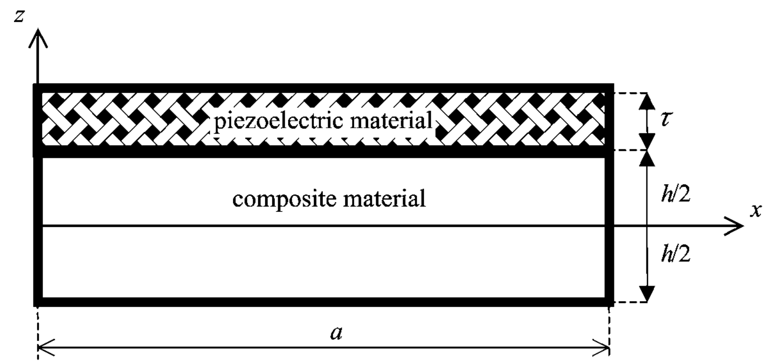

Figure 3.1. Composite beam with a layer of piezoelectric material attached to the upper surface.

the piezoelectric actuator in the direction of the beam's transverse direction, i.e. in the direction of the z-axis. It can be assumed that in a thin piezoelectric actuator, to which the external voltage $V(x,t)$ is applied, the electric potential $\varphi(x,z,t)$ varies linearly in the z-direction, therefore

$$\frac{\partial\varphi}{\partial z} \approx -\frac{V}{\tau}, \tag{35}$$

where τ is a thickness of the piezoelectric actuator. Then, from constitutive equations for the piezoelectric layer of the composite beam, with orthorhombic mm2 symmetry, such as polyvinylidene or lead-zirconate [6], we obtain the following constitutive equation for the stress $\sigma_{xx}^{(p)}$ in the piezoelectric layer

$$\sigma_{xx}^{(p)} = \frac{1}{\overline{S}_{11}^{(p)}}\,\varepsilon_{xx} - \frac{\overline{d}_{31}}{\overline{S}_{11}^{(p)}}\,\frac{V}{\tau}. \tag{36}$$

To derive the equation of motion and boundary conditions for the laminated composite beam with the piezoelectric actuator layer, we will use the virtual work principle for a piezoelectric deformable body [7],

$$\iiint\limits_{(V)} (\sigma_{ij}\delta\varepsilon_{ij} + D_i\delta\varphi_{,i})\,dV = \iiint\limits_{(V)} (\overline{F}_i - \rho\ddot{u}_i)\,\delta u_i + \iint\limits_{(S)} (\overline{t}_k\delta u_k - \overline{Q}\delta\varphi)\,dS, \tag{37}$$

where $\overline{Q}$ is a surface electric charge, $\overline{F}_i$ are components of body forces and $\overline{t}_k$ are components of surface forces. According to the assumption of equation (35), variations of the electric potential φ and the voltage V are related as

$$\delta\varphi = -\frac{\delta V}{\tau}\,z. \tag{38}$$

If the piezoelectric layer is used as the actuator, then the voltage $V(x,t)$, applied to this layer, is a known function of the coordinate x and time, and, therefore its variation δV is equal to zero. Then, according to equation (38), $\delta\varphi$ should be set to zero in the virtual work principle equation (37). So, if the piezoelectric layer is used as the actuator, then the electric field characteristics enter the virtual work principle only through the constitutive equations, and, therefore, equation (37) takes the form

$$\iiint\limits_{(V)} \sigma_{ij}\delta\varepsilon_{ij}\,dV = \iiint\limits_{(V)} (\overline{F}_i - \rho\ddot{u}_i)\,\delta u_i + \iint\limits_{(S)} \overline{t}_k \delta u_k\,dS. \tag{39}$$

Equation (39), applied to the beam with a rectangular cross-section and a piezoelectric layer of thickness τ, attached to the beam's upper surface, has the form

$$b\int\limits_0^a \int\limits_{-h/2}^{h/2+\tau} \sigma_{xx}\delta\varepsilon_{xx}\,dz\,dx = b\int\limits_0^a \int\limits_{-h/2}^{h/2+\tau} [(\overline{F}_x - \rho\ddot{u})\delta u + (\overline{F}_z - \rho\ddot{w}_0)\,\delta w_0]\,dz\,dx + \int\limits_0^a q_0\,\delta w_0\,dx. \tag{40}$$

The body force, acting on the beam, is the gravity force. Therefore,

$$\overline{F}_x = 0, \quad \overline{F}_z = -\rho g, \tag{41}$$

where ρ is mass density, and $g = 9.81\,m/s^2$ is intensity of the gravity field. With account of the constitutive equations (36), equations (41) and strain-displacement relation $\varepsilon_{xx} = u'$ (nonlinear terms are excluded), the virtual work principle (40) can be written in terms of the unknown displacements, material constants and voltage, applied to the piezoelectric actuator:

$$\begin{aligned} &b\int\limits_0^a \int\limits_{-h/2}^{h/2} \frac{1}{\overline{S}_{11}^{(0)}(z)}\,u'\,\delta u'\,dz\,dx + b\int\limits_0^a \int\limits_{h/2}^{h/2+\tau} \frac{1}{\overline{S}_{11}^{(p)}(z)}\left(u' - \overline{d}_{31}\frac{V}{\tau}\right)\delta u'\,dz\,dx \\ &+ b\int\limits_0^a \int\limits_{-h/2}^{h/2} \rho^{(0)}(g+\ddot{w})\,\delta w_0\,dz\,dx + b\int\limits_0^a \int\limits_{h/2}^{h/2+\tau} \rho^{(p)}(g+\ddot{w}_0)\,\delta w_0\,dz\,dx \\ &+ b\int\limits_0^a \int\limits_{-h/2}^{h/2} \rho^{(0)}\ddot{u}\,\delta u\,dz\,dx + b\int\limits_0^a \int\limits_{h/2}^{h/2+\tau} \rho^{(p)}\ddot{u}\,\delta u\,dz\,dx - \int\limits_0^a q_0\,\delta w_0\,dx = 0. \end{aligned} \tag{42}$$

3.2 Differential equation of motion for beam with piezoelectric actuator and without delamination

The virtual work principle (42) in conjunction with the simplifying assumptions (33) and (34), after applying standard methods of variational calculus, leads to the following differential equation of motion and boundary conditions:

$$A_0 w_0'''' + B_0\ddot{w}_0 - C_0\ddot{w}_0'' = q_0 - I_p V'' - B_0 g \quad \text{for} \quad 0 \le x \le a; \tag{43}$$

$$\text{either} \quad A_0 w_0'' + I_p V = 0 \quad \text{or } w_0 \text{ constrained at } x=0 \text{ and } x=a; \tag{44}$$

$$\text{either} \quad A_0 w_0''' - C_0\ddot{w}_0' + I_p V' = 0 \quad \text{or } w_0 \text{ constrained at } x=0 \text{ and } x=a, \tag{45}$$

where

$$A_0 = b\left(\int\limits_{-h/2}^{h/2} \frac{1}{\overline{S}_{11}^{(0)}} z^2\,dz + \int\limits_{h/2}^{h/2+\tau} \frac{1}{\overline{S}_{11}^{(p)}} z^2\,dz\right), \quad I_p = \frac{1}{\tau}\, b \int\limits_{h/2}^{h/2+\tau} \frac{\overline{d}_{31}}{\overline{S}_{11}^{(p)}} z\,dz,$$

$$B_0 = b\left(\int\limits_{-h/2}^{h/2} \rho^{(0)}\,dz + \int\limits_{h/2}^{h/2+\tau} \rho^{(p)}\,dz\right), \quad C_0 = b\left(\int\limits_{-h/2}^{h/2} \rho^{(0)} z^2\,dz \int\limits_{h/2}^{h/2+\tau} \rho^{(p)} z^2\,dz\right). \tag{46}$$

The differential equation (43) and the boundary conditions (44) and (45) imply that the voltage $V(x,t)$, applied to the piezoelectric actuator, produces the bending moment $I_p V(x,t)$ in a cross section of the beam.

If the voltage, applied to the piezoelectric actuator, is distributed uniformly along a region $x_1 \le x \le x_2$, i.e. if

$$V(x,t) = \begin{cases} V(t) & \text{in} \quad x_1 \le x \le x_2, \\ 0 & \text{for all other } x, \end{cases} \tag{47}$$

then this voltage can be presented as

$$V(x,t) = D_{x_2}^{x_1}(x)V(t) = (H_{x_1}(x) - H_{x_2}(x))V(t), \tag{48}$$

and the quantity $I_p V''(x,t)$ in the right side of the differential equation of motion (43), takes the form

$$I_p V''(x,t) = I_p V(t) H''_{x_1}(x) - I_p V(t) H''_{x_2}(x). \tag{49}$$

If a concentrated external bending moment M is applied at a point $x = x_1$ of the beam, then this bending moment can be represented by an equivalent distributed load $MH''_{x_1}(x)$ in the differential equation of motion of the beam [8], where $H''_{x_1}(x)$ is the second derivative with respect to x of the Heaviside function, defined by equation (A–5) in Appendix A. Therefore, equation (49) implies that concentrated bending moments $I_p V(t)$ are applied at points $x = x_1$ and $x = x_2$, if the voltage, applied to the piezoelectric actuator, is distributed uniformly along the region $x_1 \le x \le x_2$. This fact will be used in the next paragraph to substitute the time-dependent bending moment in a boundary condition with the equivalent distributed load, entering into the differential equation of motion, thus allowing for elimination of nonhomogeneous time-dependent boundary condition and simplification of the problem.

4 Forced Vibration of Cantilever Beam with Delamination, under Effect of Voltage, Applied to Piezoelectric Actuator. Solution in the Form of Series in Terms Eigenfunctions. Linear Model

In this paragraph, we study solutions of vibration problems for a cantilever composite beam with the crack between its plies (Figure 4.1), with the nonlinear terms being discarded in the formulation, i.e. the non-penetration constraint and the longitudinal force resultants being not taken into account. Effects of neglecting the nonlinear terms are studied in the paragraph 5, by comparing results of linear and nonlinear analysis. The

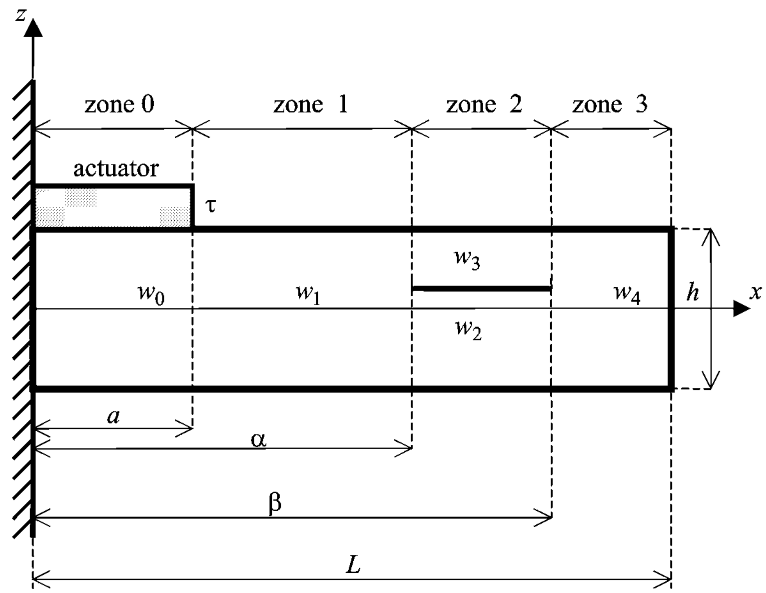

Figure 4.1. Cantilever beam with delamination and piezoelectric actuator.

a is length of the actuator; α is x-coordinate of the left crack tip; β is x-coordinate of the right crack tip; γ is z-coordinate of the crack (distance from x-axis to crack); τ is thickness of the actuator; w_0 is transverse displacement of zone 0; w_1 is transverse displacement of zone 1; w_2 is transverse displacement of lower part of zone 2 (under the crack); w_3 is transverse displacement of upper part of zone 2 (above the crack); w_4 is transverse displacement of zone 3.

voltage, applied to the piezoelectric actuator, is considered to be distributed uniformly along the length of the actuator. The partial differential equations of motion with boundary conditions, derived earlier in the general form, for this particular problem take the form presented below.

4.1 Formulation in terms of partial differential equations with boundary and initial conditions

Motion of the beam is described by the following system of five *partial differential equations*

$$A_0 w_0'''' + B_0 \ddot{w}_0 - C_0 \ddot{w}_0'' = I_p V(t) H_a''(x), \tag{50}$$

$$A_k w_k'''' + B_k \ddot{w}_k - C_k \ddot{w}_k'' = 0, \quad k = 1,2,3,4 \quad \text{(no summation with respect to } k). \tag{51}$$

The function $V(t)$ in equation (50) is the voltage, applied to the piezoelectric actuator and distributed uniformly along the region $0 \le x < a$, which does not include the point $x = a$:

$$V(x,t) = V(t) \quad \text{in} \quad 0 \le x < a.$$

The exclusion of the point $x = a$ from the region, where the voltage is applied, does not change the physics of the problem and allows to avoid having non-homogeneous time-dependent boundary condition at $x = a,$ as in equation (44). The differential equation of motion (43) and the boundary condition (44) imply that the voltage $V(x,t)$, applied to the piezoelectric actuator, produces the bending moment $I_p V(x,t)$. If $V(x,t) = V(t)$ over an interval $0 \le x \le (a - \epsilon),$ where ϵ is some very small number, and if the beam's end $x = 0$ is clamped, then the external concentrated bending moment $I_p V(t)$ is applied at the point $x = a - \epsilon,$ and this is taken into account by the term $I_p V(t) H_a''(x)$ in the right-hand side of the equation (50). The same result can be obtained from equation (43) directly. Indeed, the voltage $V(x,t) = V(t)$ in the interval $0 \le x < a$ can be written as

$$V(x,t) = V(t)(1 - H_a(x)).$$

Substitution of this expression into the expression $I_p V''(x,t)$ in the right side of equation (43) produces the result $I_p V(t) H_a''(x),$ i.e. the forcing function in the right side of equation (50).

The constants, entering into the differential equations (50) and (51), are defined by formulas (46) and (21).

Boundary conditions for the partial differential equations (50) and (51) are the following (see equations (29)–(32), (44) and (45)):

displacement boundary conditions:

$$\begin{gathered}
w_0(0) = 0, \qquad w_0'(0) = 0, \\
w_0(a) - w_1(a) = 0, \qquad w_0'(a) - w_1'(a) = 0, \\
w_1(\alpha) - w_2(\alpha) = 0, \qquad w_1'(\alpha) - w_2'(\alpha) = 0, \qquad w_2(\alpha) - w_3(\alpha) = 0, \\
w_2'(\alpha) - w_3'(\alpha) = 0, \qquad w_2(\beta) - w_4(\beta) = 0, \qquad w_2'(\beta) - w_4'(\beta) = 0, \\
w_2(\beta) - w_3(\beta) = 0, \qquad w_2'(\beta) - w_3'(\beta) = 0,
\end{gathered} \tag{52}$$

force boundary conditions:

$$\begin{gathered}
A_0 w_0''(a) - A_1 w_1''(a) = 0, \\
A_0 w_0'''(a) - C_0 \ddot{w}_0'(a) - [A_1 w_1'''(a) - C_1 \ddot{w}_1'(a)] = 0, \\
A_1 w_1''(\alpha) - A_2 w_2''(\alpha) - A_3 w_3''(\alpha) = 0, \\
[A_1 w_1'''(\alpha) - C_1 \ddot{w}_1'(\alpha)] - [A_2 w_2'''(\alpha) - C_2 \ddot{w}_2'(\alpha)] - [A_3 w_3'''(\alpha) - C_3 \ddot{w}_3'(\alpha)] = 0, \\
A_2 w_2''(\beta) + A_3 w_3''(\beta) - A_4 w_4''(\beta) = 0, \\
[A_2 w_2'''(\beta) - C_2 \ddot{w}_2'(\beta)] + [A_3 w_3'''(\beta) - C_3 \ddot{w}_3'(\beta)] - [A_4 w_4'''(\beta) - C_4 \ddot{w}_4'(\beta)] = 0, \\
A_4 w_4''(L) = 0, \\
A_4 w_4'''(L) - C_4 \ddot{w}_4'(L) = 0.
\end{gathered} \tag{53}$$

So, this problem is formulated in terms of five partial differential equations (50) and (51) and twenty boundary conditions (52) and (53). Each of the five partial differential equations is of the fourth order. So, the total order of the differential equations (twenty) is equal to the number of the boundary conditions.

Initial conditions for this problem are assumed to be

$$\begin{aligned} &w_0(0) = w_1(0) = w_2(0) = w_3(0) = w_4(0) = 0, \\ &\dot{w}_0(0) = \dot{w}_1(0) = \dot{w}_2(0) = \dot{w}_3(0) = \dot{w}_4(0) = 0. \end{aligned} \tag{54}$$

4.2 Variational formulation of the problem

The partial differential equations (50) and (51) with boundary conditions (52) and (53) are equivalent to the condition of extremum of the functional

$$\begin{aligned} J = \frac{1}{2}\int_{t_1}^{t_2}\int_0^a \big[A_0(w_0'')^2 - B_0\dot{w}_0^2 - C_0(\dot{w}_0')^2 - 2I_pV(t)H_a''(x)w_0\big]\,dx\,dt \\ + \frac{1}{2}\int_{t_1}^{t_2}\int_a^\alpha \big[A_1(w_1'')^2 - B_1\dot{w}_1^2 - C_1(\dot{w}_1')^2\big]\,dx\,dt \\ + \frac{1}{2}\int_{t_1}^{t_2}\int_\alpha^\beta \big[A_2(w_2'')^2 - B_2\dot{w}_2^2 - C_2(\dot{w}_2')^2 + A_3(w_3'')^2 - B_3\dot{w}_3^2 - C_3(\dot{w}_3')^2\big]\,dx\,dt \\ + \frac{1}{2}\int_{t_1}^{t_2}\int_\beta^L \big[A_4(w_4'')^2 - B_4\dot{w}_4^2 - C_4(\dot{w}_4')^2\big]\,dx\,dt \end{aligned} \tag{55}$$

with subsidiary conditions being the displacement boundary conditions (52).

With the use of standard methods of the calculus of variations, the partial differential equations (50) and (51) and natural (force) boundary conditions (53) follow from the condition of extremum of the functional J,

$$\delta J = 0, \tag{56}$$

with account of essential (displacement) boundary conditions (52). The same initial conditions (54) apply for the variational formulation.

4.3 Eigenvalue problem, associated with the partial differential equations and boundary conditions

To formulate the eigenvalue problem, we set the right side of equation (50) to zero and separate the variables:

$$w_k(x,t) = X_k(x)T(t) \quad (k = 0,1,2,3,4). \tag{57}$$

In the notation $X_k(x)$, the subscript k is a number of the beam's part, with which the function $X_k(x)$ are associated. A number of the eigenfunction, associated with a frequency ω_n, will be denoted by the second subscript n:

$$\omega_n \to X_{kn} \quad (k = 0,1,2,3,4; \quad n = 1,2,\dots). \tag{58}$$

The separation of the variables leads to equations

$$\ddot{T}(t) + \omega^2 T(t) = 0, \tag{59}$$

$$A_k \frac{d^4 X_k}{dx^4} + \omega^2 C_k \frac{d^2 X_k}{dx^2} = \omega^2 B_k X_k \qquad (k = 0, 1, 2, 3, 4), \tag{60}$$

where ω is a circular frequency (so far, the notation for frequency does not have an index).

General solution of the ordinary differential equations (60) has the form:

$$X_0(x) = a_1 \sin \mu_0 x + a_2 \cos \mu_0 x + a_3 \sinh \eta_0 x + a_4 \cosh \eta_0 x, \tag{61a}$$

$$X_1(x) = a_5 \sin \mu_1 x + a_6 \cos \mu_1 x + a_7 \sinh \eta_1 x + a_8 \cosh \eta_1 x, \tag{61b}$$

$$X_2(x) = a_9 \sin \mu_2 x + a_{10} \cos \mu_2 x + a_{11} \sinh \eta_2 x + a_{12} \cosh \eta_2 x, \tag{61c}$$

$$X_3(x) = a_{13} \sin \mu_3 x + a_{14} \cos \mu_3 x + a_{15} \sinh \eta_3 x + a_{16} \cosh \eta_3 x, \tag{61d}$$

$$X_4(x) = a_{17} \sin \mu_4 x + a_{18} \cos \mu_4 x + a_{19} \sinh \eta_4 x + a_{20} \cosh \eta_4 x, \tag{61e}$$

where

$$\mu_k = \sqrt{\frac{\omega}{2A_k}\Big(\omega C_k + \sqrt{\omega^2 C_k^2 + 4A_k B_k}\Big)}, \tag{62a}$$

$$\eta_k = \sqrt{\frac{\omega}{2A_k}\Big(-\omega C_k + \sqrt{\omega^2 C_k^2 + 4A_k B_k}\Big)} \qquad (k = 0, 1, 2, 3, 4). \tag{62b}$$

When equations (57), with account of equations (61), are substituted into the boundary conditions (52) and (53), one obtains a system of linear homogeneous algebraic equations, which can be written in the matrix form as

$$[D]_{(20\times 20)}\{a\}_{(20\times 1)} = \{0\}_{(20\times 1)}, \tag{63}$$

where the column-matrix $\{a\}$ consists of the coefficients $a_1, a_2, \ldots, a_{20}$ of the expressions (61), and components of the matrix $[D]$ depend on the unknown frequencies ω. Expressions for components of the matrix $[D]$ are written explicitly in reference [9]. Approximate values of frequencies $\omega \equiv \omega_n$ are computed numerically from equation

$$\det[D]_{(20\times 20)} = 0. \tag{64}$$

with the use of the bisection method. More accurate values of frequencies and the associated column-matrices $\{a\}_n$ of the dimensions (20×1) are computed by solving a nonlinear eigenvalue problem (63) by an iterative method described below, with initial approximations for the frequencies being the frequencies, computed from equation (64), by the bisection method.

4.4 Iterative solution of nonlinear eigenvalue problem

Let us consider a nonlinear eigenvalue problem of the type, represented by equations (63):

$$\mathbf{D}(\omega)\,\mathbf{a} = \mathbf{0}. \tag{65}$$

Let $\omega_n^{(0)}, \omega_n^{(1)}, \omega_n^{(2)}, \dots$ denote successive approximations of a frequency ω_n, which is one of the solutions of the nonlinear eigenvalue problem (65), the zeroth approximation, $\omega_n^{(0)}$, being an approximate value of the frequency ω_n, obtained by some other method. In the following presentation of the iterative procedure, the lower index, denoting a number of a frequency, will be omitted for simplicity of notation. Besides, let

$$\epsilon^{(k+1)} \equiv \omega^{(k+1)} - \omega^{(k)} \tag{66}$$

be a difference between successive approximations of the frequency ω. Then

$$\omega^{(k+1)} = \omega^{(k)} + \epsilon^{(k+1)}. \tag{67}$$

Assuming that the approximation with number $k+1$, i.e. $\omega^{(k+1)}$, satisfies equation (65) approximately, one can write

$$\mathbf{D}\big(\omega^{(k+1)}\big)\,\mathbf{a}^{(k+1)} \approx \mathbf{0}, \tag{68}$$

where $\mathbf{a}^{(k+1)}$ is an approximation with number $(k+1)$ of an eigenvector $\mathbf{a}$. With the use of the Taylor series expansion with two terms, we obtain

$$\mathbf{D}\big(\omega^{(k+1)}\big) \approx \mathbf{D}\big(\omega^{(k)} + \epsilon^{(k+1)}\big) \approx \mathbf{D}\big(\omega^{(k)}\big) - \epsilon^{(k+1)}\mathbf{B}\big(\omega^{(k)}\big), \tag{69}$$

where

$$\mathbf{B}(\omega) \equiv -\frac{d\mathbf{D}}{d\omega}\,. \tag{70}$$

Substitution of equation (69) into equation (68) yields

$$\big(\mathbf{D}\big(\omega^{(k)}\big) - \epsilon^{(k+1)}\mathbf{B}\big(\omega^{(k)}\big)\big)\mathbf{a}^{(k+1)} = \mathbf{0}, \tag{71}$$

which is an algebraic linear eigenvalue problem for computation of quantities $\epsilon^{(k+1)}$ as eigenvalues and vectors $\mathbf{a}^{(k+1)}$ as eigenvectors. In order for the Taylor series expansion in equation (69) to be as accurate as possible, the eigenvalue $\epsilon^{(k+1)}$ with the smallest absolute value should be chosen. The corresponding eigenvector $\mathbf{a}^{(k+1)}$ of the linear eigenvalue problem (71) is an approximation with number $(k+1)$ of the eigenvector $\mathbf{a}$ of the nonlinear eigenvalue problem (65). The updated $(k+1)$-st approximation for the frequency ω is computed by the formula (67). The iteration process continues until $\epsilon^{(k+1)} \equiv \omega^{(k+1)} - \omega^{(k)}$ becomes smaller than some chosen small number.

4.5 Forced vibration of delaminated beam with actuator (linear model)

The forced response is sought in the form

$$w_k(x,t) = \sum_{n=1}^{N} X_{kn}(x)\Theta_n(t) \quad (k = 0,1,2,3,4), \tag{72}$$

where X_{kn} are eigenfunctions (61), the subscript k denotes a number of a zone, and the subscript n denotes a number of an eigenfunction, corresponding to the frequency ω_n. Due to the fact that the shape functions in the series (72) are chosen to be the eigenfunctions $X_{kn}(x)$ of the differential operators of the problem, the series (72) satisfies not only essential (displacement) boundary conditions (52), as it is required by the Ritz method, but also the natural (force) boundary conditions (53). Therefore, the series (72) converges to the exact solution, if the unknown functions $\Theta(t)$ are computed from the condition of extremum of the functional J, defined by equation (55).

Substitution of equations (72) into the expression (55) for the functional J leads to the following result:

$$J = \int_{t_1}^{t_2} \mathcal{L}(\Theta_1(t), \ldots, \Theta_N(t);\ \dot{\Theta}_1(t), \ldots, \dot{\Theta}_N(t))\, dt, \tag{73}$$

where

$$\begin{aligned} \mathcal{L}(\Theta_1(t), \ldots, \Theta_N(t);\ \dot{\Theta}_1(t), \ldots, \dot{\Theta}_N(t)) &= \frac{1}{2}\sum_{i,j=1}^{N} K_{ij}\Theta_i(t)\Theta_j(t) \\ &- \frac{1}{2}\sum_{i,j=1}^{N} M_{ij}\dot{\Theta}_i(t)\dot{\Theta}_j(t) - \sum_{i=1}^{N} F_i(t)\Theta_i(t), \end{aligned} \tag{74}$$

and

$$\begin{aligned} K_{ij} = A_0 \int_0^a X''_{0i}X''_{0j}\,dx + A_1 \int_a^\alpha X''_{1i}X''_{1j}\,dx + A_2 \int_\alpha^\beta X''_{2i}X''_{2j}\,dx \\ + A_3 \int_\alpha^\beta X''_{3i}X''_{3j}\,dx + A_4 \int_\beta^L X''_{4i}X''_{4j}\,dx, \end{aligned} \tag{75}$$

$$\begin{aligned} M_{ij} = B_0 \int_0^a X_{0i}X_{0j}\,dx + B_1 \int_a^\alpha X_{1i}X_{1j}\,dx + B_2 \int_\alpha^\beta X_{2i}X_{2j}\,dx \\ + B_3 \int_\alpha^\beta X_{3i}X_{3j}\,dx + B_4 \int_\beta^L X_{4i}X_{4j}\,dx + C_0 \int_0^a X'_{0i}X'_{0j}\,dx \\ + C_1 \int_a^\alpha X'_{1i}X'_{1j}\,dx + C_2 \int_\alpha^\beta X'_{2i}X'_{2j}\,dx + C_3 \int_\alpha^\beta X'_{3i}X'_{3j}\,dx + C_4 \int_\beta^L X'_{4i}X'_{4j}\,dx, \end{aligned} \tag{76}$$

$$F_i(t) = -I_p X'_{0i}(a)V(t). \tag{77}$$

The necessary condition of extremum of the functional $J = \int_{t_1}^{t_2} \mathcal{L}\,dt$ (equation 73),

$$\frac{\partial\mathcal{L}}{\partial\Theta_i} - \frac{d}{dt}\frac{\partial\mathcal{L}}{\partial\dot{\Theta}_i} = 0, \tag{78}$$

produces the following system of ordinary differential equations

$$\sum_{j=1}^{N} M_{ij}\ddot{\Theta}_j(t) + \sum_{j=1}^{N} K_{ij}\Theta_j(t) = F_i(t), \tag{79}$$

or, in matrix form,

$$[M]_{(N\times N)}\{\ddot{\Theta}\}_{(N\times 1)} + [K]_{(N\times N)}\{\Theta\}_{(N\times 1)} = \{F\}_{(N\times 1)}. \tag{80}$$

Matrices $[K]$ and $[M]$ in equation (80) are symmetric, as follows from equations (75) and (76).

Example 4.1 As an example problem, we considered a clamped-free wooden beam with the following characteristics (Figure 4.1): length $L = 20 \times 10^{-2}\, m$, width $b = 2.76 \times 10^{-2}\, m$, thickness $h = 0.99 \times 10^{-2}\, m$, wood density $\rho^{(0)} = 418.02\, \dfrac{kg}{m^3}$, Young's modulus of the wood in the direction of fibers $E_1^{(0)} = 1.0897 \times 10^{10}\, \dfrac{N}{m^2}$. The piezoelectric actuator is QP10W (Active Control Experts). Thickness of the actuator is $\tau = 3.81 \times 10^{-4}\, m$, its length is $a = 5.08 \times 10^{-2}\, m$, the piezoelectric constant in the range of applied voltage (from $0\, V$ to $200\, V$) is $\overline{d}_{31} \approx -1.05 \times 10^{-9}\, \dfrac{m}{V}$, the Young's modulus of the actuator with its packaging is

$$E_1^{(p)} = 2.57 \times 10^{10}\, \frac{N}{m^2},$$

mass density of the actuator with its packaging is

$$\rho^{(p)} = 6151.1\, \frac{kg}{m^3}.$$

The voltage $V(t)$, applied to the piezoelectric actuator, is distributed uniformly along the length of the actuator and varies with time as

$$V(t) = V_a \sin(\Omega t + \phi_0), \tag{81a}$$

where

$$V_a = 200\, V, \quad \Omega = 600\, \frac{1}{s}, \quad \phi_0 = 0. \tag{81b}$$

The wooden beam is cut along its fibers, so that the angle θ in the formula (9) is equal to zero, and, therefore, the elastic compliance coefficient $\overline{S}_{11}$ for the wood is equal to

$$\overline{S}_{11}^{(0)} = \frac{1}{E_1^{(0)}} = 9.1768 \times 10^{-11}\, \frac{m^2}{N}.$$

For the piezoelectric actuator, the material coordinate system coincides with the problem coordinate system, so that the elastic compliance coefficient $\overline{S}_{11}$ for the material of the piezo-actuator is

$$\overline{S}_{11}^{(p)} = \frac{1}{E_1^{(p)}} = 3.8911 \times 10^{-11}\, \frac{m^2}{N}.$$

Results of calculation of circular frequencies for the **undelaminated** beam **with the actuator** are presented in the table below.

	ω_1	ω_2	ω_3	ω_4	ω_5	ω_6	ω_7
without rotary inertia	1398.17	8249.5	22180.	42844.6	71127.6	1.06542×10^5	1.48245×10^5
with rotary inertia	1397.435	8217.9	21985.6	42205.0	69331	1.02371×10^5	1.40641×10^5

Now, let us consider frequencies of the same beam **with the delamination and with the actuator**.

In the next table, the results are presented for the coordinates of the crack tips $\alpha = 10 \times 10^{-2}\, m,\ \beta = 11 \times 10^{-2}\, m,\ \gamma = 1.65 \times 10^{-3}\, m$.

	ω_1	ω_2	ω_3	ω_4	ω_5	ω_6	ω_7
with rotary inertia	1397.433	8217.909	21986.1	42204.9	69331.2	1.02371×10^5	1.40641×10^5

In the next table the results are presented for the coordinates of the crack tips $\alpha = 10 \times 10^{-2}\, m,\ \beta = 12 \times 10^{-2}\, m,\ \gamma = 1.65 \times 10^{-3}\, m$.

	ω_1	ω_2	ω_3	ω_4	ω_5	ω_6	ω_7
with rotary inertia	1397.433	8217.90	21986.0	42200	69330	1.02368×10^5	1.40625×10^5

In the next table the results are presented for the coordinates of the crack tips $\alpha = 10 \times 10^{-2}\, m,\ \beta = 15 \times 10^{-2}\, m,\ \gamma = 1.65 \times 10^{-3}\, m$.

	ω_1	ω_2	ω_3	ω_4	ω_5	ω_6	ω_7
with rotary inertia	1397.432	8217.62	21980.	42198	69094	1.01932×10^5	1.33019×10^5

Next, we will compare frequencies of the same cantilever beam **without the actuator**, obtained by different methods.

No delamination, no actuator:

	ω_1	ω_2	ω_3	ω_4	ω_5	ω_6	ω_7
without rotary inertia	1282.6	8037.9	22506.	44103.	72906.	1.08909×10^5	1.52113×10^5
with rotary inertia	1282.	8011.5	22330.9	43474.	71265.6	1.05385×10^5	1.51609×10^5

In the last table, the frequencies without account of rotary inertia were computed by a formula [10]

$$\omega_n = c_n^2 \frac{h}{L^2} \sqrt{\frac{E_1^{(0)}}{12\rho^{(0)}}},$$

where c_n are solutions of equation

$$\cos c_n \cosh c_n + 1 = 0.$$

With delamination, no actuator:

$$\alpha = 10 \times 10^{-2}\, m, \quad \beta = 11 \times 10^{-2}\, m, \quad \gamma = 1.65 \times 10^{-3}\, m$$

	ω_1	ω_2	ω_3	ω_4	ω_5	ω_6	ω_7
with rotary inertia	1282.0	8011.5	22330.9	43473.9	71265.6	1.05385×10^5	1.45467×10^5

$$\alpha = 10 \times 10^{-2}\, m, \quad \beta = 15 \times 10^{-2}\, m, \quad \gamma = 1.65 \times 10^{-3}\, m$$

	ω_1	ω_2	ω_3	ω_4	ω_5	ω_6	ω_7
with rotary inertia	1282.0	8011.2	22325.5	43468.0	70999.6	1.04969×10^5	1.33239×10^5

So, with the increase of the crack length, the frequencies decrease. This effect is more pronounced for higher frequencies.

4.6 Comparison of transverse displacements of cantilever beams with and without delamination at their free edges (linear analysis)

Plots of the transverse displacement as a function of time at the free end of the cantilever beam with delamination and of the same beam without delamination are presented in Figures 4.2a and 4.2b. The properties of the beams are the same as in the previous example problems (Figure 4.1 and the previous section of the text), coordinates of the crack tips are $\alpha = 10 \times 10^{-2}\, m$, $\beta = 15 \times 10^{-2}\, m$, $\gamma = 1.65 \times 10^{-3}\, m$. The beams are excited by the voltage, applied to the piezoelectric actuator. The difference in dynamic responses of the beams with and without delamination is not noticeable on the graphs, but this difference can be seen in the numerical data, used to plot the graph. This numerical data is presented below.

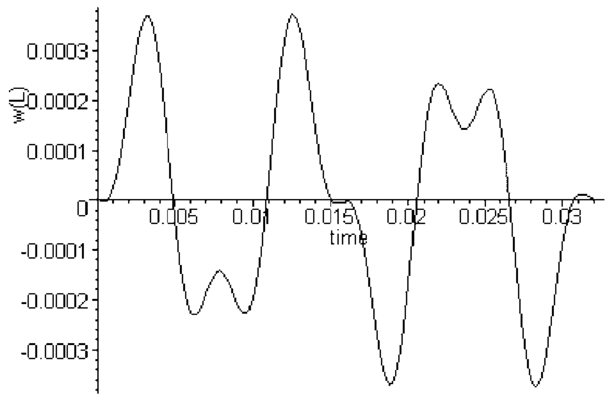

Figure 4.2a. Transverse displacement of free end of **delaminated** cantilever beam, excited by piezoelectric actuator. Beam length is $L = 0.2m$, x-coordinates of the crack tips are $\alpha = 0.1m$ and $\beta = 0.15m$, z-coordinate of the crack tips is $\gamma = 0.00165m$. **Linear analysis.**

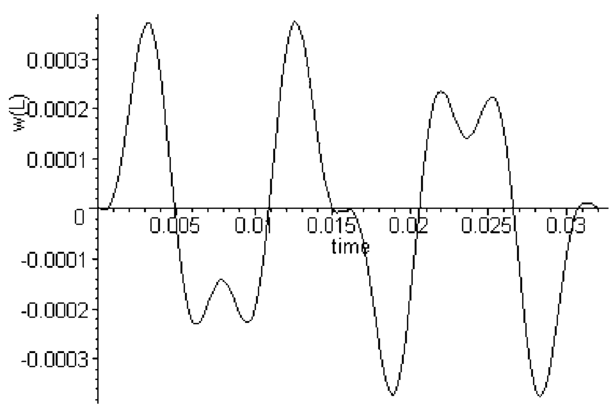

Figure 4.2b. Transverse displacement of free end of cantilever beam **without delamination**. Beam length is $L = 0.2m$. **Linear analysis.**

Displacement $w(0.2,\, t) = w(t)\big|_{x=0.2}$ **for beams with delamination and without delamination** (time is measured in seconds)

	with delamination	without delamination
$\omega(0.2, 0) =$	0	0
$\omega(0.2, 0.001) =$	4.089×10^{-5}	$4.088\,1 \times 10^{-5}$
$\omega(0.2, 0.002) =$	$2.268\,1 \times 10^{-4}$	$2.267\,8 \times 10^{-4}$
$\omega(0.2, 0.003) =$	$3.884\,6 \times 10^{-4}$	$3.884\,8 \times 10^{-4}$
$\omega(0.2, 0.004) =$	$2.740\,8 \times 10^{-4}$	$2.741\,9 \times 10^{-4}$
$\omega(0.2, 0.005) =$	$-3.944\,8 \times 10^{-5}$	-3.937×10^{-5}
$\omega(0.2, 0.006) =$	$-2.345\,3 \times 10^{-4}$	$-2.346\,5 \times 10^{-4}$
$\omega(0.2, 0.007) =$	$-2.081\,7 \times 10^{-4}$	$-2.083\,5 \times 10^{-4}$
$\omega(0.2, 0.008) =$	$-1.656\,2 \times 10^{-4}$	$-1.655\,8 \times 10^{-4}$
$\omega(0.2, 0.009) =$	$-2.242\,2 \times 10^{-4}$	$-2.240\,2 \times 10^{-4}$
$\omega(0.2, 0.010) =$	$-2.028\,5 \times 10^{-4}$	$-2.028\,5 \times 10^{-4}$
$\omega(0.2, 0.011) =$	$4.897\,5 \times 10^{-5}$	$4.871\,8 \times 10^{-5}$
$\omega(0.2, 0.012) =$	3.3710×10^{-4}	$3.370\,1 \times 10^{-4}$
$\omega(0.2, 0.013) =$	$3.663\,1 \times 10^{-4}$	$3.666\,1 \times 10^{-4}$
$\omega(0.2, 0.014) =$	$1.654\,4 \times 10^{-4}$	$1.657\,1 \times 10^{-4}$
$\omega(0.2, 0.015) =$	$1.269\,5 \times 10^{-5}$	$1.248\,9 \times 10^{-5}$
$\omega(0.2, 0.016) =$	$-5.818\,4 \times 10^{-6}$	$-6.182\,6 \times 10^{-6}$
$\omega(0.2, 0.017) =$	-8.037×10^{-5}	-8.028×10^{-5}
$\omega(0.2, 0.018) =$	$-2.855\,5 \times 10^{-4}$	$-2.851\,4 \times 10^{-4}$
$\omega(0.2, 0.020) =$	$-1.945\,2 \times 10^{-4}$	$-1.950\,2 \times 10^{-4}$

4.7 Crack opening, crack closure and interpenetration of crack faces in linear analysis

For $\alpha = 10 \times 10^{-2}\, m$, $\beta = 15 \times 10^{-2}\, m$, $\gamma = 1.65 \times 10^{-3}\, m$ at $x = 12.5 \times 10^{-2}\, m$ (at the middle of the crack's span), the difference of displacements of the upper and lower delaminated parts, $w_3(0.125, t) = w_3(t)\big|_{x=0.125}$ and $w_2(0.125, t) = w_2(t)\big|_{x=0.125}$, depends on time as shown in Figure 4.3a.

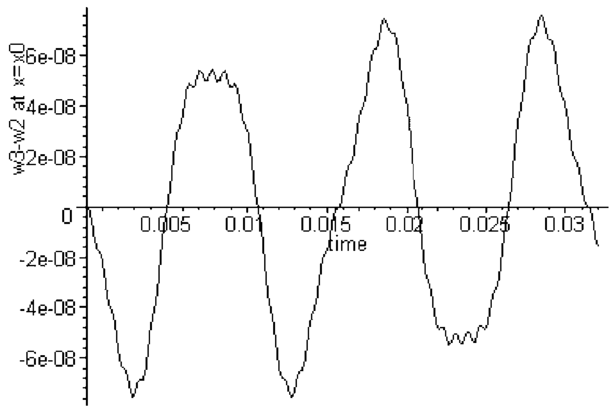

Figure 4.3a. Difference of transverse displacement of the upper and lower delaminated parts, at the middle of the crack's length, versus time, if the anti-overlapping constraint and the longitudinal force resultants are not taken into account. **Linear analysis.**

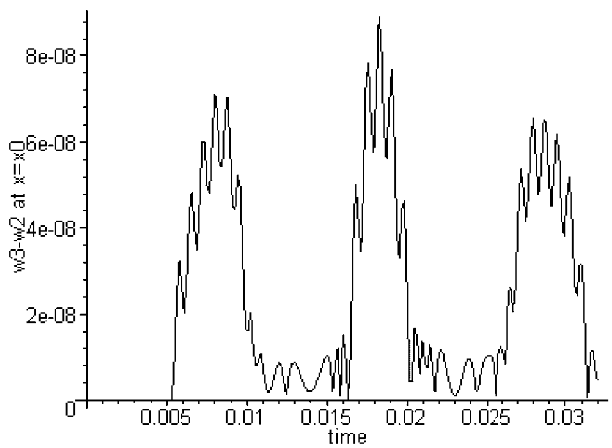

Figure 4.3b. Difference of transverse displacement of the upper and lower delaminated parts, at the middle of the crack's length, versus time, if the anti-overlapping constraint and the longitudinal force resultants are taken into account. **Linear analysis.**

Some of the numerical data, used for plotting this graph, is shown below:

$$w_3(0.125, 0) = w_2(0.125, 0) = 0;$$

$$\left.\begin{aligned} w_3(0.125, 0.001) = 1.9560 \times 10^{-5} \\ w_2(0.125, 0.001) = 1.9564 \times 10^{-5} \end{aligned}\right\} \to \text{overlapping;}$$

$$\left.\begin{aligned} w_3(0.125, 0.003) &= 1.8582 \times 10^{-4} \\ w_2(0.125, 0.003) &= 1.858,6 \times 10^{-4} \end{aligned}\right\} \rightarrow \text{overlapping;}$$

$$\left.\begin{aligned} w_3(0.125, 0.005) &= -1.8870 \times 10^{-5} \\ w_2(0.125, 0.005) &= -1.8874 \times 10^{-5} \end{aligned}\right\} \rightarrow \text{crack is open;}$$

$$\left.\begin{aligned} w_3(0.125, 0.007) &= -9.9578 \times 10^{-5} \\ w_2(0.125, 0.007) &= -9.9599 \times 10^{-5} \end{aligned}\right\} \rightarrow \text{crack is open;}$$

$$\left.\begin{aligned} w_3(0.125, 0.009) &= -1.0726 \times 10^{-4} \\ w_2(0.125, 0.009) &= -1.0728 \times 10^{-4} \end{aligned}\right\} \rightarrow \text{crack is open;}$$

$$\left.\begin{aligned} w_3(0.125, 0.011) &= 2.3427 \times 10^{-5} \\ w_2(0.125, 0.011) &= 2.3432 \times 10^{-5} \end{aligned}\right\} \rightarrow \text{overlapping;}$$

$$\left.\begin{aligned} w_3(0.125, 0.013) &= 1.7522 \times 10^{-4} \\ w_2(0.125, 0.013) &= 1.7526 \times 10^{-4} \end{aligned}\right\} \rightarrow \text{overlapping;}$$

$$\left.\begin{aligned} w_3(0.125, 0.015) &= 6.0726 \times 10^{-6} \\ w_2(0.125, 0.015) &= 6.0738 \times 10^{-6} \end{aligned}\right\} \rightarrow \text{overlapping;}$$

So, in the dynamic response of the delaminated beam, computed from the linearly formulated problem, the overlapping of the upper and lower delaminated parts is present, which, of course, is physically impossible. However, the relative difference of displacements of the crack faces in the example problem is small, less than 0.01% of the transverse displacement.

5 Forced Vibration of Cantilever Beam with Delamination, under Effect of Voltage, Applied to Piezoelectric Actuator. Solution in the Form of Series in Terms of Eigenfunctions. Nonlinear Model

Analysis, based on the linear formulation, allows for interpenetration of the crack faces. A constraint, preventing such interpenetration, leads to the nonlinear formulation of the problem, as discussed previously. The additional source of nonlinearity is due to taking account of longitudinal force resultants in the delaminated parts of the beam.

In this chapter, a comparison is made between numerical results obtained without the constraint preventing the interpenetration of the crack faces (linear model) and with such constraint (nonlinear model). It is shown that the physically impossible interpenetration of the crack faces is prevented in the nonlinear model. Besides, the effect of the longitudinal force resultants on the solution for the transverse displacement is studied

In the example problem considered below, the same problem as in the previous paragraph is considered (Figure 4.1), but in nonlinear formulation, i.e. with account of the nonpenetration constraint and longitudinal force resultants in the delaminated parts.

5.1 Variational formulation of the problem

In the following text, the function $\lambda(t)$ will denote a Lagrange multiplier, used to impose the constraint that prevents interpenetration of the crack faces in the middle of the crack's span, i.e. at $x_0 = (\alpha+\beta)/2$. This constraint is expressed by the formulas

$$f(t) \equiv (w_3(x_0,t) - w_2(x_0,t))\left(\frac{1}{2} - \lim_{\epsilon\to 0}\frac{1}{\pi}\arctan\frac{w_3(x_0,t)-w_2(x_0,t)}{\epsilon}\right) = 0, \tag{82}$$

or

$$f(t) \equiv (w_3(x_0,t) - w_2(x_0,t))\left(\frac{1}{2} - \frac{1}{\pi}\arctan\frac{w_3(x_0,t)-w_2(x_0,t)}{\epsilon}\right) = 0, \tag{83}$$

where ϵ is some small number. In our calculations, this number was chosen as $\epsilon = 5\times 10^{-12}$. For explanation of formulas (82) and (83), see comments to formulas (10a) and (10b). It is assumed that if the interpenetration of the crack faces does not occur at the point $x_0 = (\beta+\alpha)/2$, then it does not occur anywhere along the crack, $\alpha < x < \beta$. This assumption is confirmed later by numerical data, obtained from the solution of the problem. The voltage $V(t)$, applied to the piezoelectric actuator, has the form

$$V(t) = V_a \sin(\Omega t + \phi_0). \tag{84}$$

The problem can be formulated in the form of the Hamilton's principle, i.e. in the form of the condition of extremum of the functional (see formulas (12) – (23) and comments to them)

$$\begin{aligned}
J = {} & \frac{1}{2}\int\limits_{t_1}^{t_2}\int\limits_{0}^{a}\left[A_0(w_0'')^2 - B_0(\dot w_0)^2 - C_0(\dot w_0')^2\right]dx\,dt - \int\limits_{t_1}^{t_2}\int\limits_{0}^{a} I_p V(t) H_a''(x) w_0\,dx\,dt \\
& + \frac{1}{2}\int\limits_{t_1}^{t_2}\int\limits_{a}^{\alpha}\left[A_1(w_1'')^2 - B_1(\dot w_1)^2 - C_1(\dot w_1')^2\right]dx\,dt \\
& + \frac{1}{2}\int\limits_{t_1}^{t_2}\int\limits_{\alpha}^{\beta}\Bigg[A_2(w_2'')^2 - B_2(\dot w_2)^2 - C_2(\dot w_2')^2 + \frac{1}{2}N_x^{(2)}(w_2')^2 - 2\lambda(t)\,f(t) \\
& \qquad + A_3(w_3'')^2 - B_2(\dot w_3)^2 - C_3(\dot w_3')^2 + \frac{1}{2}N_x^{(3)}(w_3')^2\Bigg]dx\,dt \\
& + \frac{1}{2}\int\limits_{t_1}^{t_2}\int\limits_{\beta}^{L}\left[A_4(w_4'')^2 - B_4(\dot w_4)^2 - C_4(\dot w_4')^2\right]dx\,dt
\end{aligned} \tag{85}$$

with subsidiary conditions, represented by the following displacement (essential) boundary conditions:

$$\begin{gathered}
w_0(0) = 0, \qquad w_0'(0) = 0, \\
w_0(a) - w_1(a) = 0, \qquad w_0'(a) - w_1'(a) = 0, \\
w_1(\alpha) - w_2(\alpha) = 0, \qquad w_1(\alpha) - w_3(\alpha) = 0, \qquad w_1'(\alpha) - w_2'(\alpha) = 0, \\
w_1'(\alpha) - w_3'(\alpha) = 0, \qquad w_2(\beta) - w_4(\beta) = 0, \qquad w_3(\beta) - w_4(\beta) = 0, \\
w_2'(\beta) - w_4'(\beta) = 0, \qquad w_3'(\beta) - w_4'(\beta) = 0.
\end{gathered} \tag{86}$$

5.2 Forced vibration of delaminated beam with actuator (nonlinear model)

The forced dynamic response of the beam is sought in the form

$$w_k(x,t) = \sum_{n=1}^{N} X_{kn}(x)\,\Theta_n(t), \qquad k = 0,1,2,3,4, \tag{87}$$

where $X_{kn}(x)$ is an eigenfunction of the linearly formulated problem (equations (61)), in which the index k denotes a number of a beam's part (Figure 4.1), and the index n denotes a number of a natural frequency ω_n to which the eigenfunction $X_{kn}(x)$ corresponds.

Substitution of the series (87) into the expression for the functional (85) produces a result

$$\begin{aligned} J = &\int_{t_1}^{t_2} \mathcal{L}(\Theta_1(t),\dots,\Theta_N(t);\,\dot\Theta_1(t),\dots,\dot\Theta_N(t))dt \\ &+ \int_{t_1}^{t_2} S(\Theta_1(t),\dots,\Theta_N(t))\,dt + \int_{t_1}^{t_2} \widetilde{\lambda}(t) f(\Theta_1(t),\dots,\Theta_N(t))\,dt, \end{aligned} \tag{88}$$

where

$$\widetilde{\lambda}(t) = (\beta-\alpha)\lambda(t), \tag{89}$$

$$\begin{aligned} \mathcal{L}(\Theta_1(t),\dots,\Theta_N(t);\,\dot\Theta_1(t),\dots,\dot\Theta_N(t)) &= \frac{1}{2}\sum_{m,n=1}^{N} K_{mn}\Theta_m\Theta_n \\ &- \frac{1}{2}\sum_{m,n=1}^{N} M_{mn}\dot\Theta_m\dot\Theta_n - \sum_{n=1}^{N} F_n(t)\Theta_n(t), \end{aligned} \tag{90}$$

$$S(\Theta_1(t),\dots,\Theta_N(t)) = \frac{1}{4}\sum_{k,l,m,n=1}^{N} \mathcal{A}_{klmn}\Theta_k\Theta_l\Theta_m\Theta_n - \frac{1}{4}\sum_{l,m,n=1}^{N} \mathcal{B}_{lmn}\Theta_l\Theta_m\Theta_n, \tag{91}$$

$$\begin{aligned} f(\Theta_1(t),\dots,\Theta_N(t)) &= \left[\sum_{n=1}^{N} (X_{3n}(x_0) - X_{2n}(x_0))\,\Theta_n\right] \\ &\times \left[\frac{1}{\pi}\arctan\sum_{n=1}^{N}\frac{1}{\epsilon}(X_{3n}(x_0) - X_{2n}(x_0))\Theta_n - \frac{1}{2}\right] = 0. \end{aligned} \tag{92}$$

The constants K_{mn} and M_{mn} and components of the force vector $F_n(t)$, entering into equations (90), are defined by formulas (75)–(77). The constants $\mathcal{A}_{klmn}$ and $\mathcal{B}_{lmn}$ in equation (91) are defined as follows:

$$\begin{aligned} \mathcal{A}_{klmn} &= Q_2 \int\limits_{\alpha}^{\beta} X'_{2k} X'_{2l} X'_{2m} X'_{2n}\, dx + Q_3 \int\limits_{\alpha}^{\beta} X'_{3k} X'_{3l} X'_{3m} X'_{3n}\, dx, \\ \mathcal{B}_{lmn} &= H_2 \int\limits_{\alpha}^{\beta} X''_{2l} X'_{2m} X'_{2n}\, dx + H_3 \int\limits_{\alpha}^{\beta} X''_{3l} X'_{3m} X'_{3n}\, dx. \end{aligned} \tag{93}$$

In the equation (88), the last two terms, $\int\limits_{t_1}^{t_2} S\, dt$ and $\int\limits_{t_1}^{t_2} \widetilde{\lambda} f\, dt$, are due to the nonlinearity of the formulation of the problem. The term $\int\limits_{t_1}^{t_2} S\, dt$ is due to taking into account the longitudinal force resultants in the delaminated parts, and the term $\int\limits_{t_1}^{t_2} \widetilde{\lambda} f\, dt$ is due to taking account of the constraint that prevents the interpenetration of the crack faces.

The condition of extremum of the functional (88), $\delta J = 0$, leads to the following differential equations

$$\frac{\partial \mathcal{L}}{\partial \Theta_i} - \frac{d}{dt}\left(\frac{\partial \mathcal{L}}{\partial \dot{\Theta}_i}\right) + \frac{\partial S}{\partial \Theta_i} + \widetilde{\lambda}(t)\, \frac{\partial f}{\partial \Theta_i} = 0, \qquad i = 1, 2, \ldots N, \tag{94}$$

and the equation of constraint

$$f(\Theta_1, \ldots, \Theta_N) = 0. \tag{95}$$

The equation of constraint (95) is the same as the equation (92).

Following the penalty function method [11], the equation of constraint (95) can be written in the form

$$f(t) - \frac{1}{\mu}\, \widetilde{\lambda}(t) = 0, \tag{96}$$

where μ is some large number, or

$$\widetilde{\lambda}(t) = \mu f(t). \tag{97}$$

Then, substituting equation (97) into equation (94), we receive

$$\frac{\partial \mathcal{L}}{\partial \Theta_i} - \frac{d}{dt}\left(\frac{\partial \mathcal{L}}{\partial \dot{\Theta}_i}\right) + \frac{\partial S}{\partial \Theta_i} + \mu f\, \frac{\partial f}{\partial \Theta_i} = 0, \qquad i = 1, 2, \ldots N. \tag{98}$$

The substitution of equations (90) – (92) into equation (98) leads to the following ordinary differential equations

$$\sum_{m=1}^{N} M_{im} \ddot{\Theta}_m + \sum_{m=1}^{N} K_{im} \Theta_m + R_i(\Theta_1, \ldots, \Theta_N) = F_i, \qquad i = 1, \ldots, N, \tag{99}$$

where

$$R_i(\Theta_1,\dots,\Theta_N) = \sum_{k,l,m=1}^{N} \mathcal{A}_{iklm}\Theta_k\Theta_l\Theta_m + \sum_{l,m=1}^{N} \mathcal{C}_{ilm}\Theta_l\Theta_m + \mu G_i(\Theta_1,\dots,\Theta_N), \quad (100)$$

where

$$\mathcal{C}_{ilm} = -\frac{1}{4}(\mathcal{B}_{ilm} + \mathcal{B}_{lim} + \mathcal{B}_{mli}),$$

quantities $\mathcal{A}_{klmn}$ and $\mathcal{B}_{lmn}$ are defined by equations (93), and

$$G_i(\Theta_1,\dots,\Theta_N) = \big(X_{3i}(x_0) - X_{2i}(x_0)\big)\left[\frac{1}{\pi}\arctan\frac{\sum\limits_{m=1}^{N}\left(X_{3m}(x_0) - X_{2m}(x_0)\right)\Theta_m}{\epsilon} - \frac{1}{2}\right]^2$$
$$\times \sum_{n=1}^{N}\big(X_{3n}(x_0) - X_{2n}(x_0)\big)\Theta_n, \qquad i = 1,\dots,N. \quad (101)$$

Equations (99) are a system of nonlinear ordinary differential equations, which can be written in matrix form as follows:

$$[M]_{(N\times N)}\{\ddot{\Theta}\}_{(N\times 1)} + [K]_{(N\times N)}\{\Theta\}_{(N\times 1)} + \{R\}_{(N\times 1)} = \{F\}_{(N\times 1)}. \quad (102)$$

In computation of the example problems, equations (102) were reduced to the system of first-order differential equations and solved by an implicit Adams method with direct iteration [12]. Some details on the method of the solution are presented in reference [9].

For the cantilever beam, excited by the piezoelectric actuator (Figure 4.1), with the same numerical values of material and geometric characteristics as in the previous paragraph, and with coordinates of the crack tips $\alpha = 10\times 10^{-2}\,m$, $\beta = 15\times 10^{-2}\,m$ and $\gamma = 1.65\times 10^{-3}\,m$, the difference of the transverse displacements of the crack's faces at $x = 0.125\,m$, computed as the solution of the nonlinearly formulated problem, is presented in Figure 4.3b. The graph in this figure shows that interpenetration of the crack faces is prevented in the nonlinear analysis.

For the same beam, the transverse displacements of the free end of the delaminated beam, obtained from the linear and nonlinear analysis, are presented on graphs in Figure 5.1. As can be seen form these graphs, the results of the linear and nonlinear analysis are slightly different.

In the case of small amplitudes of vibration, neglecting the longitudinal force resultants in the delaminated parts (i.e. neglecting the nonlinear terms in the strain-displacement relations) does not produce a significant effect on results of the nonlinear analysis. This can be seen from graphs in Figure 5.2, obtained for the same beam as considered above.

At the free end of the beam, the transverse displacements of the delaminated and undelaminated beams, obtained from the nonlinear analysis, are presented by graphs in Figure 5.3. These graphs are noticeably different.

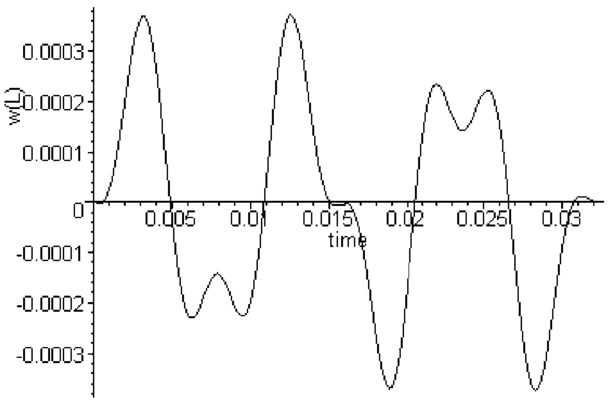

Figure 5.1a. Transverse displacement of free end of **delaminated** cantilever beam, excited by piezoelectric actuator. Beam length is $L = 0.2m,$ x-coordinates of the crack tips are $\alpha = 0.1m$ and $\beta = 0.15m,$ z-coordinate of the crack tips is $\gamma = 0.00165m.$ **Linear analysis.**

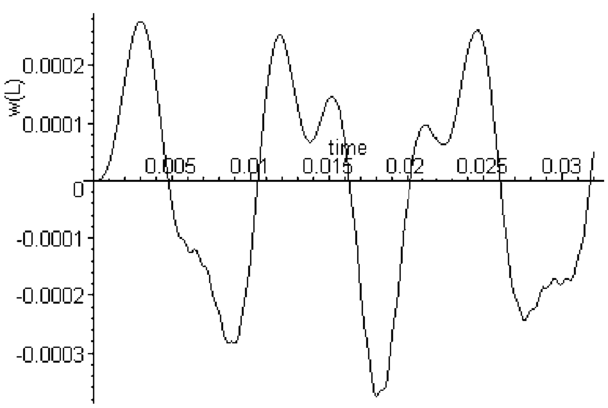

Figure 5.1b. Transverse displacement of free end of **delaminated** cantilever beam, excited by piezoelectric actuator. Beam length is $L = 0.2m,$ x-coordinates of the crack tips are $\alpha = 0.1m$ and $\beta = 0.15m,$ z-coordinate of the crack tips is $\gamma = 0.00165m.$ **Nonlinear analysis.**

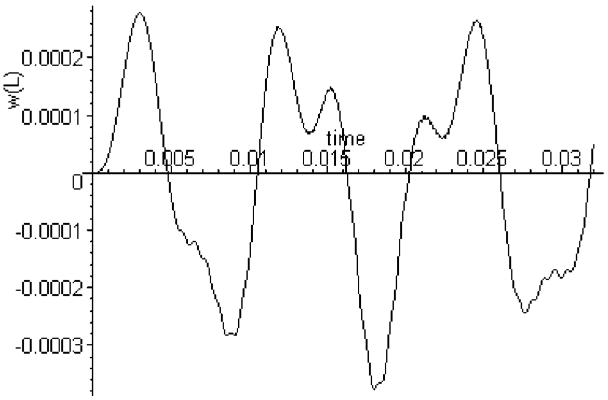

Figure 5.2a. Transverse displacement of free end of **delaminated** cantilever beam, excited by piezoelectric actuator. Beam length is $L = 0.2m,$ x-coordinates of the crack tips are $\alpha = 0.1m$ and $\beta = 0.15m,$ z-coordinate of the crack tips is $\gamma = 0.00165m.$ Linear analysis. **Both types of nonlinearity** are taken into account: due to non-penetration constraint and due to longitudinal force resultants.

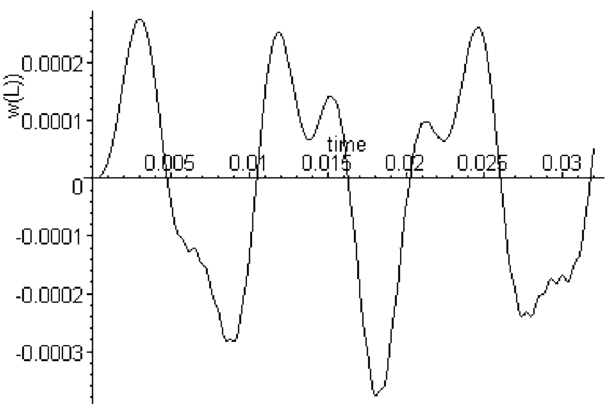

Figure 5.2b. Transverse displacement of free end of **delaminated** cantilever beam, excited by piezoelectric actuator. Beam length is $L = 0.2m,$ x-coordinates of the crack tips are $\alpha = 0.1m$ and $\beta = 0.15m,$ z-coordinate of the crack tips is $\gamma = 0.00165m.$ Nonlinear analysis. **Only one types of nonlinearity** is take into account: due to non-penetration constraint.

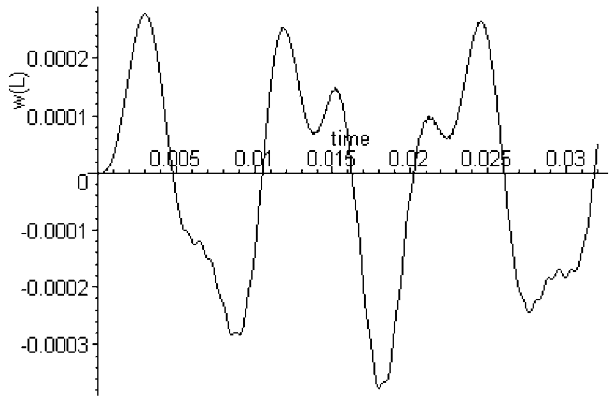

Figure 5.3a. Transverse displacement of free end of **delaminated** cantilever beam, excited by piezoelectric actuator. Beam length is $L = 0.2m,$ x-coordinates of the crack tips are $\alpha = 0.1m$ and $\beta = 0.15m,$ z-coordinate of the crack tips is $\gamma = 0.001165m$. **Nonlinear analysis.**

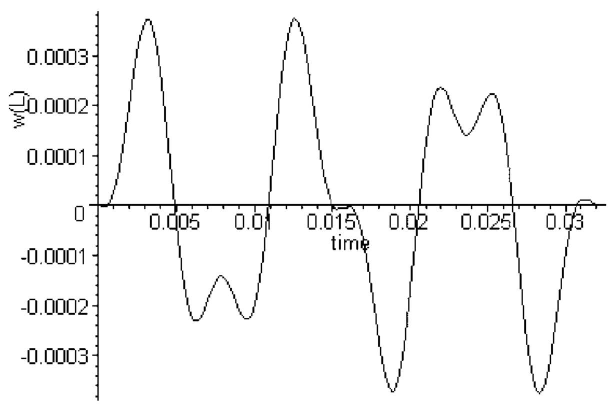

Figure 5.3b. Transverse displacement of free end of **undelaminated** cantilever beam, excited by piezoelectric actuator. Beam length is $L = 0.2m,$ x-coordinates of the crack tips are $\alpha = 0.1m$ and $\beta = 0.15m,$ z-coordinate of the crack tips is $\gamma = 0.001165m$. **Nonlinear analysis.**

Acknowledgements

Financial support for this work is provided by the Air Force Research Laboratory and the Air Force Institute of Technology, program managers — Mark Derriso and professor Athony N. Palazotto.

Appendix A. Properties of the Heaviside function

It can be shown [13] that the Heaviside function (unit step-function) $H_\alpha(x)$, defined by formula (3), has the following property

$$\frac{dH_\alpha(x)}{dx} = \delta_\alpha(x), \tag{A-1}$$

where $\delta_\alpha(x)$ is the Dirac's delta-function, defined as a function that has the following properties:

$$\delta_\alpha(x) = \begin{cases} 0 & \text{for} \quad x \neq \alpha, \\ \infty & \text{for} \quad x = \alpha \end{cases} \tag{A-2}$$

and

$$\int_{x_1}^{x_2} f(x)\delta_\alpha(x)\,dx = \begin{cases} f(\alpha) & \text{for} \quad x_1 < \alpha < x_2, \\ 0 & \text{for} \quad \alpha < x_1 \ \text{ and for } \ \alpha > x_2. \end{cases} \tag{A-3}$$

The delta-function has several analytical representations, one of which has the form [14]:

$$\delta_\alpha(x) = \lim_{\epsilon \to 0} \frac{1}{\pi} \frac{\epsilon}{\epsilon^2 + (x-\alpha)^2}. \tag{A-4}$$

According to formula (A-1), the analytical representation of the Heaviside function, corresponding to the analytical representation (A-4) of the delta-function is

$$H_\alpha(x) = \lim_{\epsilon \to 0} \frac{1}{\pi} \arctan \frac{x-\alpha}{\epsilon} + \frac{1}{2} = \begin{cases} 0 & \text{for} \quad x < \alpha, \\ \dfrac{1}{2} & \text{for} \quad x = \alpha, \\ 1 & \text{for} \quad x > \alpha. \end{cases} \tag{A-5}$$

We see that at the point $x = \alpha$ the Heaviside function, defined by the formula (A-5), is equal to $\frac{1}{2}$, while the Heaviside function, defined by the formula (3), is equal to 0. Such a change of the definition of the Heaviside function does not change a physical meaning and numerical solution of differential equations of motion, which contain the Heaviside function.

Carrying out the Heaviside function $H_\alpha(x)$ beyond the integral sign in an indefinite integral is done with the use of the formula

$$\int H_\alpha(x)\,f(x)\,dx = H_\alpha(x) \int_\alpha^x f(\eta)\,d\eta. \tag{A-6}$$

With the use of properties (A-1) and (A-3), it can be shown that

$$\int_{x_1}^{x_2} f(x) \frac{d^2 H_\alpha(x)}{dx^2}\,dx = \begin{cases} -\dfrac{df}{dx}(\alpha) & \text{for} \quad x_1 < \alpha < x_2, \\ 0 & \text{for} \quad \alpha < x_1 \ \text{ and for } \ \alpha > x_2. \end{cases} \tag{A-7}$$

The double-sided unit step-function $D_{\alpha}^{\beta}(x)$, defined by formula (2), can be expressed in terms of the Heaviside function $H_{\alpha}(x)$ as follows:

$$D_{\beta}^{\alpha}(x) = H_{\alpha}(x) - H_{\beta}(x). \tag{A-8}$$

References

[1] Ramkumar, R.L., Kulkarni, S.V. and Pipes, R.B. Free vibration frequencies of a delaminated beam. In: *34th Annual Technical Conference, 1979. Reinforced Plastics/Composites Institute.* The Society of the Plastics Industry Inc. **22-E**, 1979, P.1–5.

[2] Wang, J.T.S., Liu, Y.Y. and Gibby, J.A. Vibrations of split beams. *J. of Sound and Vibr.* **84**(4) (1982) 491–502.

[3] Mujumdar, P.M. and Suryanarayan, S. Flexural vibrations of beams with delaminations. *J. of Sound and Vibr.* **125**(3) (1988) 441–461.

[4] Luo, H. and Hanagud, S. Dynamics of delaminated beams. *Int. J. of Solids and Structures* **37**(10) (2000) 1501–1519.

[5] Wang, J. and Tong, L. A study of the vibration of delaminated beams using a nonlinear anti-interpenetration constraint model. *Composite Structures* **57**(4) (2002) 483–488.

[6] Perel, V.Y. and Palazotto, A.N. Finite element formulation for dynamics of delaminated composite beams with piezoelectric actuators. *Int. J. of Solids and Structures* **39**(17) (2002) 4457–4483.

[7] Tiersten, H.F. *Linear Piezoelectric Plate Vibrations.* Plenum Press, New York, 1969.

[8] Simvulidi, I.A. *Analysis of Engineering Structures on Elastic Foundations.* Visshaya Shkola, Moscow, 1987. [Russian].

[9] Perel, V.Y. *Nonlinear Dynamics of Composite Delaminated Beam with Piezoelectric Actuator.* Trafford, Victoria, B.C., Canada, 2003.

[10] Paz, M. *Structural Dynamics.* Van Nostrand Reinhold, New York, 1984.

[11] Reddy, J.N. *Energy and Variational Methods in Applied Mechanics.* John Wiley & Sons, New York, 1984.

[12] Burden, R.L. and Faires, J.D. *Numerical Analysis.* Brooks/Cole, Pacific Grove, CA, 2001.

[13] Dirac, P.A.M. *The Principles of Quantum Mechanics.* Clarendon Press, Oxford, 1978.

[14] Rubinowicz, A. *Quantum Mechanics.* Elsevier Pub. Co., New York, 1968.

Nonlinear Dynamics and Systems Theory, **4**(2) (2004) 195–216

Robust Active Control for Structural Systems with Structured Uncertainties

Sheng-Guo Wang[1], H.Y. Yeh[2] and P.N. Roschke[3]

[1] *Department of Engineering Technology and Department of ECE, University of North Carolina at Charlotte, Charlotte, NC 28223-0001, USA*
[2] *Department of Civil Engineering, Prairie View A&M University, Prairie View, TX 77446-0397, USA*
[3] *Department of Civil Engineering, Texas A&M University, College Station, TX 77843-3136, USA*

Received: April 23, 2003; Revised: March 4, 2004

Abstract: Although control theory has been widely applied to constrain motion response of tall, slender structures and long bridges undergoing large forces from natural hazards such as earthquakes and strong wind, numerous uncertainties in these structures such as model errors, stress calculations, material properties, and load environments need to be included in design of the control algorithm. This paper develops a robust active control approach to treat structured uncertainties in the system, control input, and especially, disturbance input matrices that have not been treated previously. Special SVD decomposition is applied to all forms of the structured uncertainties. Robust active control provides multi-objectives, including robust α-degree relative stability, robust H_∞ disturbance attenuation and robust H_2 optimality. The H_∞ norm of the transfer function from the external disturbance forces (e.g., earthquake, wind, and etc.) to the observed system states is restricted by a prescribed attenuation index δ. Settling time of the controlled structural system is robustly less than $4/\alpha$. Preservation of robust H_2 optimality of uncertain structural systems is also discussed. Numerical simulations of a four-story building under robust control are carried out for motion induced by the 1940 El Centro earthquake. Evaluation of controller performance is measured by application of six indices, including a comparison with an LQR controller. Results of the proposed approach may be applied to robust control design of structural systems.

Keywords: *Robust active control; structural systems; structured uncertainties; multi-objective; H_∞/H_2 optimality.*

Mathematics Subject Classification (2000): 93B36, 93D21, 93C05.

1 Introduction

Since the advance of new technologies and the advent of high strength materials, civil engineering structures are becoming taller, longer, and more flexible. To warrant safety and comfort of inhabitants, it is deemed necessary to limit the motion of these structures. Application of modern control theory to restrain the structural motion was first proposed by Yao [18]. Since then, considerable progress has been made to reduce effects of undesirable external forces such as earthquakes and strong winds. Among noteworthy contributions to this field of research are those by Soong [9], Spencer, *et al.* [11], Fujino, *et al.* [2], Yang, *et al.* [17], and many others. Housner, *et al.* [5] detailed recent developments in active control strategies for civil engineering structures. In 1997, Housner, *et al.* provided a summary and general overview of structural control: past and present [4]. A survey paper by Spencer and Sain [10] extensively summarizes recent research progress and describes new efforts in feedback control of buildings.

Most control strategies of structural systems focus on application of linear models and control laws. However, structural uncertainties occur from modeling errors, linearization approximations, stress calculations, material properties, and external disturbances. Effects of these uncertainties on stability and robustness of structural control have been previously examined [3, 11]. Consequently, one primary research issue is robustness of control systems. In particular, numerous studies of this kind have focused on control of buildings. In this regard the H_∞ approach is advantageous in that it may consider both attenuation of disturbance effects and perturbation of unstructured parameters. H_∞ design methods may be found in many references such as [7, 19].

It is well known that dynamics of a civil engineering structure can be described by a Lagrangian system of equations. Many physical problems, such as aeronautical systems, mechanical systems, structural systems, and flexible structures can be described via Lagrange's equation using a state-space model [14]. Since there are numerous uncertainties in stresses, material properties, and loadings that pertain to descriptive numerical models, unanticipated variations of these design parameters may cause instability or degradation of a structural system. In such cases robustness of a control system for stability and its performance toward attenuating disturbance from external hazards is important. Wang, *et al.* [14] have discussed robust optimal pole clustering in a vertical strip and H_∞-norm disturbance rejection for uncertain Lagrangian systems. Considered uncertainties are in both the system matrix and the control input matrix. Wang, *et al.* [12, 14] have also discussed a state-feedback controller and an observer-based output-feedback controller for robust pole clustering in a vertical strip and disturbance attenuation in general uncertain systems with structured and unstructured uncertainties, respectively. They [12] also show that this new method is more flexible and less conservative than the traditional approaches. However, no uncertainties are considered in the disturbance input matrix.

Furthermore, there have been no recent treatments of uncertainties with regard to the disturbance input matrix in the literature [7, 12, 14, 15, 19]. However, the disturbance input matrix has uncertainties, e.g., in view of the uncertainties existing in mass, as well as in the inverse mass matrix, and so on. Recently, Wang, *et al.* [13] discussed robust control for structural systems via Lagrange's model with unstructured uncertainties, including those in the disturbance input matrix. In [16] they further discussed parametric uncertainties in system and control input matrices, as well as unstructured uncertainties in the disturbance input matrix. However, some uncertainties may be structured uncertainties, such as from mass, spring constants, and damping ratios. Thus, it is meaningful to investigate robust control for structural systems with structured uncertainties in the disturbance input matrix. Herein lies the motivation for research reported in this paper.

Therefore, the objective of this paper is to develop an approach for active control of structural systems that includes robust stability and performance control with H_∞-norm disturbance attenuation that takes into account structured uncertainties in the structural systems, including those in the disturbance input matrices, to reject/attenuate disturbances such as earthquake and wind forces for a family of structural systems with these uncertainties. Applicable uncertain structural systems include uncertainties among system, control input, and disturbance input matrices. Robust state feedback control is considered here, while robust output feedback control is considered in a future paper. The proposed control algorithm provides a robust α-degree relative stability, i.e., the closed-loop system poles robustly stay in the left-half plane with the real part less than $-\alpha$. It also guarantees a prescribed H_∞-norm disturbance attenuation constraint δ from the external hazard forces to the observed states of the structure. The approach is based on the algebraic Riccati equation (ARE). A group of several flexible scalars is introduced to enable solution of the ARE. Then, H_2 optimality of the design controller is also proved.

It is noted that there are many publications concerning robust H_∞ control and multi-objective control in the literature [19]. For structured uncertainties, the μ-theory [19] makes a breakthrough. However, calculation and design based on μ theory is an NP-hard problem. Therefore, this paper uses a new method to deal with structured uncertainties, extended from Wang, *et al.* [12] to include structured uncertainties in the disturbance input matrix. It uses special SVD-type decomposition and introduces a group of adjustable design parameters to control design to enable control with robust performance, including robust relative stability, robust H_∞ disturbance attenuation and robust H_2 optimal control for the whole uncertain system family. It is noticed that the treatment may be taken into some conventional framework from H_∞-control view point. However, Wang, *et al.* [12] have shown that the conventional framework will not be as flexible and is more-conservative than the proposed method that renders conventional treatment of this problem as a special case of their approach as shown by theoretical proof and an example. Therefore, this paper develops an approach that extends work presented by Wang, *et al.* [12, 14].

Salient contributions of this paper are as follows:

1) an uncertain Lagrangian system with uncertainties not only in system and control input matrices but also in disturbance input matrix is treated;
2) structured uncertainties in the disturbance input matrix are taken into account;
3) a special weighted SVD-type decomposition for all structured uncertainties is described;
4) a group of tuning scalars is used;
5) discussion of robust H_2 optimality together with robust H_∞ disturbance attenuation and robust relative stability is included;
6) numerical simulation of control for an uncertain building model, including a nominal model and a worst case model, excited by the 1940 El Centro, California, earthquake data is demonstrated; and
7) finally, six performance indices are used for evaluation and comparison with the traditional LQR control.

The paper is organized as follows. Section 2 formulates an analytical approach to control of uncertain structural systems with structured uncertainties. Section 3 provides robust control algorithms with robust relative stability and H_∞-norm disturbance attenuation for uncertain structural systems. Furthermore, in Section 4 preservation of H_2 optimality of the design controller with respect to a special performance index is derived. In Section 5, a numerical example of robust control design is presented that illustrates robust controller design. Section 6 provides six indices for performance evaluation and Section 7 demonstrates simulations excited by the 1940 El Centro earthquake data and compares results from three robust controllers and an LQR controller. Finally, Section 8 concludes the paper.

2 Control System Formulation

It is well known that motion of a structural system can be described by Lagrange's equations in state-space as follows:

$$\frac{d}{dt}\left(\frac{\partial L}{\partial \dot{q}_i}\right) - \frac{\partial L}{\partial q_i} + \frac{\partial D_f}{\partial \dot{q}_i} = Q_i, \tag{1}$$

where $L = T - V$, T is the system kinetic energy, V is the system potential energy, D_f is the system dissipation function, Q_i represents the generalized force, and q_i is the partial state. For example, dynamic motion of a structural system may be described by

$$\mathbf{M}\ddot{\mathbf{q}} + \mathbf{C}_d\dot{\mathbf{q}} + \mathbf{K}_s\mathbf{q} = \mathbf{f} \tag{2}$$

where $\mathbf{q}$ is a displacement vector, $\mathbf{M}$ is a mass matrix, $\mathbf{C}_d$ is a damping coefficient matrix, $\mathbf{K}_s$ is a stiffness coefficient matrix, and $\mathbf{f}$ is an external force vector that includes both undesired forces from an external hazard and desired control forces. Mass matrix $\mathbf{M}$ is a full rank matrix, i.e., its inverse exists. Sometimes, it is simply considered to be a diagonal matrix. The dynamic system (2) may be rewritten as

$$\ddot{\mathbf{q}} + \mathbf{M}^{-1}\mathbf{C}_d\dot{\mathbf{q}} + \mathbf{M}^{-1}\mathbf{K}_s\mathbf{q} = \mathbf{M}^{-1}\mathbf{f}. \tag{3}$$

However, uncertainties in structural parameters that are derived from modeling errors, linearized approximation, stress calculations, variation in materials properties, and external disturbances are inevitable. If uncertainties, perturbations, and disturbances are taken into account, equations (1) – (3) can be reformulated as a monic vector differential equation with parametric perturbations and external disturbances as follows:

$$\ddot{\mathbf{q}} + (\mathbf{D}_c + \Delta\mathbf{D}_c)\dot{\mathbf{q}} + (\mathbf{D}_k + \Delta\mathbf{D}_k)\mathbf{q} = (\mathbf{B}_u + \Delta\mathbf{B}_u)\mathbf{u} + (\mathbf{F}_w + \Delta\mathbf{F}_w)\mathbf{w}, \tag{4a}$$

$$\mathbf{z} = \mathbf{C}_1\mathbf{q} + \mathbf{C}_2\dot{\mathbf{q}}, \tag{4b}$$

where $\mathbf{q} \in R^n$, $\mathbf{u} \in R^m$, $\mathbf{w} \in R^\omega$, and $\mathbf{z} \in R^p$ are the partial state, input, disturbance, and output (vibration specification signals), respectively; $\mathbf{D}_c$, $\mathbf{D}_k$, $\mathbf{B}_u$, $\mathbf{F}_w$, $\mathbf{C}_1$, and $\mathbf{C}_2$ are nominal structural system parameter matrices with appropriate dimensions; $\Delta\mathbf{D}_c$, $\Delta\mathbf{D}_k$, $\Delta\mathbf{B}_u$ and $\Delta\mathbf{F}_w$ are perturbation matrices that can be time-varying with appropriate dimensions. The considered disturbance vector $\mathbf{w}(t)$ may include an earthquake force vector $\mathbf{w}_e(\mathrm{t})$ and/or a wind force vector $\mathbf{w}_w(\mathrm{t})$. Thus, the uncertain structural system can be described by the following specific state-space block companion form:

$$\dot{\mathbf{x}}(\mathbf{t}) = (\mathbf{A} + \Delta\mathbf{A})\mathbf{x}(t) + (\mathbf{B} + \Delta\mathbf{B})\mathbf{u}(t) + (\mathbf{F} + \Delta\mathbf{F})\mathbf{w}(t), \tag{5a}$$

$$\mathbf{z}(t) = \mathbf{C}\mathbf{x}(t) \tag{5b}$$

$$\mathbf{A} = \begin{bmatrix} \mathbf{0} & \mathbf{I} \\ -\mathbf{D}_k & -\mathbf{D}_c \end{bmatrix}, \quad \Delta\mathbf{A} = \begin{bmatrix} \mathbf{0} & \mathbf{0} \\ -\Delta\mathbf{D}_k & -\Delta\mathbf{D}_c \end{bmatrix}, \quad \mathbf{B} = \begin{bmatrix} \mathbf{0} \\ \mathbf{B}u \end{bmatrix},$$
$$\Delta\mathbf{B} = \begin{bmatrix} \mathbf{0} \\ \Delta\mathbf{B}u \end{bmatrix}, \quad \mathbf{F} = \begin{bmatrix} \mathbf{0} \\ \mathbf{F}_w \end{bmatrix}, \quad \Delta\mathbf{F} = \begin{bmatrix} \mathbf{0} \\ \Delta\mathbf{F}_w \end{bmatrix},$$
$$\text{and} \quad \mathbf{C} = [\,\mathbf{C}_1 \quad \mathbf{C}_2\,], \tag{5c}$$

where the state $\mathbf{x} = \begin{bmatrix} \mathbf{q}^{\mathrm{T}} & \dot{\mathbf{q}}^{\mathrm{T}} \end{bmatrix}^{\mathrm{T}} \in R^{2n}$, all matrices have appropriate dimensions, and $(\mathbf{A}, \mathbf{B})$ is assumed to be controllable.

Based on the form of block matrices given in equation (5), results are directly derived with respect to the low dimensional uncertainties $\Delta\mathbf{D}_c$, $\Delta\mathbf{D}_k$, $\Delta\mathbf{B}_u$, and $\Delta\mathbf{F}_w$ for simple and less conservative constraints to robust active structural control problems. In light of perturbations of physical parameters, structured or unstructured uncertainties, especially structured ones, usually exist in $\mathbf{A}(\mathbf{D}_k, \mathbf{D}_c)$, $\mathbf{B}_u$, and $\mathbf{F}_w$, and are described as $\Delta\mathbf{A}(\Delta\mathbf{D}_k, \Delta\mathbf{D}_c)$, $\Delta\mathbf{B}_u$, and $\Delta\mathbf{F}_w$, respectively. The case of unstructured uncertainties is considered in [13]. Here, structured uncertainties are treated.

Structured uncertainties can be described as:

$$\begin{aligned} \Delta\mathbf{D}_k &= \sum_{j=1}^{l_k} a_{kj}\mathbf{A}_{kj}, & \Delta\mathbf{D}_c &= \sum_{j=1}^{l_c} a_{cj}\mathbf{A}_{cj}, \\ \Delta\mathbf{B}_{\mathbf{u}} &= \sum_{j=1}^{l_b} b_j\mathbf{B}_j, & \Delta\mathbf{F}_w &= \sum_{j=1}^{l_f} f_j\mathbf{F}_j, \end{aligned} \tag{6}$$

where $\Delta\mathbf{D}_c$, $\Delta\mathbf{D}_k$, $\Delta\mathbf{B}_u$, and $\Delta\mathbf{F}_w$ are the uncertain stiffness matrix, uncertain damping matrix, uncertain control input matrix, and uncertain disturbance input matrix, respectively. They are described as structured uncertainties, i.e., matrices $\mathbf{A}_{kj}$, $\mathbf{A}_{cj}$, $\mathbf{B}_j$, and $\mathbf{F}_j$ represent the structures of uncertainties, while scalars a_{kj}, a_{cj}, b_j, and f_j represent the uncertain values of uncertainties on their corresponding structures, respectively, and are bounded by ± 1 without loss of generality.

Here, weighted SVD (singular value decomposition) is applied to the uncertainty structure matrices $\mathbf{A}_{kj}$, $\mathbf{A}_{cj}$, $\mathbf{B}_j$, and $\mathbf{F}_j$. Then, it follows that

$$\mathbf{A}_{kj} = \mathbf{T}_{kj}\mathbf{U}_{kj}^{\mathrm{T}}, \quad \mathbf{A}_{cj} = \mathbf{T}_{cj}\mathbf{U}_{cj}^{\mathrm{T}}, \quad \mathbf{B}_j = \mathbf{T}_{bj}\mathbf{U}_{bj}^{\mathrm{T}}, \quad \text{and} \quad \mathbf{F}_j = \mathbf{T}_{fj}\mathbf{U}_{fj}^{\mathrm{T}}, \tag{7}$$

respectively. Next, the following definitions are made:

$$\begin{aligned} \mathbf{T}_k &= \sum_{j=1}^{l_k} \mathbf{T}_{kj}\mathbf{T}_{kj}^{\mathrm{T}}, & \mathbf{U}_k &= \sum_{j=1}^{l_k} \mathbf{U}_{kj}\mathbf{U}_{kj}^{\mathrm{T}}, & \mathbf{T}_c &= \sum_{j=1}^{l_c} \mathbf{T}_{cj}\mathbf{T}_{cj}^{\mathrm{T}}, & \mathbf{U}_c &= \sum_{j=1}^{l_c} \mathbf{U}_{cj}\mathbf{U}_{cj}^{\mathrm{T}}, \\ \mathbf{T}_b &= \sum_{j=1}^{l_b} \mathbf{T}_{bj}\mathbf{T}_{bj}^{\mathrm{T}}, & \mathbf{U}_b &= \sum_{j=1}^{l_b} \mathbf{U}_{bj}\mathbf{U}_{bj}^{\mathrm{T}}, & \mathbf{T}_f &= \sum_{j=1}^{l_f} \mathbf{T}_{fj}\mathbf{T}_{fj}^{\mathrm{T}}, & \mathbf{U}_f &= \sum_{j=1}^{l_f} \mathbf{U}_{fj}\mathbf{U}_{fj}^{\mathrm{T}} \end{aligned} \tag{8}$$

Furthermore, it is defined that

$$\mathbf{T}_A = \begin{bmatrix} 0 & 0 \\ 0 & \mathbf{T}_k + \mathbf{T}_c \end{bmatrix}, \quad \mathbf{U}_A = \begin{bmatrix} \mathbf{U}_k & 0 \\ 0 & \mathbf{U}_c \end{bmatrix}, \quad \mathbf{T}_B = \begin{bmatrix} 0 & 0 \\ 0 & \mathbf{T}_b \end{bmatrix},$$
$$\mathbf{U}_B = \mathbf{U}_b, \quad \mathbf{T}_F = \begin{bmatrix} 0 & 0 \\ 0 & \mathbf{T}_f \end{bmatrix}, \quad \mathbf{U}_F = \mathbf{U}_f, \quad \mathbf{F}_\Delta = \sum_{j=1}^{l_f} \mathbf{F}_j \mathbf{F}_j^{\mathrm{T}}. \tag{9}$$

Notice that some Lagrangian representations of structures with the block companion form in (5) may be formulated as matched uncertain systems (extended from [8]). That is, the matched uncertainties are within the range of the nominal control-input matrix $\mathbf{B}$. This implies that all uncertainties can be reached by suitable control signals through the control-input matrix $\mathbf{B}$. Thus, a system with matched uncertainties can be compensated if a suitable designed robust controller is applied. In other words, a robust controller is guaranteed to exist and there exists a robust controller that can overcome all these matched uncertainties. In this case these structured matched uncertainties can be described as follows:

$$\Delta\mathbf{A} = \mathbf{B} \cdot \Delta\mathbf{A}_B, \quad \Delta\mathbf{B} = \mathbf{B} \cdot \Delta\mathbf{B}_B, \quad \mathbf{F} = \mathbf{B} \cdot \mathbf{F}_B, \quad \Delta\mathbf{F} = \mathbf{B} \cdot \Delta\mathbf{F}_B, \quad \text{i.e.,} \tag{10a}$$

$$\Delta\mathbf{A}_B = [-\Delta\mathbf{D}_{Bk} \quad -\Delta\mathbf{D}_{Bc}], \quad \Delta\mathbf{D}_{Bk} = \sum_{j=1}^{l_k} a_{bkj}\mathbf{A}_{bkj}, \quad \Delta\mathbf{D}_{Bc} = \sum_{j=1}^{l_c} a_{bcj}\mathbf{A}_{bcj};$$
$$\Delta\mathbf{B}_B = \Delta\mathbf{B}_{Bu} = \sum_{j=1}^{l_b} b_{bj}\mathbf{B}_{bj}, \quad \Delta\mathbf{F}_w = \mathbf{B}_u \Delta\mathbf{F}_{Bw}, \quad \Delta\mathbf{F}_B = \Delta\mathbf{F}_{Bw} = \sum_{j=1}^{l_f} f_{bj}\mathbf{F}_{bj}; \tag{10b}$$
$$\text{with} \quad \Delta\mathbf{B}_{Bu} + \Delta\mathbf{B}_{Bu}^{\mathrm{T}} + 2\mathbf{I} > \mathbf{0}. \tag{10c}$$

This uncertain system can be called a matched uncertain system, i.e., with matched uncertainties. Applying weighted SVD for all of the above uncertainty structures similar to the above (7) – (9) leads to the following:

$$\mathbf{A}_{bkj} = \mathbf{T}_{bkj}\mathbf{U}_{bkj}^{\mathrm{T}}, \quad \mathbf{A}_{bcj} = \mathbf{T}_{bcj}\mathbf{U}_{bcj}^{\mathrm{T}}, \quad \mathbf{B}_{bj} = \mathbf{T}_{bbj}\mathbf{U}_{bbj}^{\mathrm{T}}, \quad \mathbf{F}_{bj} = \mathbf{T}_{bfj}\mathbf{U}_{bfj}^{\mathrm{T}}, \tag{11}$$

Finally, it is defined that

$$\mathbf{T}_{bk} = \sum_{j=1}^{l_k} \mathbf{T}_{bkj}\mathbf{T}_{bkj}^{\mathrm{T}}, \quad \mathbf{U}_{bk} = \sum_{j=1}^{l_k} \mathbf{U}_{bkj}\mathbf{U}_{bkj}^{\mathrm{T}}, \quad \mathbf{T}_{bc} = \sum_{j=1}^{l_c} \mathbf{T}_{bcj}\mathbf{T}_{bcj}^{\mathrm{T}}, \quad \mathbf{U}_{bc} = \sum_{j=1}^{l_c} \mathbf{U}_{bcj}\mathbf{U}_{bcj}^{\mathrm{T}}, \tag{12a}$$
$$\mathbf{T}_{bb} = \sum_{j=1}^{l_b} \mathbf{T}_{bbj}\mathbf{T}_{bbj}^{\mathrm{T}}, \quad \mathbf{U}_{bb} = \sum_{j=1}^{l_b} \mathbf{U}_{bbj}\mathbf{U}_{bbj}^{\mathrm{T}}, \quad \mathbf{T}_{bf} = \sum_{j=1}^{l_f} \mathbf{T}_{bfj}\mathbf{T}_{bfj}^{\mathrm{T}}, \quad \mathbf{U}_{bf} = \sum_{j=1}^{l_f} \mathbf{U}_{bfj}\mathbf{U}_{bfj}^{\mathrm{T}}, \tag{12b}$$
$$\mathbf{T}_{bA} = \mathbf{T}_{bk} + \mathbf{T}_{bc}, \quad \mathbf{U}_{bA} = \begin{bmatrix} \mathbf{U}_{bk} & 0 \\ 0 & \mathbf{U}_{bc} \end{bmatrix}, \quad \mathbf{T}_{bB} = \mathbf{T}_{bb}, \quad \mathbf{U}_{bB} = \mathbf{U}_{bb}, \quad \mathbf{T}_{bF} = \mathbf{T}_{bf},$$
$$\mathbf{U}_{bF} = \mathbf{U}_{bf}, \quad \mathbf{F}_{b\Delta} = \sum_{j=1}^{l_f} \mathbf{F}_{bj}\mathbf{F}_{bj}^{\mathrm{T}}. \tag{12c}$$

The objective is to find a linear state-feedback control law such that it can accomplish the above-mentioned robust active control that is valid for the whole family of uncertain structural systems in (5) in face of disturbances and perturbations in (6) – (12). Thus, the goal is to design a state feedback controller

$$\mathbf{u}(t) = -\mathbf{K}\mathbf{x}(t) \tag{13}$$

such that the closed loop uncertain linear system

$$\dot{\mathbf{x}}(\mathbf{t}) = (\mathbf{A} + \Delta\mathbf{A} - \mathbf{B}\mathbf{K} - \Delta\mathbf{B}\mathbf{K})\mathbf{x}(t) + (\mathbf{F} + \Delta\mathbf{F})\mathbf{w}(t), \tag{14a}$$

$$\mathbf{z}(t) = \mathbf{C}\mathbf{x}(t), \tag{14b}$$

has a robust disturbance attenuation with a prescribed H_∞-norm constraint δ (a specified disturbance attenuation index) that satisfies the following:

$$\|\mathbf{T}_{zw}(s)\|_\infty = \left\|\mathbf{C}(s\mathbf{I} - \mathbf{A}_c)^{-1}(\mathbf{F} + \Delta\mathbf{F})\right\|_\infty \leq \delta \tag{15}$$

and a robust α-degree relative stability, i.e.,

$$\mathrm{Re}\,\{\lambda(\mathbf{A}_c)\} < -\alpha, \tag{16}$$

where $\mathbf{A}_c = \mathbf{A} + \Delta\mathbf{A} - \mathbf{B}\mathbf{K} - \Delta\mathbf{B}\mathbf{K}$, and $\mathbf{T}_{zw}(s)$ is a transfer function matrix from the disturbance vector $\mathbf{w}$ to the observation vector $\mathbf{z}$ of the structural system. The disturbance vector $\mathbf{w}$ may include a wind and/or earthquake disturbance. The observation vector $\mathbf{z}$ may include a vibration vector, i.e., displacement vector, velocity vector, and other salient observation states. This indicates that the gain of the structural system from the disturbance energy $\|\mathbf{w}\|^2$ to the structural vibration energy $\|\mathbf{z}\|^2$ is bounded by δ even in the worst case in view of the H_∞-norm property. The control law also provides robust relative stability with an index α to the structural system. In the case of matched uncertainties in (10) – (14), the existence of this desired controller is guaranteed. Also, the optimality of the controller is proved in an H_2 sense.

3 Robust Feedback Control

In this section, a state feedback controller is developed in (13) that provides robust α-degree relative stability in (16) and an H_∞ disturbance attenuation with a prescribed index δ in (15) for the uncertain structural system given in (5) and (14). The controller (13) is obtained by solving a Riccati equation as derived in this section. A set of tuning parameters is introduced to enhance flexibility in defining the controller.

Before deriving the main result, the following lemmas are cited to provide a basis for the derivation. As a preliminary statement, a matrix $\mathbf{Q}$ that is > 0, ≥ 0, and < 0 is said to be positive definite, positive semi-definite, and negative definite, respectively.

Lemma 1 ([1]) *Matrix $\mathbf{A}$ is robust α-degree relatively stable if and only if there exists a unique positive matrix $\mathbf{P}$ for any positive definite matrix $\mathbf{Q}$ such that*

$$(\mathbf{A} + \alpha\mathbf{I})^{\mathrm{T}}\mathbf{P} + \mathbf{P}(\mathbf{A} + \alpha\mathbf{I}) = -\mathbf{Q}, \tag{17}$$

i.e., all eigenvalues of matrix $\mathbf{A}$ lie in the left plane of the line $-\alpha$, $\mathrm{Re}\,\{\lambda(\mathbf{A})\} < -\alpha$.

Lemma 2 ([14]) *For any $n \times m$ matrices $\mathbf{X}$ and $\mathbf{Y}$, and any scalar $\xi > 0$,*

$$\xi \mathbf{X}\mathbf{X}^* + \frac{1}{\xi}\mathbf{Y}\mathbf{Y}^* \pm (\mathbf{X}\mathbf{Y}^* + \mathbf{Y}\mathbf{X}^*) \geq 0. \tag{18}$$

Lemma 3 *For given scalars $\alpha \geq 0$ and $\delta > 0$, if there exist a positive definite matrix $\mathbf{P}$ and positive adjustable scalars ε and ε_3 such that*

$$(\mathbf{A}_c + \alpha\mathbf{I})^{\mathrm{T}}\mathbf{P} + \mathbf{P}(\mathbf{A}_c + \alpha\mathbf{I}) + \frac{\varepsilon}{\delta}\mathbf{P}[\mathbf{F}(\mathbf{I} + \varepsilon_3\mathbf{U}_F)\mathbf{F}^{\mathrm{T}} + \frac{1}{\varepsilon_3}\mathbf{T}_F + l_f\mathbf{F}_\Delta]\mathbf{P} + \frac{1}{\varepsilon\delta}\mathbf{C}^{\mathrm{T}}\mathbf{C} < 0, \tag{19}$$

then the closed-loop system (14) with structured uncertainties in (6)–(9) is of the α-degree relatively stable as (16) and δ-degree disturbance attenuated as (15).

Proof By Lemma 1, it is obvious that system A_c is of α-degree relatively stable. By extension of Lemma 2 in [14], it is known that the closed-loop system (14) with structured uncertainties in (6) − (9) is of α-degree relatively stable as (16) and there is δ-degree disturbance attenuation in (15) if

$$(\mathbf{A}_c + \alpha\mathbf{I})^{\mathrm{T}}\mathbf{P} + \mathbf{P}(\mathbf{A}_c + \alpha\mathbf{I}) + \frac{\xi}{\delta}\mathbf{P}(\mathbf{F} + \Delta\mathbf{F})(\mathbf{F} + \Delta\mathbf{F})^{\mathrm{T}}\mathbf{P} + \frac{1}{\xi\delta}\mathbf{C}^{\mathbf{T}}\mathbf{C} < 0. \tag{20a}$$

In view of Lemma 2, it follows that

$$\mathbf{P}(\mathbf{F} + \Delta\mathbf{F})(\mathbf{F} + \Delta\mathbf{F})^{\mathrm{T}}\mathbf{P} \leq \mathbf{P}\Big[\mathbf{F}(\mathbf{I} + \varepsilon_3\mathbf{U}_F)\mathbf{F}^{\mathrm{T}} + \frac{1}{\varepsilon_3}\mathbf{T}_F + l_f\mathbf{F}_\Delta\Big]\mathbf{P}. \tag{20b}$$

Then, it is obvious that this Lemma holds.

Now, a primary concept for this paper is described as follows.

Theorem 3.1 *Let the disturbance attenuation index $\delta > 0$ and the robust relative stability index $\alpha > 0$, where δ and α are prescribed scalars that are determined according to performance requirements of the structure. Consider a given uncertain structural system (5) with structured uncertainties in (6)–(9). Then, if there exist positive adjustable scalars ε_1, ε_2, ε_3, and ε, an adjustable matrix $\mathbf{Q} > 0$, and a solution matrix $\mathbf{P} > 0$ satisfying the following Riccati equation:*

$$\begin{gathered}(\mathbf{A} + \alpha\mathbf{I})^{\mathrm{T}}\mathbf{P} + \mathbf{P}(\mathbf{A} + \alpha\mathbf{I}) - \mathbf{P}\Big\{\mathbf{B}(\mathbf{I} - \frac{\varepsilon_2}{2}\mathbf{U}_B)\mathbf{B}^{\mathrm{T}} \\ -\varepsilon_1\mathbf{T}_A - \frac{1}{2\varepsilon_2}\mathbf{T}_B - \frac{\varepsilon}{\delta}\Big[\mathbf{F}(\mathbf{I} + \varepsilon_3\mathbf{U}_F)\mathbf{F}^{\mathrm{T}} + \frac{1}{\varepsilon_3}\mathbf{T}_F + l_f\mathbf{F}_\Delta\Big]\Big\}\mathbf{P} \\ + \frac{1}{\varepsilon_1}\mathbf{U}_A + \frac{1}{\varepsilon\delta}\mathbf{C}^{\mathrm{T}}\mathbf{C} + \mathbf{Q} = \mathbf{0}, \qquad 0 < \varepsilon_2 < \frac{2}{\bar{\sigma}(\mathbf{U}_B)}\end{gathered} \tag{21}$$

where $\mathbf{T}_A$, $\mathbf{U}_A$, $\mathbf{T}_B$, $\mathbf{U}_B$, $\mathbf{T}_F$, $\mathbf{U}_F$ and $\mathbf{F}_\Delta$ are as in (9), then the state-feedback controller

$$\mathbf{u}(t) = -\mathbf{K}\mathbf{x}(t) = -r\mathbf{B}^{\mathrm{T}}\mathbf{P}\mathbf{x}(t), \tag{22}$$

$$\frac{1}{\varepsilon_2\bar{\sigma}(\mathbf{U}_B)} - 0.5 \geq r \geq 0.5 \qquad \textit{or} \qquad 0.5 \geq r \geq \frac{1}{\varepsilon_2\underline{\sigma}(\mathbf{U}_B)} - 0.5, \tag{23}$$

guarantees a robust α-degree relative stability (16) and a δ-degree H_∞ disturbance attenuation (15) for the uncertain structural system (5) with all admissible structured uncertainties as shown in (6)–(9).

Proof To prove this theorem, equation (19) is investigated for the uncertain system (5) with uncertainties in (6)–(9). Control vector $\mathbf{u}(t)$ is given by equation (22), and

$$\mathbf{A}_c = \mathbf{A} + \Delta\mathbf{A} - \mathbf{B}\mathbf{K} - \Delta\mathbf{B}\mathbf{K} = \mathbf{A} + \Delta\mathbf{A} - r\mathbf{B}\mathbf{B}^{\mathrm{T}}\mathbf{P} - r\Delta\mathbf{B}\mathbf{B}^{\mathrm{T}}\mathbf{P}.$$

Thus, by using the Riccati equation (21), Lemmas 2 and 3, and conditions in (21) and (23), we have

$$\begin{aligned}
&(\mathbf{A}_c+\alpha\mathbf{I})^{\mathrm{T}}\mathbf{P} + \mathbf{P}(\mathbf{A}_c + \alpha\mathbf{I}) + \frac{\varepsilon}{\delta}\mathbf{P}\Big[\mathbf{F}(\mathbf{I}+\varepsilon_3\mathbf{U}_F)\mathbf{F}^{\mathrm{T}} + \frac{1}{\varepsilon_3}\mathbf{T}_F + l_f\mathbf{F}_\Delta\Big]\mathbf{P} + \frac{1}{\varepsilon\delta}\mathbf{C}^{\mathrm{T}}\mathbf{C} \\
&\quad = (\mathbf{A}+\alpha\mathbf{I})^{\mathrm{T}}\mathbf{P} + \mathbf{P}(\mathbf{A}+\alpha\mathbf{I}) + \frac{\varepsilon}{\delta}\mathbf{P}\Big[\mathbf{F}(\mathbf{I}+\varepsilon_3\mathbf{U}_F)\mathbf{F}^{\mathrm{T}} + \frac{1}{\varepsilon_3}\mathbf{T}_F + l_f\mathbf{F}_\Delta\Big]\mathbf{P} \\
&\quad + \frac{1}{\varepsilon\delta}\mathbf{C}^{\mathrm{T}}\mathbf{C} + (\Delta\mathbf{A} - r\mathbf{B}\mathbf{B}^{\mathrm{T}}P - r\Delta\mathbf{B}\mathbf{B}^{\mathrm{T}}\mathbf{P})^{\mathrm{T}}\mathbf{P} \\
&\quad + \mathbf{P}(\Delta\mathbf{A} - r\mathbf{B}\mathbf{B}^{\mathrm{T}}\mathbf{P} - r\Delta\mathbf{B}\mathbf{B}^{\mathrm{T}}\mathbf{P}) = \mathbf{P}\Big[\mathbf{B}(\mathbf{I} - \frac{\varepsilon_2}{2}\mathbf{U}_B)\mathbf{B}^{\mathrm{T}} - \varepsilon_1\mathbf{T}_A - \frac{1}{2\varepsilon_2}\mathbf{T}_B\Big]\mathbf{P} \\
&\quad - \frac{1}{\varepsilon_1}\mathbf{U}_A - \mathbf{Q} + \Delta\mathbf{A}^{\mathrm{T}}\mathbf{P} + \mathbf{P}\Delta\mathbf{A} - r\mathbf{P}(2\mathbf{B}\mathbf{B}^{\mathrm{T}} + \Delta\mathbf{B}\mathbf{B}^{\mathrm{T}} + \mathbf{B}\Delta\mathbf{B}^{\mathrm{T}})\mathbf{P} \\
&\quad \le \mathbf{P}\Big[-2r^2\varepsilon_2\mathbf{B}\mathbf{U}_B\mathbf{B}^{\mathrm{T}} - \frac{1}{2\varepsilon_2}\mathbf{T}_B - r(\Delta\mathbf{B}\mathbf{B}^{\mathrm{T}} + \mathbf{B}\Delta\mathbf{B}^{\mathrm{T}})\Big]\mathbf{P} - \varepsilon_1\mathbf{P}\mathbf{T}_A\mathbf{P} \\
&\quad - \frac{1}{\varepsilon_1}\mathbf{U}_A + \mathbf{P}(\Delta\mathbf{A}^{\mathrm{T}} + \Delta\mathbf{A})\mathbf{P} - \mathbf{Q} \le -\mathbf{Q} < \mathbf{0}.
\end{aligned}$$

Thus, controller (22) makes inequality (19) hold. Then, by Lemma 3, Theorem 3.1 is proved.

The proposed controller (22) in Theorem 3.1 is not only a robust controller with H_∞ disturbance attenuation and robust relative stability, but also an optimal controller in the H_2 optimal sense under a certain meaning as discussed in the next section.

Now, consider matched uncertain systems with matched uncertainties in (10)–(12).

Theorem 3.2 *Consider a matched uncertain system (5) with the matched structured uncertainties in (10)–(12), a specified relative stability degree α, and a disturbance attenuation index δ. Select an assigned matrix $\mathbf{Q} > 0$, and positive adjustable scalars ε_1, ε_2, ε_3, ε, and r within the following regions*

$$\begin{aligned}
&\frac{\underline{\sigma}\Big(\mathbf{I} - 0.5\varepsilon_2\mathbf{U}_{bB} - 0.5\dfrac{1}{\varepsilon_2}\mathbf{T}_{bB}\Big)}{\bar{\sigma}(\mathbf{T}_{bA})} > \varepsilon_1 > 0, \\
&\frac{\underline{\sigma}\Big[\Big(\mathbf{I} - 0.5\varepsilon_2\mathbf{U}_{bB} - 0.5\dfrac{1}{\varepsilon_2}\mathbf{T}_{bB}\Big) - \varepsilon_1\mathbf{T}_{bA}\Big]\delta}{\bar{\sigma}\Big[\dfrac{1}{\varepsilon_3}\mathbf{T}_{bF} + \mathbf{F}_B(\mathbf{I}+\varepsilon_3\mathbf{U}_{bF})\mathbf{F}_B^{\mathrm{T}} + l_f\mathbf{F}_{b\Delta}\Big]} > \varepsilon > 0, \qquad r \ge 0.5,
\end{aligned} \tag{24}$$

where $\bar{\sigma}$ and $\underline{\sigma}$ denote the maximum and minimum singular values of a matrix, respectively. Then, there always exists a solution matrix $\mathbf{P} > 0$ that satisfies the following Riccati equation

$$
\begin{aligned}
&(\mathbf{A}+\alpha\mathbf{I})^{\mathrm{T}}\mathbf{P}+\mathbf{P}(\mathbf{A}+\alpha\mathbf{I})-\mathbf{PB}\Big\{\mathbf{I}-\frac{\varepsilon_2}{2}\mathbf{U}_{bB}-\frac{1}{2\varepsilon_2}\mathbf{T}_{bB}-\varepsilon_1\mathbf{T}_{bA}\\
&-\frac{\varepsilon}{\delta}\Big[\mathbf{F}_B(I+\varepsilon_3\mathbf{U}_{bF})\mathbf{F}_B^{\mathrm{T}}+\frac{1}{\varepsilon_3}\mathbf{T}_{bF}+l_f\mathbf{F}_{b\Delta}\Big]\Big\}\mathbf{B}^{\mathrm{T}}\mathbf{P}+\frac{1}{\varepsilon_1}\mathbf{U}_{bA}+\frac{1}{\varepsilon\delta}\mathbf{C}^{\mathrm{T}}\mathbf{C}+\mathbf{Q}=\mathbf{0}
\end{aligned}
\tag{25}
$$

The robust active state-feedback controller in (22) guarantees a robust α-degree relative stability (16) and a δ-degree disturbance attenuation (15) for the uncertain structural system (5) with all admissible matched structured uncertainties as shown in (10) – (12).

Proof Because of matched uncertainty conditions, $\mathbf{I}-0.5\varepsilon_2\mathbf{U}_{bB}-0.5\,\frac{1}{\varepsilon_2}\,\mathbf{T}_{bB} > 0$ for some ε_2. Based on optimal control theory [1] it is obvious that selection of ε_1 and ε in (24) guarantees that the Riccati equation (25) has a solution matrix $\mathbf{P} > 0$ for any selected positive semi-definite matrix $\mathbf{Q}$. Following a line of proof similar to that used in Theorem 3.1 and using Lemma 2 lead to the following:

$$
\begin{aligned}
&(\mathbf{A}_c+\alpha\mathbf{I})^{\mathrm{T}}\mathbf{P}+\mathbf{P}(\mathbf{A}_c+\alpha\mathbf{I})+\frac{\varepsilon}{\delta}\mathbf{P}\Big[\mathbf{F}(\mathbf{I}+\varepsilon_3\mathbf{U}_F)\mathbf{F}^{\mathrm{T}}+\frac{1}{\varepsilon_3}\mathbf{T}_F+l_f\mathbf{F}_\Delta\Big]\mathbf{P}+\frac{1}{\varepsilon\delta}\mathbf{C}^{\mathrm{T}}\mathbf{C}\\
&\quad=\mathbf{PB}\Big[\mathbf{I}-\frac{\varepsilon_2}{2}\mathbf{U}_{bB}-\frac{1}{2\varepsilon_2}\mathbf{T}_{bB}-\varepsilon_1\mathbf{T}_{bA}\Big]\mathbf{B}^{\mathrm{T}}\mathbf{P}-\frac{1}{\varepsilon_1}\mathbf{U}_{bA}+\Delta\mathbf{A}_B^{\mathrm{T}}\mathbf{B}^{\mathrm{T}}\mathbf{P}+\mathbf{PB}\Delta\mathbf{A}_B\\
&\quad-r\mathbf{PB}(2\mathbf{I}+\Delta\mathbf{B}_B+\Delta\mathbf{B}_B^{\mathrm{T}})\mathbf{B}^{\mathrm{T}}\mathbf{P}-\mathbf{Q}\le-\mathbf{Q}<0
\end{aligned}
$$

Thus, by Lemma 3, the proof is complete.

Remark 3.1 The disturbance attenuation index $\delta > 0$ and the robust relative stability index $\alpha > 0$ are prescribed based on engineering requirements. Riccati equations (21) or (25) are solved for matrix $\mathbf{P}$ after selection of a set of adjustable parameters. $\mathbf{Q}$ is a small positive definite matrix. Then, the robust active control law in equation (22) is used with $\mathbf{P}$ from Riccati equation (21) or (25).

Remark 3.2 For tuning the adjustable scalars in Theorem 3.2, ε_2 is usually selected such that $\underline{\sigma}(\mathbf{I}-0.5\varepsilon_2\mathbf{U}_{bB}-0.5\frac{1}{\varepsilon_2}\mathbf{T}_{bB})$ is large, and ε_3 is selected such that $\bar{\sigma}(\varepsilon_3\mathbf{F}_B\mathbf{U}_{bF}\mathbf{F}_B^{\mathrm{T}} + \frac{1}{\varepsilon_3}\mathbf{T}_{bF})$ is small.

It is noticed that for uncertain structural systems $\Delta\mathbf{F}=\mathbf{0}$ is a special case of what was discussed above. The following remark addresses this case.

Remark 3.3 Theorems 3.1 – 3.2 are valid for the case in which disturbance input uncertainties are not considered, i.e., $\Delta\mathbf{F}=\mathbf{0}$. For this special case, we simply let $\mathbf{T}_F=\mathbf{0}$, $\mathbf{U}_F=\mathbf{0}$, and $\mathbf{F}_\Delta=\mathbf{0}$ for Theorem 3.1 and $\mathbf{T}_{bF}=\mathbf{0}$, $\mathbf{U}_{bF}=\mathbf{0}$, and $\mathbf{F}_{b\Delta}=\mathbf{0}$ for Theorem 3.2. Therefore, for the case of $\Delta\mathbf{F}=\mathbf{0}$, Riccati equations (21) and (25) in Theorems 3.1 and 3.2 are reduced to

$$
\begin{aligned}
&(\mathbf{A}+\alpha\mathbf{I})^{\mathrm{T}}\mathbf{P}+\mathbf{P}(\mathbf{A}+\alpha\mathbf{I})-\mathbf{P}\Big[\mathbf{B}(\mathbf{I}-\frac{\varepsilon_2}{2}\mathbf{U}_B)\mathbf{B}^{\mathrm{T}}-\varepsilon_1\mathbf{T}_A-\frac{1}{2\varepsilon_2}\mathbf{T}_B-\frac{\varepsilon}{\delta}\mathbf{F}\mathbf{F}^{\mathrm{T}}\Big]\mathbf{P}\\
&\qquad+\frac{1}{\varepsilon_1}\mathbf{U}_A+\frac{1}{\varepsilon\delta}\mathbf{C}^{\mathrm{T}}\mathbf{C}+\mathbf{Q}=\mathbf{0},
\end{aligned}
\tag{26}
$$

$$(\mathbf{A}+\alpha\mathbf{I})^{\mathrm{T}}\mathbf{P}+\mathbf{P}(\mathbf{A}+\alpha\mathbf{I})-\mathbf{P}\mathbf{B}\left\{\mathbf{I}-\frac{\varepsilon_2}{2}\,\mathbf{U}_{bB}-\frac{1}{2\varepsilon_2}\,\mathbf{T}_{bB}-\varepsilon_1\mathbf{T}_{bA}-\frac{\varepsilon}{\delta}\,\mathbf{F}_B\mathbf{F}_B^{\mathrm{T}}\right\}\mathbf{B}^{\mathrm{T}}\mathbf{P} + \frac{1}{\varepsilon_1}\,\mathbf{U}_{bA}+\frac{1}{\varepsilon\delta}\,\mathbf{C}^{\mathrm{T}}\mathbf{C}+\mathbf{Q}=\mathbf{0}, \tag{27}$$

respectively. These equations coincide with the results in [14], in which no uncertainty is considered for the disturbance input matrix, i.e., $\Delta\mathbf{F}=\mathbf{0}$ and also $\varepsilon_2=1$.

Selection of the set of adjustable scalars ε_i $(i=1,2,3)$, ε, gain parameter r, and adjustable positive definite matrix $\mathbf{Q}$ requires some experience. However, these adjustable scalars, parameter, and matrix provide flexibility for obtaining a desired robust active controller for an uncertain structural system. Some general guidance for selection of this adjustable set is summarized in the following remarks.

Remark 3.4 The set of adjustable scalars ε_i $(i=1,2,3)$, and ε is usually chosen in (21) or (25) of Theorems 3.1 – 3.2, such that

$$\mathbf{B}\left(\mathbf{I}-\frac{\varepsilon_2}{2}\mathbf{U}_B\right)\mathbf{B}^{\mathrm{T}}-\varepsilon_1\mathbf{T}_A-\frac{1}{2\varepsilon_2}\mathbf{T}_B-\frac{\varepsilon}{\delta}\left[\mathbf{F}(\mathbf{I}+\varepsilon_3\mathbf{U}_F)\mathbf{F}^{\mathrm{T}}+\frac{1}{\varepsilon_3}\mathbf{T}_F+l_f\mathbf{F}_\Delta\right] \tag{28a}$$

or $$\mathbf{I}-\frac{\varepsilon_2}{2}\mathbf{U}_{bB}-\frac{1}{2\varepsilon_2}\mathbf{T}_{bB}-\varepsilon_1\mathbf{T}_{bA}-\frac{\varepsilon}{\delta}\left[\frac{1}{\varepsilon_3}\mathbf{T}_{bF}+\mathbf{F}_B(\mathbf{I}+\varepsilon_3\mathbf{U}_{bF})\mathbf{F}_B^{\mathrm{T}}+l_f\mathbf{F}_{b\Delta}\right] \tag{28b}$$

is semi-positive definite if possible. Positive definite matrix $\mathbf{Q}$ is usually assigned as a small matrix. Then, matrix $\mathbf{P}$ is solved from Riccati equations (21) and (25), respectively. Gain parameter r is selected to satisfy Riccati equations. A small r means a small energy requirement for the controller. However, a large r provides a fast decay response to disturbances (earthquake and wind disturbances, etc.). Also, another consideration for selection of gain r is to let conditions in Section 4 hold for H_2 optimality in Theorems 4.1 – 4.2. Therefore, selection of gain parameter r depends on physical conditions and requirements. Due to the special block companion form of structural systems, and even the special block diagonal structure, selection of appropriate adjustable scalars is accomplished easily.

Remark 3.5 For a matched uncertain structural system, selection of adjustable scalars ε and ε_i $(i=1,2,3)$, is very easy from (24) since solution of the Riccati equation (25) always exists from (24).

4 Preservation of H_2 Optimality

The proposed controllers (22) in Theorems 3.1 – 3.2 are not only robust with H_∞ disturbance attenuation and robust relatively stability, but also optimal in the H_2 optimal sense as discussed in this section. Thus, many H_2 optimal properties [1] hold for these robust controlled uncertain structural systems via the designed controller. The following theorems provide these results with H_2 optimality.

Theorem 4.1 *Under conditions in Theorem 3.1, if*

$$2\alpha\mathbf{P}+\mathbf{P}\left\{r\left[\mathbf{B}(\mathbf{I}-\varepsilon_2\mathbf{U}_B)\mathbf{B}^{\mathrm{T}}-\frac{1}{\varepsilon_2}\mathbf{T}_B\right]-\left[\mathbf{B}(\mathbf{I}-\frac{\varepsilon_2}{2}\mathbf{U}_B)\mathbf{B}^{\mathrm{T}}-\frac{1}{2\varepsilon_2}\mathbf{T}_B\right] + \frac{\varepsilon}{\delta}\left[\mathbf{F}(\mathbf{I}+\varepsilon_3\mathbf{U}_F)\mathbf{F}^{\mathrm{T}}+\frac{1}{\varepsilon_3}\mathbf{T}_F+l_f\mathbf{F}_\Delta\right]\right\}\mathbf{P}+\frac{1}{\varepsilon\delta}\mathbf{C}^{\mathrm{T}}\mathbf{C}+\mathbf{Q}\ge\mathbf{0}, \tag{29}$$

then the robust active controller (24) is also H_2 optimal for the uncertain structural system (5) regarding a specific performance index

$$J = \int [\mathbf{x}^{\mathrm{T}}(t)\tilde{\mathbf{Q}}\mathbf{x}(t) + \mathbf{u}^{\mathrm{T}}(t)\tilde{\mathbf{R}}\mathbf{u}(t)]\,dt \tag{30}$$

with

$$\tilde{\mathbf{Q}} = -\tilde{\mathbf{A}}^{\mathrm{T}}\mathbf{P} - \mathbf{P}\tilde{\mathbf{A}} + \mathbf{P}\mathbf{B}\tilde{\mathbf{R}}^{-1}\mathbf{B}^{\mathrm{T}}\mathbf{P} \geq 0, \qquad \tilde{\mathbf{R}} = \frac{1}{r}\mathbf{I}, \tag{31}$$

where

$$\tilde{\mathbf{A}} = \mathbf{A} + \Delta\mathbf{A} - r\Delta\mathbf{B}\mathbf{B}^{\mathrm{T}}\mathbf{P}. \tag{32}$$

Proof To show that the designed controller (22) is optimal, matrix $\tilde{\mathbf{Q}}$ is expanded as follows:

$$\begin{aligned}\tilde{\mathbf{Q}} &= -\tilde{\mathbf{A}}^{\mathrm{T}}\mathbf{P} - \mathbf{P}\tilde{\mathbf{A}} + \mathbf{P}\mathbf{B}\tilde{\mathbf{R}}^{-1}\mathbf{B}^{\mathrm{T}}\mathbf{P} \\ &= -(\mathbf{A} + \Delta\mathbf{A} - r\Delta\mathbf{B}\mathbf{B}^{\mathrm{T}}\mathbf{P})^{\mathrm{T}}\mathbf{P} - \mathbf{P}(\mathbf{A} + \Delta\mathbf{A} - r\Delta\mathbf{B}\mathbf{B}^{\mathrm{T}}\mathbf{P}) + r\mathbf{P}\mathbf{B}\mathbf{B}^{\mathrm{T}}\mathbf{P}.\end{aligned}$$

It follows from the proof of Theorem 3.1 and equation (21) that

$$\begin{aligned}\tilde{\mathbf{Q}} \geq 2\alpha\mathbf{P} + \mathbf{P}\bigg\{ & r\left[\mathbf{B}(\mathbf{I} - \varepsilon_2\mathbf{U}_B)\mathbf{B}^{\mathrm{T}} - \frac{1}{\varepsilon_2}\mathbf{T}_B\right] - \left[\mathbf{B}\left(\mathbf{I} - \frac{\varepsilon_2}{2}\mathbf{U}_B\right)\mathbf{B}^{\mathrm{T}} - \frac{1}{2\varepsilon_2}\mathbf{T}_B\right] \\ & + \frac{\varepsilon}{\delta}\left[\mathbf{F}(\mathbf{I} + \varepsilon_3\mathbf{U}_F)\mathbf{F}^{\mathrm{T}} + \frac{1}{\varepsilon_3}\mathbf{T}_F + l_f\mathbf{F}_\Delta\right]\bigg\}\mathbf{P} + \frac{1}{\varepsilon\delta}\mathbf{C}^{\mathrm{T}}\mathbf{C} + \mathbf{Q}.\end{aligned}$$

Therefore, if (29) holds, $\tilde{\mathbf{Q}} \geq 0$, and equation (31) is true. Since $\tilde{\mathbf{R}} > 0$ and $\tilde{\mathbf{Q}} \geq 0$, the perturbed uncertain system (14) is optimal with respect to the specific performance index (30) by the active robust controller (22) based on well-known H_2 optimal control theory. Thus, this theorem is proved.

For other cases, the following theorem for H_2 optimality is listed. Due to the similarity of proofs, details are omitted here.

Theorem 4.2 Under conditions in Theorem 3.2, if

$$\begin{aligned}2\alpha\mathbf{P} + P\mathbf{B}\bigg\{ & r\left(\mathbf{I} - \varepsilon_2\mathbf{U}_{bB} - \frac{1}{\varepsilon_2}\mathbf{T}_{bB}\right) - \left(I - \frac{\varepsilon_2}{2}\mathbf{U}_{bB} - \frac{1}{2\varepsilon_2}\mathbf{T}_{bB}\right) \\ & + \frac{\varepsilon}{\delta}\left[\mathbf{F}_B(I + \varepsilon_3\mathbf{U}_{bF})\mathbf{F}_B^{\mathrm{T}} + \frac{1}{\varepsilon_3}\mathbf{T}_{bF} + l_f\mathbf{F}_{b\Delta}\right]\bigg\}\mathbf{B}^{\mathrm{T}}\mathbf{P} + \frac{1}{\varepsilon\delta}\mathbf{C}^{\mathrm{T}}\mathbf{C} + \mathbf{Q} \geq \mathbf{0},\end{aligned} \tag{33}$$

then the robust active controller (22) is also H_2 optimal for the uncertain structural system (5) regarding a specific performance index J in (30) with $\tilde{\mathbf{Q}}$ and $\tilde{\mathbf{R}}$ in (31).

Remark 4.1 Notice that H_2 optimality is for the uncertain structural system (5) regarding a specific performance index J in (30) with $\tilde{\mathbf{Q}}$ and $\tilde{\mathbf{R}}$ in (31), where $\tilde{\mathbf{Q}}$ is uncertain. Also, it is noticed that uncertainties in the uncertain system are unknown but only their bound and structures are known. The importance of the above theorems is that when the respective condition of (29) or (33) holds, the robust controller (22) provides H_2 optimality in face of any admissible uncertainties as described in the respective theorems

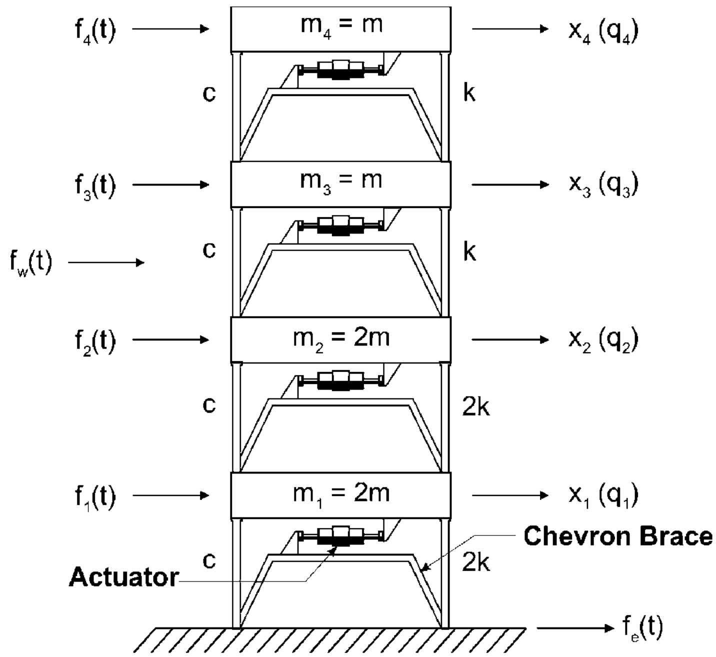

Figure 5.1. Building model for numerical example.

in Section 3 even though their exact values are not known. This means that the robust controller (22) provides a gain margin of infinity and at least a 60°-phase margin for whole uncertain structural systems with all admissible uncertainties even though the exact performance due to unknown uncertainties is not known.

5 Numerical Example

In order to illustrate effectiveness of the proposed approach for robust control, a numerical example of a four-degree-of-freedom system is taken and extended from [6] (see Figure 5.1). For this model of a tall building, stiffness, mass, and damping values of $k = 350 \times 10^6$N/m, $m = 1.05 \times 10^6$kg, and $c = 1.575 \times 10^6$N-s/m, respectively, are assumed. Total weight of the building is 61.74MN. In order to design a robust controller that is valid for both earthquake and wind disturbances, the considered external disturbance force applied to each floor level is $f_{di}(t) = f_{wi}(t) + f_{ei}(t),\ i = 1, \dots, 4$, where $f_{wi}(t)$ is from a strong wind event and $f_{ei}(t)$ is from an earthquake event. The total external force for each floor level is $f_i(t) = f_{ui}(t) + f_{di}(t)$, where $f_{ui}(t)$ is the control force. The system is described as

$$\mathbf{M}\ddot{\mathbf{q}} + \mathbf{C}_d\dot{\mathbf{q}} + \mathbf{K}_s\mathbf{q} = \mathbf{f} \quad \text{or} \quad \ddot{\mathbf{q}} + \mathbf{M}^{-1}\mathbf{C}_d\dot{\mathbf{q}} + \mathbf{M}^{-1}\mathbf{K}_s\mathbf{q} = \mathbf{M}^{-1}\mathbf{f}, \tag{34}$$

where $\mathbf{M}$ only has elements on the diagonal, $\mathbf{q}$ is a relative displacement vector to the ground,

$$
\mathbf{K}_s = \begin{bmatrix} 4k & -2k & 0 & 0 \\ -2k & 3k & -k & 0 \\ 0 & -k & 2k & -k \\ 0 & 0 & -k & k \end{bmatrix} = 175 \cdot 10^6 \begin{bmatrix} 8 & -4 & 0 & 0 \\ -4 & 6 & -2 & 0 \\ 0 & -2 & 4 & -2 \\ 0 & 0 & -2 & 2 \end{bmatrix},
$$

$$
\mathbf{C}_d = \begin{bmatrix} 2c & -c & 0 & 0 \\ -c & 2c & -c & 0 \\ 0 & -c & 2c & -c \\ 0 & 0 & -c & c \end{bmatrix} = 1.575 \cdot 10^6 \begin{bmatrix} 2 & -1 & 0 & 0 \\ -1 & 2 & -1 & 0 \\ 0 & -1 & 2 & -1 \\ 0 & 0 & -1 & 1 \end{bmatrix}, \tag{35}
$$

$$
\mathbf{M} = 1.05 \cdot 10^6 \begin{bmatrix} 2 & 0 & 0 & 0 \\ 0 & 2 & 0 & 0 \\ 0 & 0 & 1 & 0 \\ 0 & 0 & 0 & 1 \end{bmatrix}, \quad \mathbf{f} = \begin{bmatrix} f_1(t) \\ f_2(t) \\ f_3(t) \\ f_4(t) \end{bmatrix}.
$$

From equations (34) and (35), we have

$$
\mathbf{D}_{k0} = \begin{bmatrix} 2000/3 & -1000/3 & 0 & 0 \\ -1000/3 & 500 & -500/3 & 0 \\ 0 & -1000/3 & 2000/3 & -1000/3 \\ 0 & 0 & -1000/3 & 1000/3 \end{bmatrix},
$$

$$
\mathbf{D}_{c0} = \begin{bmatrix} 1.5 & -0.75 & 0 & 0 \\ -0.75 & 1.5 & -0.75 & 0 \\ 0 & -1.5 & 3.0 & -1.5 \\ 0 & 0 & -1.5 & 1.5 \end{bmatrix}, \quad \mathbf{A}_0 = \begin{bmatrix} \mathbf{0} & \mathbf{I} \\ -\mathbf{D}_{k0} & -\mathbf{D}_{c0} \end{bmatrix} \tag{36}
$$

If it is assumed that each story has a controller and is connected to a Chevron brace, then

$$
\mathbf{B}_{ch} = \begin{bmatrix} 1 & -1 & 0 & 0 \\ 0 & 1 & -1 & 0 \\ 0 & 0 & 1 & -1 \\ 0 & 0 & 0 & 1 \end{bmatrix}, \quad \mathbf{B}_0 = \begin{bmatrix} \mathbf{0} \\ \mathbf{M}^{-1}\mathbf{B}_{ch} \end{bmatrix}, \quad \text{and} \quad \mathbf{B}_{u0} = \mathbf{M}^{-1}\mathbf{B}_{ch}. \tag{37}
$$

State variables are chosen to be the displacement and velocity of each level (relative to the ground), $\mathbf{z}(t) = \mathbf{x}(t)$, i.e., $\mathbf{C} = \mathbf{I}$. Consider $\mathbf{w}(t) = [\, w_w^{\mathrm{T}}(t) \quad w_e(t)\,]^{\mathrm{T}}$, where $w_w(t)$ and $w_e(t)$ are wind and earthquake forces, respectively. Then,

$$
\mathbf{F}_{w0} = \mathbf{M}^{-1}\mathbf{F}_0,
$$

where

$$
\mathbf{F}_0 = \begin{bmatrix} & 2 \\ \mathbf{I}_4 & 2 \\ & 1 \\ & 1 \end{bmatrix}, \quad w_w(t) = \begin{bmatrix} f_{w1}(t) \\ f_{w2}(t) \\ f_{w3}(t) \\ f_{w4}(t) \end{bmatrix}
$$

and $w_e(t)$ is an earthquake force for a mass m. For simplicity, only an earthquake loading is considered here and it follows that $\mathbf{F}_{w0}$ and $\mathbf{w}(t)$ reduce to

$$
\mathbf{F}_{w0} = \mathbf{M}^{-1} \begin{bmatrix} 2 \\ 2 \\ 1 \\ 1 \end{bmatrix} = \frac{1}{m} \begin{bmatrix} 1 \\ 1 \\ 1 \\ 1 \end{bmatrix} = \frac{1}{m}\mathbf{F}_{wI}, \tag{38}
$$

$$
\mathbf{F}_{wI} = [\, 1, 1, 1, 1 \,]^{\mathrm{T}}, \quad \text{and} \quad \mathbf{w}(t) = w_e(t).
$$

Uncertainties are taken to be as follows: $\Delta m = \pm 10\% \cdot m$, $\Delta k = \pm 10\% \cdot k$, and $\Delta c = \pm 10\% \cdot c$. Thus, $\Delta\mathbf{K}_s = a_k \cdot 0.1\mathbf{K}_s$, $\Delta\mathbf{C}_d = a_c \cdot 0.1\mathbf{C}_d$, and $\Delta\mathbf{M} = a_m \cdot 0.1\mathbf{M}$, where $|a_k| \le 1$, $|a_c| \le 1$, and $|a_m| \le 1$. Then, $(\mathbf{M}+\Delta\mathbf{M})^{-1} = (0.90909 \sim 1.11111)\mathbf{M}^{-1}$. These are parametric perturbations, i.e., structured uncertainties. Also, it is obvious that the disturbance input matrix $\mathbf{F}_w$ has uncertainties when parameter m changes with uncertainties. $\mathbf{D}_k$ is perturbed by a factor $(0.818181 \sim 1.22222)$, as is $\mathbf{D}_c$. The central matrix $1.0101\mathbf{M}^{-1}$ is taken as a nominal $\mathbf{M}_0^{-1}$ and $\Delta\mathbf{M}_0^{-1} = a_{m1} \cdot 0.10101\mathbf{M}^{-1} = a_{m1} \cdot 0.1\mathbf{M}_0^{-1}$, where $|a_{m1}| \le 1$. Further, take central matrices as nominal models for new $\mathbf{D}_k$ and $\mathbf{D}_c$ for design, i.e.,

$$\mathbf{D}_k = 1.0202\mathbf{D}_{k0}, \quad \mathbf{D}_c = 1.0202\mathbf{D}_{c0}, \quad \mathbf{A} = \begin{bmatrix} \mathbf{0} & \mathbf{I} \\ -\mathbf{D}_k & -\mathbf{D}_c \end{bmatrix}, \quad \mathbf{B}_u = \mathbf{M}_0^{-1}\mathbf{B}_{ch},$$

then

$$\begin{gathered} \Delta\mathbf{D}_k = a_{k1}0.198\mathbf{D}_k, \quad \Delta\mathbf{D}_c = a_{c1}0.198\mathbf{D}_c, \quad \Delta\mathbf{A} = \begin{bmatrix} \mathbf{0} & \mathbf{0} \\ -\Delta\mathbf{D}_k & -\Delta\mathbf{D}_c \end{bmatrix}, \\ \text{and} \quad \Delta\mathbf{B}_u = 0.1a_{m1}\mathbf{M}_0^{-1}\mathbf{B}_{ch}, \end{gathered} \tag{39}$$

where $|a_{k1}| \le 1$, and $|a_{c1}| \le 1$. These matrices are actually structured uncertainties. Similarly, a new central disturbance input matrix is taken as follows: $\mathbf{F}_w = \mathbf{M}_0^{-1}[2,2,1,1]^{\mathrm{T}}$, $\Delta\mathbf{F}_w = 0.1f_1\mathbf{F}_w$ and $|f_1| \le 1$. This case is obviously a matched uncertainty model, so that $\Delta\mathbf{B}_{Bu}$, $\Delta\mathbf{D}_{Bk}$, $\Delta\mathbf{D}_{Bc}$, $\mathbf{F}_{Bw}$ and $\Delta\mathbf{F}_{Bw}$ are available and can be obtained by a left multiplication of $\mathbf{B}_w$ with the respective uncertainties and matrices.

Next, the SVD decomposition is applied to all of the above uncertainty structures to obtain $\mathbf{T}_{bk}$, $\mathbf{U}_{bk}$, $\mathbf{T}_{bc}$, $\mathbf{U}_{bc}$, $\mathbf{T}_{bb}$, $\mathbf{U}_{bb}$, $\mathbf{T}_{bf}$, $\mathbf{U}_{bf}$, and $\mathbf{F}_{b\Delta}$. The final step is to design a robust controller for this uncertain structure system with all above structured uncertainties in $\Delta\mathbf{A}$, $\Delta\mathbf{B}$, and $\Delta\mathbf{F}$. A relative degree of stability and a disturbance attenuation index are taken to be $\alpha = 1.5$ and $\delta = 0.01$, respectively. Based on Theorem 3.2 and Remarks 3.2, 3.4, and 3.5, $\mathbf{Q} = 0.05\mathbf{I}$, $\varepsilon_1 = 3.9 \cdot 10^{-9}$, $\varepsilon_2 = 1$, $\varepsilon_3 = 1$, and $\varepsilon = 10^{-7}$. From Theorem 3.2, Riccati equation (25) has the solution matrix $\mathbf{P}$. For optimality, we choose $r = 1.04$. Also, equation (33) satisfies Theorem 4.2. Then, the robust control law (22) is $\mathbf{u}(t) = -\mathbf{K}\mathbf{x}(t) = -r\mathbf{B}^{\mathrm{T}}\mathbf{P}\mathbf{x}(t)$ with

$$\begin{gathered} \mathbf{K} = r\mathbf{B}^{\mathrm{T}}\mathbf{P} = r \cdot 10^8 \\ \times \begin{bmatrix} 0.1611 & 1.1376 & -0.7897 & 0.7668 & 0.4093 & 0.0358 & 0.0693 & 0.0949 \\ -0.8795 & -0.7291 & 2.1767 & -0.4508 & -0.3735 & 0.4524 & 0.1012 & 0.0631 \\ 3.2609 & -2.8101 & -0.0195 & 0.7873 & 0.1028 & -0.1471 & 0.2127 & 0.1394 \\ -2.4035 & 1.7595 & -0.7564 & 0.4764 & 0.0511 & -0.0252 & -0.0859 & 0.1903 \end{bmatrix}. \end{gathered} \tag{40}$$

6 Evaluation Indices

In order to evaluate the controller, special consideration is given to absolute accelerations $\mathbf{a}_a(t)$, interstory drifts $\mathbf{d}_x(t)$, and control forces $\mathbf{u}(t)$. Maximum peak values and maximum RMS values for all four floors and over the entire simulation period are monitored and recorded. Elements of the relative acceleration vector $\mathbf{a}(t)$ are determined by numerical differentiation of the output velocities. Then, the absolute accelerations $\mathbf{a}_a(t)$ are computed as follows:

$$\begin{aligned}\mathbf{a}_a(t) &= \begin{bmatrix} a_{a1}(t) \\ a_{a2}(t) \\ a_{a3}(t) \\ a_{a4}(t) \end{bmatrix} = \mathbf{a}(t) + (1+\Delta f)a_e(t) \begin{bmatrix} 1 \\ 1 \\ 1 \\ 1 \end{bmatrix} = \begin{bmatrix} a_1(t) \\ a_2(t) \\ a_3(t) \\ a_4(t) \end{bmatrix} + (1+\Delta f)a_e(t) \begin{bmatrix} 1 \\ 1 \\ 1 \\ 1 \end{bmatrix} \\ &= \begin{bmatrix} \dot{x}_5(t) \\ \dot{x}_6(t) \\ \dot{x}_7(t) \\ \dot{x}_8(t) \end{bmatrix} + (1+\Delta f)a_e(t) \begin{bmatrix} 1 \\ 1 \\ 1 \\ 1 \end{bmatrix},\end{aligned} \tag{41}$$

where $a_e(t)$ is the acceleration time-history of the earthquake, and Δf is the enlarged ratio of earthquake acceleration (for the nominal model $\Delta f = 0$). The interstory drift vector is

$$\mathbf{d}_x = [d_{x1},\, d_{x2},\, d_{x3},\, d_{x4}]^{\mathrm{T}} = [x_1,\, x_2 - x_1,\, x_3 - x_2,\, x_4 - x_3]^{\mathrm{T}}. \tag{42}$$

In order to facilitate an evaluation of the merits of the proposed approach for control, six performance indices are defined as listed in Tables 7.1 and 7.2. The maximum peak value of absolute acceleration is defined as follows:

$$J_1 = \max_{i,t}\{|a_{ai}(t)|\}. \tag{43}$$

The second evaluation criterion, J_2, is the maximum RMS value of absolute acceleration and is given by:

$$J_2 = \max_i \left[\frac{1}{T_f} \int_0^{T_f} a_{ai}^2(t)\, dt \right]^{1/2}. \tag{44}$$

The third and fourth indices, J_3 and J_4, are the maximum peak value and the maximum RMS value of the interstory drifts, respectively:

$$J_3 = \max_{i,t}\{|d_{xi}(t)|\}, \qquad J_4 = \max_i \left[\frac{1}{T_f} \int_0^{T_f} d_{xi}^2(t)\, dt \right]^{1/2}. \tag{45}$$

Finally, J_5 and J_6 are the maximum peak value and the maximum RMS value of the control forces, respectively,

$$J_5 = \max_{i,t}\{|u_i(t)|\}, \qquad J_6 = \max_i \left[\frac{1}{T_f} \int_0^{T_f} u_i^2(t)\, dt \right]^{1/2}.$$

7 Simulations

Numerical simulations are carried out for both a nominal case without perturbations and a worst case where $\Delta\mathbf{M} = 0.1\mathbf{M}$, $\Delta\mathbf{K}_s = 0.1\mathbf{K}_s$, and $\Delta\mathbf{C}_d = -0.1\mathbf{C}_d$ (i.e., $\Delta m = 0.1m$,

$\Delta k = 0.1k,\ \Delta c = -0.1c$). The basic concept is to take the worst case for $\mathbf{D}_c + \Delta\mathbf{D}_c$, i.e., the smallest one from $\Delta c = -0.1c$ and $\Delta m = 0.1m$, and the largest $\mathbf{K}_s + \Delta\mathbf{K}_s$ from $\Delta k = 0.1k$ when $\Delta m = 0.1m$. It follows that $\Delta\mathbf{D}_k = 0$, $\Delta\mathbf{D}_c = -0.1818\mathbf{D}_{c0}$, $\Delta\mathbf{B}_B = [\mathbf{0}\ \ -0.1\mathbf{I}]^{\mathrm{T}}$, and $\Delta\mathbf{F}_w = 0.1\mathbf{F}_{w0}$. Thus, one simulated uncertain system model in the worst case is taken as

$$\begin{aligned}\dot{\mathbf{x}}(t) &= \left\{\begin{bmatrix}\mathbf{0} & \mathbf{I}\\ -\mathbf{D}_{k0} & -0.81818\mathbf{D}_{c0}\end{bmatrix} - \begin{bmatrix}\mathbf{0}\\ 0.9\mathbf{B}_{u0}\end{bmatrix}\mathbf{K}\right\}\mathbf{x}(t) + 1.1\begin{bmatrix}\mathbf{0}\\ \mathbf{F}_{w0}\end{bmatrix}\mathbf{w}(t)\\ &= \left\{\begin{bmatrix}\mathbf{0} & \mathbf{I}\\ -\mathbf{D}_{k0} & -0.81818\mathbf{D}_{c0}\end{bmatrix} - \begin{bmatrix}\mathbf{0}\\ 0.9\mathbf{B}_{u0}\end{bmatrix}\mathbf{K}\right\}\mathbf{x}(t) - 1.1a_e(t)\begin{bmatrix}\mathbf{0}\\ \mathbf{F}_{wI}\end{bmatrix},\\ \mathbf{z}(t) &= \mathbf{x}(t),\end{aligned} \tag{47}$$

where $\mathbf{D}_{k0}$ and $\mathbf{D}_{c0}$ are given by (36), $\mathbf{K}$ is from (40), $\mathbf{w}(t) = w_e(t)$, and $a_e(t)$ is the earthquake acceleration time-history. The simulated nominal system model is

$$\begin{aligned}\dot{\mathbf{x}}(t) &= \left\{\begin{bmatrix}\mathbf{0} & \mathbf{I}\\ -\mathbf{D}_{k0} & -\mathbf{D}_{c0}\end{bmatrix} - \begin{bmatrix}\mathbf{0}\\ \mathbf{B}_{u0}\end{bmatrix}\mathbf{K}\right\}\mathbf{x}(t) + \begin{bmatrix}\mathbf{0}\\ \mathbf{F}_{w0}\end{bmatrix}\mathbf{w}(t)\\ &= \left\{\begin{bmatrix}\mathbf{0} & \mathbf{I}\\ -\mathbf{D}_{k0} & -\mathbf{D}_{c0}\end{bmatrix} - \begin{bmatrix}\mathbf{0}\\ \mathbf{B}_{u0}\end{bmatrix}\mathbf{K}\right\}\mathbf{x}(t) - a_e(t)\begin{bmatrix}\mathbf{0}\\ \mathbf{F}_{wI}\end{bmatrix},\\ \mathbf{z}(t) &= \mathbf{x}(t).\end{aligned} \tag{48}$$

A time history of acceleration $a_e(t)$ from the 1940 El Centro, California, earthquake is applied to the base of the structure.

It is noted that numerical simulations for the perturbed building apply the disturbance earthquake forces and corresponding accelerations enlarged by 10%.

For comparison, the numerical simulations are also conducted on the same structure using an LQR controller. Weighting matrices for the LQR design, $\mathbf{Q} = 10^{12} \times \mathbf{I}$ and $\mathbf{R} = \mathbf{I}$, are selected by a trial and error procedure in order to produce an allowable maximum peak control force that is physically realizable. Under these conditions, the maximum control force for the LQR controller is 811 kN. Likewise, the robust control force is limited to 810 kN for comparison. Then, a small gain robust controller is included with an adjustable gain of $r = 1.637 \times 10^{-2}$ which requires a maximum force 810 kN. Finally, a clipped robust controller with an 810 kN force limit is simulated as well, which is also physically realizable. However, by contrast, the robust controller provides information about how much force is required for a very high level of performance, without a trial and error procedure.

Output of numerical simulations for the uncontrolled, LQR controlled, and clipped robust controlled cases is shown in Figures 7.1 – 7.4. These graphs show fourth floor interstory drift and absolute acceleration for 30-sec of motion. Figures 7.1 and 7.2 illustrate results for the nominal model. Figures 7.3 and 7.4 show the corresponding information for the perturbed model. Results indicate that reduction in response of the structure is very good for both interstory drift and absolute acceleration. Note that the robust controller requires a much larger maximum control force if it is not clipped.

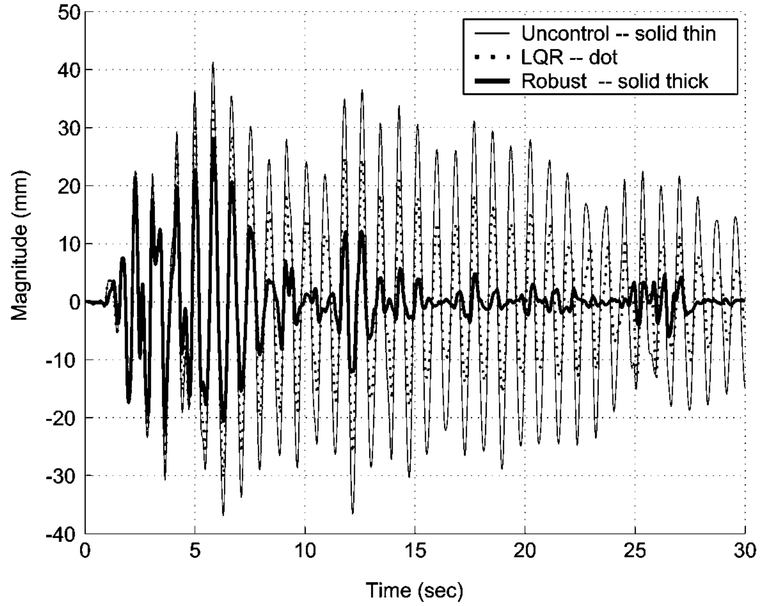

Figure 7.1. Nominal model: Uncontrolled and controlled interstory drift of the 4-th floor.

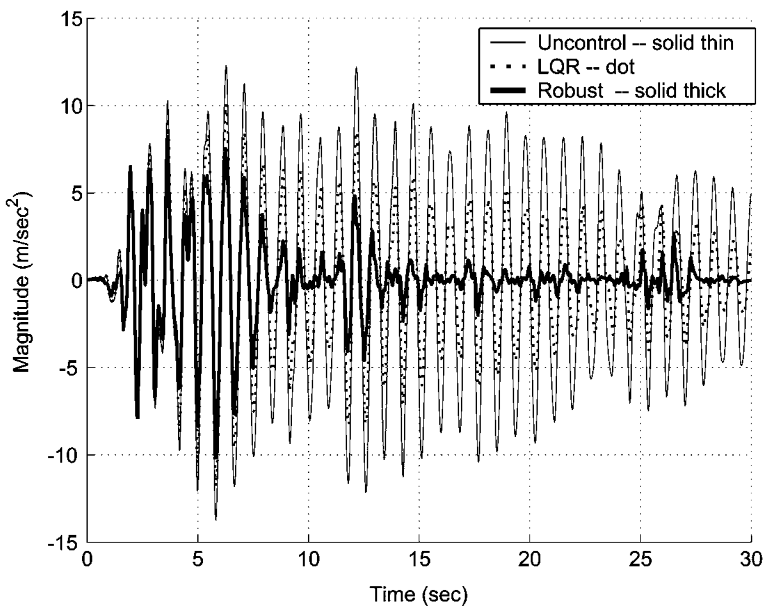

Figure 7.2. Nominal model: Uncontrolled and controlled absolute acceleration of the 4-th floor.

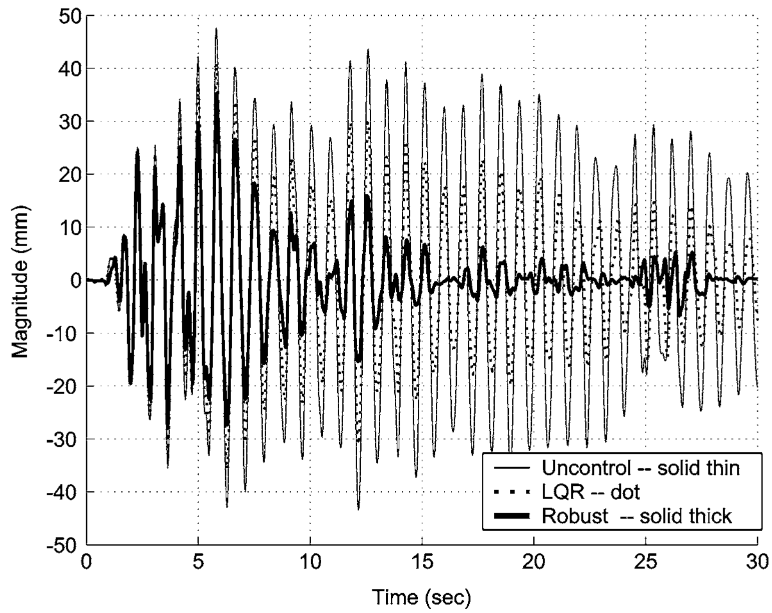

Figure 7.3. Perturbed model: Uncontrolled and controlled interstory drift of the 4-th floor.

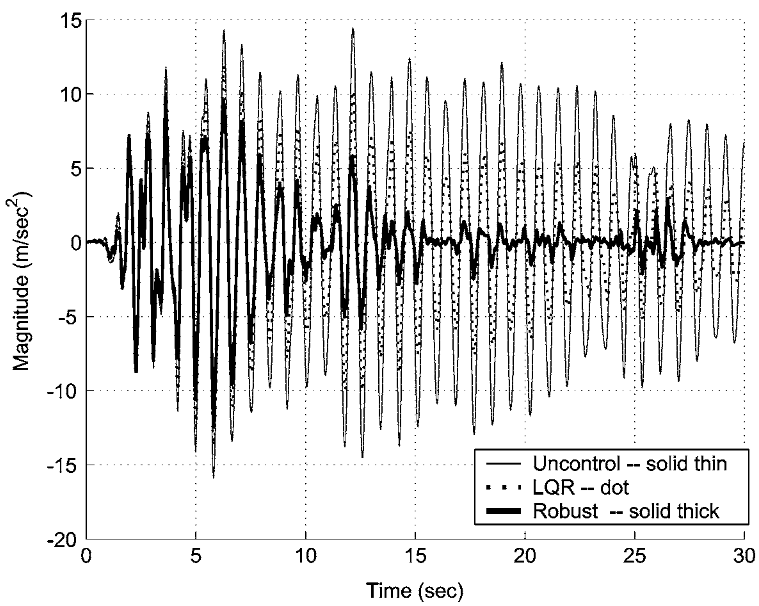

Figure 7.4. Perturbed model: Uncontrolled and controlled absolute acceleration of the 4-th floor.

Quantitative results from numerical simulations for the nominal and perturbed structure are listed in Tables 7.1 and 7.2, respectively. Cases presented include uncontrolled, LQR-controlled, robust controlled ($r = 1.04$), small gain robust controlled ($r = 1.637 \times 10^{-2}$), and clipped robust controlled ($r = 1.04$, $u_{max} = 810\,\text{kN}$). Simulation results in this paper and [13] appear to bode well for experimental implementation.

Table 7.1 Comparison of simulation performance: Nominal model.

Performance Index	Uncontrolled Model	LQR Control $Q = 1\times10^{12}I$, $R = I$	Robust Control $r = 1.04$	Small Gain Robust Control $r = 1.637\times10^{-2}$	Clipped Robust Control $r = 1.06$
Max Peak Absolute Accel. (m/s^2)	13.72	11.79	3.58	11.72	10.18
Max RMS Absolute Accel. (m/s^2)	5.84	3.82	0.68	3.81	2.15
Max Peak Interstory Drift. (mm)	73.0	63.1	1.2	62.8	49.9
Max RMS Interstory Drift. (mm)	31.8	20.6	0.3	20.5	11.2
Max Peak Force (kN)	—	711	12,274	706	810
Max RMS Force (kN)	—	251.7	2,194.4	247.6	720.7

Table 7.2 Comparison of simulation performance: Perturbed model.

Performance Index	Uncontrolled Model	LQR Control $Q = 1\times10^{12}I$, $R = I$	Robust Control $r = 1.04$	Small Gain Robust Control $r = 1.637\times10^{-2}$	Clipped Robust Control $r = 1.06$
Max Peak Absolute Accel. (m/s^2)	15.90	13.70	3.98	13.61	12.47
Max RMS Absolute Accel. (m/s^2)	7.13	4.63	0.75	4.61	2.77
Max Peak Interstory Drift. (mm)	82.8	72.5	1.4	72.0	61.4
Max RMS Interstory Drift. (mm)	38.9	25.0	0.3	24.9	14.5
Max Peak Force (kN)	—	811	14,398	810	810
Max RMS Force (kN)	—	305.4	2,559.8	300.4	734.9

8 Conclusions

In this paper, a general structural system model based on Lagrange's equation has been introduced. Its form is that of a special structural block companion matrix form, and an active robust controller for the uncertain structural system is described. General structured uncertainties and matched structured uncertainties are described and considered for uncertain structural systems. Considered structured uncertainties include those in the system, control input, and especially disturbance input matrices. In addition, special weighted SVD decomposition is applied to all structured uncertainties. An approach to design robust state-feedback algorithms for matched and general uncertain structural systems has been proposed. The active robust controller has robust α-degree relative stability, robust H_∞ δ-degree disturbance rejection, and robust H_2 optimality for a family of uncertain systems. Settling time of the controlled system is always less than $4/\alpha$. Moreover, the H_∞-norm of the transfer function from the disturbance vector $\mathbf{w}$ to the observed output vector $\mathbf{z}$ is not greater than δ, i.e., $\|\mathbf{T}_{zw}(s)\|_\infty \le \delta$. Thus, hazardous effects of disturbances such as earthquakes and strong winds to the structural system are controlled and attenuated due to robust H_∞ δ-degree disturbance rejection. In addition, response to the disturbance is quickly reduced due to robust α-degree relative stability and a judicious selection of the gain parameter r. The proposed controller is also H_2 optimal with a special performance index that is shown in Section 4. Thus, the designed robust controller provides infinity gain margin and at least a 60°-phase margin for entire uncertain structural system with all admissible uncertainties. A set of adjustable parameters provides flexibility in design of the robust controller. An example of an uncertain four-story building is used to illustrate results. Numerical simulations are carried on the building excited by the 1940 El Centro earthquake data and compared with the LQR controller by the six performance evaluation indices. Results show that the performance of the robust controller is very good.

References

[1] Anderson, B.D.O. and Moore, J.B. *Linear Optimal Control*. Prentice Hall, Englewood Cliffs, NJ, 1971.

[2] Fujino,Y., Soong, T.T., and Spencer, B.F. Jr. Structural control: Basic concepts and applications. *Proc. ASCE Struct. Cong. XIV*, Chicago, IL, 1996. P. 1277–1287.

[3] Grandhi, R.V., Haq, I. and Khot, N.S. Enhanced robustness in integrated structural/control system design. *AIAA Journal* **29** (1991) 1168–1173.

[4] Housner, G.W., Bergman, L.A., Caughey, T.K., Chassiakos, A.G., Claus, R.O., Masri, S.F., Skelton, R.E., Soong, T.T., Spencer, B.F. and Yao, J.T.P. Structural control: Past and present. *J. Engin. Mech.* **123** (1997) 897–971.

[5] Housner, G.W., Soong, T.T. and Masri, S.F. Second generation of active structural control in civil engineering. *First World Conference on Structural Control*, Los Angeles, CA, 1994, P.3–18.

[6] James, M.L., Smith, G.M., Wolford, J.C. and Whaley, P.W. *Vibration of Mechanical and Structural Systems.* Harper Collins College Publishers, 1994.

[7] Kwakernaak, H. Robust control and H_∞-optimization: Tutorial paper. *Automatica* **29** (1987) 255–273.

[8] Leitmann, G. Guaranteed asymptotic stability for some linear systems with bounded uncertainties. *Dynamics Syst., Measurement and Contr.* **101** (1979) 212–216.

[9] Soong, T.T. *Active Structural Control: Theory and Practice*. Longman Scientific and Technical, Essex, England, 1990.

[10] Spencer, B.F. Jr. and Sain, M.K. Controlling buildings: A new frontier in feedback. *IEEE Control Systems* **17** (1997) 19–35.

[11] Spencer, B.F. Jr., Sain, M.K., Kaspari, D.C. and Kantor, J.C. Reliability-based design of active control strategies. *Proc. ATC 17–1 Seminar on Seismic Isolation, Passive Energy Dissipation and Active Control*, San Francisco, Vol. 2, 1994. P. 761–772.

[12] Wang, S.-G., Lin, S., Shieh, L.S. and Sunkel, J.W. Observer-based controller for robust pole clustering in a vertical strip and disturbance rejection in structured uncertain systems. *Int. J. Robust and Nonlinear Control* **8** (1998) 1073–1084.

[13] Wang, S.-G., Roschke, P.N. and Yeh, H.Y. Robust control for structural systems with uncertainties. *Proc. of SPIE's 6th Annual Int. Symp. on Smart Structures and Materials, Conf. of Smart Systems for Bridges, Structures, and Highways, (SS06)*, Vol. 3671, 1999. P. 206–216.

[14] Wang, S.-G., Shieh, L.S. and Sunkel, J.W. Optimal pole-clustering in a vertical strip and disturbance rejection for Lagrange's systems. *Int. J. Dynamics and Control* **5** (1995) 295–312.

[15] Wang, S.-G., Shieh, L.S. and Sunkel, J.W. Robust optimal pole-placement in a vertical strip and disturbance rejection. *Int. J. of Systems Science* **26** (1995) 1839–1853.

[16] Wang, S.-G., Yeh, H.Y. and Roschke, P.N. Robust control for structural systems with parametric and unstructured uncertainties. *J. Vibration and Control* **7** (2001) 753–772.

[17] Yang, J.N., Wu, J.C., Reinhorn, A.M., Riley, M., Schmitendorf, W.E. and Jabbari, F. Experimental verifications of H_∞ and sliding mode control for seismic-excited buildings. *J. of Structural Engin.* **122** (1996) 69–75.

[18] Yao, J.T.P. Concept of structural control. *J. Struct. Div.* **98** (1972) 1567–1574.

[19] Zhou, K., Doyle, J.C. and Glover, K. *Robust and Optimal Control.* Prentice Hall, Upper Saddle River, NJ, 1996.

Nonlinear Dynamics and Systems Theory, 4(2) (2004) 217–229

A Criterion for Stability of Nonlinear Time-Varying Dynamic System

Yongmao Wang[1], Yan Shi[2] and Hirofumi Sasaki[3]

[1] *School of Science, Yanshan University, Qinhuangdao, 066004, China*
[2] *School of Information Science, Kyushu Tokai University, Kumamoto, 862-8652, Japan*
[3] *School of Engineering, Kyushu Tokai University, Kumamoto, 862-8652, Japan*

Received: May 2, 2003; Revised: April 27, 2004

Abstract: In this paper, based on the assumption that both the leading principal submatrix of r-order and its complementary submatrix in $A(t)$ have eigenvalues with only negative real parts, we establish a criterion for the stability of a class of nonlinear time-varying dynamic system $dx/dt = A(t)x + f(t,x)$. Also a feasible method for decomposition and aggregation of large-scale system is provided. Moreover, we shall show the efficiency of the presented criterion by a numerical example.

Keywords: *Vector Liapunov function; nonlinear time-varying dynamic system; stability of system.*

Mathematics Subject Classification (2000): 93D30, 34D20, 93D05; 93A15.

1 Introduction

The problem of constructing Liapunov functions for non-autonomous systems in general case still remains open. The concept of vector Liapunov functions (see [1, 2]) in terms of differential inequalities (see Lakshmikantham, *et al.* [3]) allowed to express the existence conditions for certain dynamical properties of the initial system via the existence of the corresponding properties in the comparison system. This approach has been intensively developed in the stability investigation of large-scale systems (see [4 − 6]). For recent results of the direct Liapunov method development and some approaches to the problem of Liapunov functions construction see [7 − 10].

In this paper, based on the assumption that both the leading principal submatrix of matrix $A(t)$ and its complementary submatrix have eigenvalues with only negative real parts, we give a feasible method of constructing vector Liapunov function of dynamic system (1), and establish sufficient conditions for stability of the system

$$\frac{dx}{dt} = A(t)x + f(x,t), \tag{1}$$

where $A(t) = a_{ij}(t)_{n\times n}$, $x = (x_1, x_2, \dots, x_n)^{\mathrm{T}}$, $f(x,t) = (f_1(t, x_1, \dots, x_n), \dots, f_n(t, x_1, \dots, x_n))^{\mathrm{T}}$, $a_{ij}(t)$ is differentiable and bounded on $[0, +\infty)$, $f(x,t)$ is continuous on field $t \geq 0$, $|x| \leq h$, $i = 1, 2, \dots, n$, and assume the system (1) have unique solution for any initial condition on the field.

Moreover, we also extend the result [11], and show that it is a special case of this paper for $r = 1$, $m = n - 1$. Finally, we give a numerical example to show the efficiency of the presented criterion.

2 Notations and Definitions

Let $A(t) = (a_{ij})_{n\times n}$, and partition $A(t)$ into the following:

$$A(t) = \begin{bmatrix} A_r & A_{r\times m} \\ A_{m\times r} & A_m \end{bmatrix}, \quad m = n - r, \quad 1 \leq r < n, \tag{2}$$

where A_r is a $r \times r$ matrix, which is called leading principal submatrix of order r and A_m is an $m \times m$ matrix, called complementary submatrix of A_r. The matrix $B(s,n)$ of order $(n-s+1)(n-s+2)/2$ is defined as

$$B(s,n) = \begin{bmatrix} a(ss,ss)+\delta_{ss} & \dots & a(sn,ss) & \dots & a(nn,ss) \\ \dots & \dots & \dots & \dots & \dots \\ a(ss,sn) & \dots & a(sn,sn)+\delta_{sn} & \dots & a(nn,sn) \\ a(ss,(s+1)(s+1)) & \dots & a(sn,(s+1)(s+1)) & \dots & a(nn,(s+1)(s+1)) \\ \dots & \dots & \dots & \dots & \dots \\ a(ss,nn) & \dots & a(sn,nn) & \dots & a(nn,nn)+\delta_{nn} \end{bmatrix}. \tag{3}$$

When $s = 1$ and $n = r$, let $B_r = B(1,r)$; when $s = r+1$ and $n = n$, let $B_m = B(r+1,n)$. Thus, B_r is a matrix of order $r(r+1)/2$, and B_m is a matrix of order $m(m+1)/2$, where $m = n - r$. The elements $a(ik,jl)$ in either matrix B_r or B_m satisfy the equalities $a(ik,jl) = a(ki,jl) = a(ki,lj)$ and

$$a(ik,jl) = \begin{cases} 0, & \text{if} \quad i \neq j, \quad k \neq l, \quad k \neq j, \quad j \neq l, \\ a_{kl}, & \text{if} \quad i = j, \quad k \neq l, \\ a_{ii} + a_{kk}, & \text{if} \quad i = j, \quad k = l, \quad i \neq k, \\ a_{ii}, & \text{if} \quad i = j = k = l, \end{cases}$$

where a_{ij} is an element either in A_r for $i, j = 1, 2, \dots, r$, or in A_m for $i, j = r+1, \dots, n$.

In matrix B_r, $\delta_{ik} = \alpha/2$ if $i = k$, and $\delta_{ik} = \alpha$ if $i \neq k$. In matrix B_m, $\delta_{ik} = \delta/2$ if $i = k$, and $\delta_{ik} = \delta$ if $i \neq k$. And $\alpha = \min(\inf|\operatorname{Re}\lambda_1|, \dots, \inf|\operatorname{Re}\lambda_r|)$ and $\delta = \min(\inf|\operatorname{Re}\mu_1|, \dots, \inf|\operatorname{Re}\mu_s|)$, where λ_i and μ_j are eigenvalues of A_r and A_m $(i = 1, \dots, r;\ j = 1, \dots, m)$, respectively.

Let p be an unknown variable, and $p_1, \dots, p_r$ be r roots of the equation

$$\left|\left(p - \frac{\alpha}{2}\right)E_r - A_r\right| = p^r + a_1 p^{r-1} + \dots + a_r = 0, \tag{4}$$

and let

$$\Delta_1 = a_1, \qquad \Delta_2 = \begin{vmatrix} a_1 & a_3 \\ a_0 & a_2 \end{vmatrix}, \qquad \dots, \qquad \Delta_r = \begin{vmatrix} a_1 & a_3 & \dots & a_{2r-1} \\ a_0 & a_2 & \dots & a_{2r-2} \\ \dots & \dots & \dots & \dots \\ 0 & 0 & \dots & a_r \end{vmatrix},$$

where $a_0 = 1$, and $a_k = 0$ for $k > r$.

Let q be an unknown variable, and $q_1, \dots, q_m$ be m roots of the equation

$$\left|\left(q - \frac{\delta}{2}\right)E_m - A_m\right| = q^m + b_1 q^{m-1} + \dots + b_m = 0, \tag{5}$$

and let

$$\Delta_1^* = b_1, \qquad \Delta_2^* = \begin{vmatrix} b_1 & b_3 \\ b_0 & b_2 \end{vmatrix}, \qquad \dots, \qquad \Delta_r^* = \begin{vmatrix} b_1 & b_3 & \dots & b_{2m-1} \\ b_0 & b_2 & \dots & b_{2m-2} \\ \dots & \dots & \dots & \dots \\ 0 & 0 & \dots & b_m \end{vmatrix}$$

where $b_0 = 1$, and $b_k = 0$ for $k > m$.

The quadratic forms ω_1 and v_1 are respectively defined as

$$\omega_1 = -\Delta_1\Delta_2 \dots \Delta_r(x_1^2 + x_2^2 + \dots = +x_r^2), \tag{6}$$

$$v_1 = \frac{\prod_{i=1}^{r} \Delta_i}{\det B_r} \begin{vmatrix} 0 & x_1^2 \quad 2x_1x_2 \quad \dots \quad 2x_1x_r \quad x_2^2 \quad \dots \quad 2x_{r-1}x_r \quad x_r^2 \\ 1 & \\ 0 & \\ \vdots & \\ 1 & B_r \\ 0 & \\ \vdots & \\ 1 & \end{vmatrix} = c_1 \sum_{i,j=1}^{r} v_{ij}x_ix_j, \tag{7}$$

where $c_1 = \Delta_1\Delta_2 \dots \Delta_r / \det B_r$, and for $i, j = 1, 2, \dots, r$, v_{ij} and v_{ji} are both half the algebraic cofactor of the element $2x_ix_j$, while v_{ii} is the algebraic cofactor of x_i^2.

The quadratic forms ω_2 and v_2 are respectively defined as

$$\omega_2 = -\Delta_1^*\Delta_2^* \dots = \Delta_m^*(x_{r+1}^2 + x_{r+2}^2 + \dots + x_n^2), \tag{8}$$

$$v_2 = \frac{\prod_{i=1}^{m} \Delta_i^*}{\det B_m} \begin{vmatrix} 0 & x_{r+1}^2 \quad 2x_{r+1}x_{r+2} \quad \dots \quad 2x_{r+1}x_n \quad x_{r+2}^2 \quad \dots \quad 2x_{n-1}x_n \quad x_n^2 \\ 1 & \\ 0 & \\ \vdots & \\ 1 & B_m \\ 0 & \\ \vdots & \\ 1 & \end{vmatrix} \tag{9}$$

$$= c_2 \sum_{i,j=r+1}^{n} v_{ij}x_ix_j,$$

where $c_2 = \Delta_1^*\Delta_2^*\dots\Delta_m^*/\det B_m$ and for $i, j = r+1, r+2, \dots, n$, v_{ij} and v_{ji} are both half the algebraic cofactor of the element $2x_ix_j$, while v_{ij} is the algebraic cofactor of x_i^2.

For all $t \in [t_0, +\infty)$, the meanings of the letters v_1^*, v_2^*, Δ, Δ^*, b_r, b_m, M_1, M_2, β, γ, ε_1 and ε_2 are given by the following equalities, respectively:

$$v_1^* = \inf_{x_1^2+\dots+x_r^2=1} v_1(t, x_1, \dots, x_r), \quad v_2^* = \inf_{x_{r+1}^2+\dots+x_n^2=1} v_2(t, x_{r+1}, \dots, x_n),$$

$$\Delta = \sup(\Delta_1\Delta_2\dots\Delta_r), \quad \Delta^* = \sup(\Delta_1^*\Delta_2^*\dots\Delta_m^*),$$

$$b_r = \inf|\det B_r|, \quad b_m = \inf|\det B_m|,$$

$$M_1 = \sup(|v_{ij}|, \ i, j = 1, 2, \dots, r), \quad M_2 = \sup(|v_{i=j}|, \ i, j = r+1, r+2, \dots, n),$$

$$\varepsilon_1 < \frac{b_r}{3r^2M_1}, \quad \varepsilon_2 < \frac{b_r}{3(n-r)^2M_2}, \quad \beta = r(n-r)M_1\left(\frac{\Delta r M_1 m_1^2}{b_r^2} + \frac{\Delta\varepsilon_1}{b_r}\right)\Big/v_2^*,$$

$$\gamma = r(n-r)M_2\left(\frac{\Delta^*(n-r)M_2m_2^2}{b_m^2} + \frac{\Delta^*\varepsilon_2}{b_m}\right)\Big/v_1^*,$$

where m_1 and m_2 are positive numbers.

3 Main Results

In the sequel, we shall give main results of this paper, that is, a criterion for stability of nonlinear time-varying dynamic system (1), and show the efficiency of the presented criterion by a numerical example.

3.1 A criterion for stability of nonlinear time-varying dynamic system

Theorem 3.1 *The trivial solution of (1) is asymptotically stable if*

(i) $\operatorname{Re}\lambda_i \le -\alpha < 0$, $\operatorname{Re}\mu_j \le -\delta < 0$, $i = 1, \dots, r$, $j = 1, \dots, m$;

(ii) *every* a_{ij} $(i, j = 1, \dots, n)$ *is differentiable and bounded on* $[t_0, +\infty)$, *especially, when* a_{ij} *is an element of* $A_{r\times m}$, $|a_{ij}| \le m_1$, *when* a_{ij} *is that of* $A_{m\times r}$, $|a_{ij}| \le m_2$;

(iii) $\alpha\delta - \beta\gamma > 0$, $|f_i(t, x_1, t_2, \dots, x_n)| \le \varepsilon(|x_1| + |x_2| + \dots + |x_n|)$, $i = 1, \dots, n$;

(iv) $\tilde{\lambda}_i < \left(1 - \dfrac{3r^2M_1\varepsilon}{b_r}\right)\Delta_1\dots\Delta_r$, $\tilde{\mu}_j < \left(1 - \dfrac{3(n-r)^2M_2\varepsilon}{b_m}\right)\Delta_1^*\dots\Delta_s^*$, *where* $\varepsilon = \min(\varepsilon_1, \varepsilon_2)$, $\tilde{\lambda}_i$ *and* $\tilde{\mu}_j$ *are eigenvalues of the matrixes* $\tilde{A}_r$ *and* $\tilde{A}_m$ *respectively, where*

$$\tilde{A}_r = ((c_1v_{ij})')_{r\times r}, \quad \tilde{A}_m = ((c_2v_{i=j})')_{m\times m}.$$

Proof Partition (1) into two correlative subsystems

$$\frac{d\zeta_1}{dt} = A_{11}(t)\zeta_1 + A_{12}(t)\zeta_2 + f^*(x, t), \tag{10}$$

$$\frac{d\zeta_2}{dt} = A_{21}(t)\zeta_1 + A_{22}(t)\zeta_2 + f^{**}(x, t), \tag{11}$$

where

$$A(t) = [a_{ij}(t)|_{n\times n} = \begin{bmatrix} A_{11}(t) & A_{12}(t) \\ A_{21}(t) & A_{22}(t) \end{bmatrix}, \quad i,j = 1,2,\dots,n,$$

$$A_{11} = \begin{bmatrix} a_{11}(t) & \dots & a_{1r}(t) \\ \dots & \dots & \dots \\ a_{r1}(t) & \dots & a_{rr}(t) \end{bmatrix}, \quad A_{22} = \begin{bmatrix} a_{r+1,r+1}(t) & \dots & a_{r+1,n}(t) \\ \dots & \dots & \dots \\ a_{n,r+1}(t) & \dots & a_{n,n}(t) \end{bmatrix},$$

$$f^* = [f_1(x,t),\dots,f_r(x,t)]^{\mathrm{T}}, \quad f^{**} = [f_{r+1}(x,t),\dots,f_n(x,t)]^{\mathrm{T}},$$

$$\zeta_1 = (x_1,\dots,x_r)^{\mathrm{T}}, \quad \zeta_2 = (x_{r+1},\dots,x_n)^{\mathrm{T}}.$$

Taking v_1 and v_2 as components of Liapunov function of systems (10) and (11) respectively, we have the following results:

$$\left.\frac{dv_1}{dt}\right|_{(10)} = \nabla_x v_1(x,t)A_{11}(t)\zeta_1 + \nabla_x v_1(x,t)A_{12}(t)\zeta_2 + \frac{\partial v_1}{\partial t} + \nabla_x f^*, \tag{12}$$

$$\left.\frac{dv_2}{dt}\right|_{(11)} = \nabla_x v_2(x,t)A_{21}(t)\zeta_1 + \nabla_x v_2(x,t)A_{22}(t)\zeta_2 + \frac{\partial v_2}{\partial t} + \nabla_x f^{**}. \tag{13}$$

Obviously, the eigenvalue λ_i of A_r, and the root p_i of (4) are related by expression $p_i = \lambda_i + \alpha/2$, which shows $\operatorname{Re} p_i \le -\alpha/2$ when $\operatorname{Re}\lambda_i \le -\alpha$ for $i = 1,\dots,r$. Hence, $\Delta_1 > 0$, $\Delta_2 > 0$, $\dots$, $\Delta_r > 0$. Moreover, $\Delta_2 \dots \Delta_r > k$, where k is such a positive as is decided by α, and not dependent on t.

Based on [12], we can prove that v_1 is positively definite function, and obtain the following result

$$\sum_{i=1}^{r} \frac{\partial v_1}{\partial x_i}\left[a_{i1}x_1 + \dots + \left(a_{ii} + \frac{\alpha}{2}\right)x_i + \dots + a_{ir}x_r\right] = 2\omega_1. \tag{14}$$

According to Barbashin formula [13], the v_1 is unique quadratic form that satisfies the equality (14). Therefore, v_1 should be in accordance with Liapunov function constructed in [12], that is,

$$v_1 = \Delta_2(t)\dots\Delta_r(t)\sum_{j=1}^{r} x_j^2 + \sum_{\sigma=1}^{r-1}\sum_{j=1}^{r}\prod_{s=1(\ne\sigma\pm1)}^{r} \Delta_s(t)\Delta_{\sigma j}^2(t)(x_1\dots x_r), \tag{15}$$

where the meaning of $\Delta_{\sigma j}$ is the same as in [12], if $a_{ii} + \alpha/2$ is substituted for a_{ii} in $\Delta_{\sigma j}$ from [12] for $i = 1,\dots,r$. Consequently, the following inequality holds

$$v_1 \ge \Delta_2\dots\Delta_r \sum_{j=1}^{r} x_j^2 \ge k\sum_{j=1}^{r} x_j^2$$

which means that v_1 is positive definite with respect to t, x_1, $\dots$, x_r. It can be proved similarly that quadratic form v_2 is positive definite with respect to t, x_{r+1}, $\dots$, x_n.

By means of Euler theorem on homogeneous function we can change (14) into

$$\sum_{i=1}^{r}\frac{\partial v_1}{\partial x_i}[a_{i1}x_1+\cdots+a_{ii}x_i+\cdots+a_{ir}x_r]=-\frac{\alpha}{2}\sum_{i=1}^{r}x_i\frac{\partial v_1}{\partial=x_i}+2\omega_1=-\alpha v_1+2\omega_1, \quad (16)$$

namely,

$$\nabla_x v_1(x,t)A_{11}(t)\zeta_1=-\alpha v_1+2\omega_1.$$

For the same reason, it can be done that

$$\nabla_x v_2(x,t)A_{22}(t)\zeta_2=-\frac{\delta}{2}\sum_{i=r+1}^{n}x_i\frac{\partial v_2}{\partial x_i}+2\omega_2=-\delta v_2+2\omega_2. \quad (17)$$

Calculating the second terms on the right-hand side of (12), we have

$$\begin{aligned}
&\nabla_x v_1(x,t)A_{12}(t)\zeta_2\\
&\quad=\left(a_{1,r+1}\frac{\partial v_1}{\partial x_1}+a_{2,r+1}\frac{\partial v_1}{\partial x_2}+\cdots+a_{r,r+1}\frac{\partial v_1}{\partial x_r}\right)x_{r+1}+\dots\\
&\qquad+\left(a_{1,n}\frac{\partial v_1}{\partial x_1}+a_{2,n}\frac{\partial v_1}{\partial x_2}+\cdots+a_{r,n}\frac{\partial v_1}{\partial x_r}\right)x_n\\
&\quad=2c_1\left(a_{1,r+1}\sum_{j=1}^{r}v_{1j}x_j+a_{2,r+1}\sum_{j=1}^{r}v_{2j}x_j+\dots\right.\\
&\qquad\left.+a_{r,r+1}\sum_{j=1}^{r}v_{rj}x_j\right)x_{r+1}+\dots\\
&\qquad+2c_1\left(a_{1,n}\sum_{j=1}^{r}v_{1j}x_j+a_{2,n}\sum_{j=1}^{r}v_{2j}x_j+\cdots+a_{r,n}\sum_{j=1}^{r}v_{rj}x_j\right)x_n\\
&\quad=2c_1x_1\left(x_{r+1}\sum_{i=1}^{r}a_{i,r+1}v_{i1}+\cdots+x_n\sum_{i=1}^{r}a_{i,n}v_{i1}\right)\\
&\qquad+2c_1x_2\left(x_{r+1}\sum_{i=1}^{r}a_{i,r+1}v_{i2}+\cdots+x_n\sum_{i=1}^{r}a_{i,n}v_{i2}\right)+\dots\\
&\qquad+2c_1x_r\left(x_{r+1}\sum_{i=1}^{r}a_{i,r+1}v_{ir}+\cdots+x_n\sum_{i=1}^{r}a_{i,n}v_{ir}\right).
\end{aligned} \quad (18)$$

In order to reduce the sum on the right-hand side of (12) into the form of linear combination of v_1 and v_2, we set up the estimation, with the aid of condition (ii) and inequality $-az^2+bz\le -az^2/2+b^2/2a$ $(a>0)$, as follows:

$$\begin{aligned}
&-2c_1x_1^2\det B_r+2c_1x_1\left(x_{r+1}\sum_{i=1}^{r}a_{i,r+1}v_{i1}+\cdots+x_n\sum_{i=1}^{r}a_{i,n}v_{i1}\right)\\
&\qquad\le -c_1x_1^2\det B_r+\frac{c_1}{\det B_r}\left(x_{r+1}\sum_{i=1}^{r}a_{i,r+1}v_{i1}+\cdots+x_n\sum_{i=1}^{r}a_{i,n}v_{i1}\right)^2
\end{aligned}$$

$$\leq -c_1x_1^2\det B_r + \frac{c_1m_1^2}{\det B_r}\bigg(\sum_{i=1}^r |v_{i1}|\bigg)^2(|x_{r+1}|+\dots+|x_n|)^2$$

. . . .

$$\begin{aligned}
&-2c_1x_r^2\det B_r + 2c_1x_r\bigg(x_{r+1}\sum_{i=1}^r a_{i,r+1}v_{ir} + \dots + x_n\sum_{i=1}^r a_{i,n}v_{ir}\bigg)\\
&\leq -c_1x_r^2\det B_r + \frac{c_1}{\det B_r}\bigg(x_{r+1}\sum_{i=1}^r a_{i,r+1}v_{ir} + \dots + x_n\sum_{i=1}^r a_{i,n}v_{ir}\bigg)^2\\
&\leq -c_1x_r^2\det B_r + \frac{c_1m_1^2}{\det B_r}\bigg(\sum_{i=1}^r |v_{ir}|\bigg)^2(|x_{r+1}|+\dots+|x_n|)^2.
\end{aligned}$$

The inequality obtained by adding corresponding terms on both sides of r inequalities above shows that

$$\begin{aligned}
\frac{dv_1}{dt}\bigg|_{(10)} &\leq -\alpha v_1 + \omega_1 + \frac{c_1m_1^2}{\det B_r}(|x_{r+1}|+\dots+|x_n|)^2\\
&\times\bigg[\bigg(\sum_{i=1}^r|v_{i1}|\bigg)^2 + \bigg(\sum_{i=1}^r|v_{i2}|\bigg)^2 + \dots + \bigg(\sum_{i=1}^r|v_{ir}|\bigg)^2\bigg] + \frac{\partial v_1}{\partial t} + |\nabla_x v_1 f^*| \\
&\leq -\alpha v_1 + \omega_1 + \frac{c_1m_1^2}{\det B_r}(|x_{r+1}|+\dots+|x_n|)^2\sum_{i,j=1}^r v_{ij}^2 + \frac{\partial v_1}{\partial t} + |\nabla_x v_1 f^*|.
\end{aligned} \tag{19}$$

We estimate the last sum expression on the right-hand side of (19)

$$\begin{aligned}
|\nabla_x v_1 f^*| &= \bigg|2c_1\sum_{i=1}^r\sum_{j=1}^r v_{ij}x_jf_i(t,x_1,\dots,x_n)\bigg|\\
&\leq 2\varepsilon|c_1|(|x_1|+|x_2|+\dots+|x_n|)\bigg(\sum_{i=1}^r\sum_{j=1}^r|v_{ij}|\,|x_j|\bigg)\\
&\leq 2\varepsilon|c_1|\,rM_1(|x_1|+|x_2|+\dots+|x_n|)(|x_1|+|x_2|+\dots+|x_r|)\\
&\leq 3r^2|c_1|M_1\varepsilon(x_1^2+\dots+x_r^2) + r(n-r)|c_1|M_1\varepsilon(x_{r+1}^2+\dots+x_n^2).
\end{aligned} \tag{20}$$

Based on the deduction above, for (19) there is following estimation:

$$\begin{aligned}
\frac{dv_1}{dt}\bigg|_{(10)} &= -\alpha v_1 + (3r^2|c_1|M_1\varepsilon - \Delta_1\Delta_2\dots\Delta_r)(x_1^2+\dots+x_r^2)\\
&\quad + (x_{r+1}^2+\dots+x_n^2)\beta v_2^* + \frac{\partial v_1}{\partial t}\\
&\leq -\alpha v_1 + \beta v_2 + [(x_{r+1}^2+\dots+x_n^2)\beta v_2^* - \beta v_2]\\
&\quad + \bigg[\Delta_1\Delta_2\dots\Delta_r\bigg(\frac{3r^2M_1\varepsilon}{b_r} - 1\bigg)(x_1^2+\dots+x_r^2) + \frac{\partial v_1}{\partial t}\bigg].
\end{aligned} \tag{21}$$

In the same way, taking (17) into consideration, we can obtain

$$\frac{dv_2}{dt}\bigg|_{(11)} = -\delta v_2 + 2\omega_2 + 2c_2x_{r+1}\bigg(x_1\sum_{i=r+1}^n a_{i1}v_{i,r+1} + \dots + x_r\sum_{i=r+1}^n a_{ir}v_{i,r+1}\bigg)$$

$$+ 2c_2x_{r+2}\left(x_1\sum_{i=r+1}^{n} a_{i1}v_{i,r+2} + \cdots + x_r \sum_{i=r+1}^{n} a_{ir}v_{i,r+2}\right) + \ldots$$
$$+ 2c_2x_n\left(x_1\sum_{i=r+1}^{n} a_{i1}v_{i,n} + \cdots + x_r \sum_{i=r+1}^{n} a_{ir}v_{i,n}\right) + \frac{\partial v_2}{\partial t} + |\nabla_x v_2 f^{**}|.$$

Similarly to the way of getting (21), we can estimate (13) as follows

$$\begin{aligned}
\left.\frac{dv_2}{dt}\right|_{(11)} &= -\delta v_2 + 2\omega_2 + \frac{c_2m_2^2}{\det B_m}(|x_1| + \cdots + |x_r|)^2 \\
&\quad \times \left[\left(\sum_{i=r+1}^{n} |v_{i,r+1}|\right)^2 + \cdots + \left(\sum_{i=r+1}^{n} |v_{in}|\right)^2\right] + \frac{\partial v_2}{\partial t} + \nabla_x v_2 f^{**} \\
&\le -\delta v_2 + \omega_2 + \frac{c_2m_2^2}{\det B_m}(|x_1| + \cdots + |x_r|)^2 \sum_{i,j=r+1}^{n} v_{ij}^2 + \frac{\partial v_2}{\partial t} + \nabla_x v_2 f^{**} \\
&\le -\delta v_2 + \gamma v_1 + [\gamma v_1^*(x_1^2 + \cdots + x_n^2) - \gamma v_1] \\
&\quad + \left[\Delta_1^*\Delta_2^*\ldots\Delta_m^*\left(\frac{3(n-r)^2M_2\varepsilon}{b_m} - 1\right)(x_{r+1}^2 + \cdots + x_n^2) + \frac{\partial v_2}{\partial t}\right].
\end{aligned} \tag{22}$$

The simultaneous existence of (21) and (22) leads to the inequality system

$$\begin{aligned}
\frac{dv_1}{dt} &\le -\alpha v_1 + \beta v_2 + [(x_1^2 + \cdots + x_n^2)\beta v_2^* - \beta v_2] + \left[1 - \frac{3r^2M_1\varepsilon}{b_r}\right]\omega_1 + \frac{\partial v_1}{\partial t}, \\
\frac{dv_2}{dt} &\le \gamma v_1 - \delta v_2 + [(x_1^2 + \cdots + x_r^2)\gamma v_1^* - \gamma v_1] + \left[1 - \frac{3(n-r)^2M_2\varepsilon}{b_m}\right]\omega_2 + \frac{\partial v_2}{\partial t}.
\end{aligned} \tag{23}$$

Let $x_i = \rho_1\alpha_i$, where $i = r+1, r+2, \ldots, n$, $\rho_1 = \sqrt{x_{r+1}^2 + \cdots + x_n^2}$, then $\alpha_{r+1}^2 + \cdots + \alpha_n^2 = 1$. It follows for arbitrary $t \in [t_0, +\infty)$ that

$$v_2^* = \inf_{x_{r+1}^2 + \cdots + x_n^2 = 1} v_2(t, x_{r+1}, \ldots, x_n) = \inf v_2(t, \alpha_{r+1}, \ldots, \alpha_n) > 0.$$

The sum of the first expression in the system of inequalities (23) is

$$(x_{r+1}^2 + \cdots + x_n^2)\beta v_2^* - v_2(t, x_{r+1}, \ldots, x_n)\beta \le [v_2^* - v_2(t, \alpha_{r+1}, \ldots, \alpha_n)]\beta\rho_1^2 = 0. \tag{24}$$

For the same reason, it follows that

$$(x_1^2 + \cdots + x_r^2)\gamma v_1^* - v_1(t, x_1, \ldots, x_r)\gamma \le [v_1^* - v_1(t, \alpha_1, \ldots, \alpha_r)]\gamma\rho_2^2 = 0, \tag{25}$$

where $\rho_2 = \sqrt{x_1^2 + \cdots + x_n^2}$.

Since $\tilde{A}_r$ and $\tilde{A}_m$ are real symmetric matrices, there exist orthogonal transformations

$$\zeta = P_r\eta \quad \text{and} \quad \zeta_1 = P_m\eta_1$$

to make the following equations to hold.

$$\frac{\partial v_1}{\partial t} = \zeta^{\mathrm{T}}\tilde{A}_r\zeta = \eta^{\mathrm{T}}P_r^{\mathrm{T}}\tilde{A}_rP_r\eta = \tilde{\lambda}_1y_1^2 + \dots + \tilde{\lambda}_ry_r^2,$$
$$\frac{\partial v_2}{\partial t} = \zeta_1^{\mathrm{T}}\tilde{A}_m\zeta_1 = \eta_1^{\mathrm{T}}P_m^{\mathrm{T}}\tilde{A}_mP_m\eta_1 = \tilde{\mu}_1y_{r+1}^2 + \dots + \tilde{\mu}_my_n^2,$$

where

$$\eta = (y_1,\dots,y_r)^{\mathrm{T}}, \quad \eta_1 = (y_{r+1},\dots,y_n)^{\mathrm{T}},$$

P_r and P_m are orthogonal matrices in correspondence with order r and m $(m = n-r)$, respectively. By using the orthogonal transformations above, we can change ω_1 and ω_2 into:

$$\begin{aligned} -\omega_1 &= \Delta_1\Delta_2\dots\Delta_r\zeta^{\mathrm{T}}E_r\zeta = \Delta_1\Delta_2\dots\Delta_r\eta^{\mathrm{T}}P_r^{\mathrm{T}}P_r\eta \\ &= \Delta_1\Delta_2\dots\Delta_r(y_1^2+\dots+y_r^2), \end{aligned} \tag{26}$$

$$\begin{aligned} -\omega_2 &= \Delta_1^*\Delta_2^*\dots\Delta_m^*\zeta_1^{\mathrm{T}}E_m\zeta_1 = \Delta_1^*\Delta_2^*\dots\Delta_m^*\eta_1^{\mathrm{T}}P_m^{\mathrm{T}}P_m\eta_1 \\ &= \Delta_1^*\Delta_2^*\dots\Delta_m^*(y_{r+1}^2+\dots+y_n^2). \end{aligned} \tag{27}$$

Taking (iv) into consideration, we can obtain

$$\begin{aligned} \left(1-\frac{3r^2M_1\varepsilon}{b_r}\right)\omega_1 + \frac{\partial v_1}{\partial t} &= \left[\tilde{\lambda}_1 - \left(1-\frac{3r^2M_1\varepsilon}{b_r}\right)\Delta_1\dots\Delta_r\right]y_1^2 + \dots \\ &+ \left[\tilde{\lambda}_r - \left(1-\frac{3r^2M_1\varepsilon}{b_r}\right)\Delta_1\dots\Delta_r\right]y_r^2 \le 0; \\ \left(1-\frac{3(n-r)^2M_2\varepsilon}{b_m}\right)\omega_1 + \frac{\partial v_2}{\partial t} &= \left[\tilde{\mu}_1 - \left(1-\frac{3(n-r)^2M_2\varepsilon}{b_m}\right)\Delta_1^*\dots\Delta_m^*\right]y_{r+1}^2 + \dots \\ &+ \left[\tilde{\mu}_m - \left(1-\frac{3(n-r)^2M_2\varepsilon}{b_m}\right)\Delta_1^*\dots\Delta_m^*\right]y_n^2 \le 0. \end{aligned}$$

The discussion above shows that (23) can take the form

$$\begin{aligned} \frac{dv_1}{dt} &\le -\alpha v_1 + \beta v_2, \\ \frac{dv_2}{dt} &\le \gamma v_1 - \delta v_2, \end{aligned} \tag{28}$$

where α, β, γ, δ are all positive number. Define vector Liapunov function $v = (v_1, v_2)^{\mathrm{T}}$, we rewrite inequality (28) as follows:

$$\frac{dv}{vt} \le Dv, \tag{29}$$

and establish differential equation system as

$$\frac{dX}{dt} = DX, \tag{30}$$

where D is a 2×2 order aggregation matrix

$$D = \begin{bmatrix} -\alpha & \beta \\ \gamma & -\delta \end{bmatrix}.$$

Let $v(t, v_0, t_0)$ and $X(t, X_0, t_0)$ be solution of (29) and (30), respectively. For $v_0 = X_0$, based on the result of [4], the following inequality holds for all $t \in [t_0, +\infty)$.

$$v(t, v_0, t_0) \leq X(t, v_0, t_0). \tag{31}$$

Because $\alpha\delta - \beta\gamma > 0$, $-\alpha < 0$, $-\delta > 0$, we can conclude that zero solution of (30) is asymptotically stable, this means $\lim_{t\to+\infty} X(t, v_0, t_0) = 0$. By (31) and the positive definite character of v_1 and v_2, we have $t \to +\infty$, $v = (v_1, v_2)^{\mathrm{T}} \to (0, 0)^{\mathrm{T}}$, and the zero solution of the system (1) is asymptotically stable.

Remark 1 It should be noted that Theorem 3.1 is different from the approach proposed by Razumikhin (see, e.g., [14]). Especially, one can see this from the following numerical example.

3.2 Numerical example

Next, we give a numerical example to show the efficiency of the presented criterion. Consider the following nonlinear time-varying dynamic system:

$$\frac{dx}{dt} = A(t)x + f(x, t),$$

where

$$A(t) = \begin{bmatrix} -10 & 0 & 0 & -\frac{1}{20}\cos t \\ 0 & -8 & \frac{1}{20}\sin t & \frac{1}{50}e^{-t} \\ \frac{1}{60}e^{-t} & \frac{1}{40} & -6 & 0 \\ -\frac{1}{40}\cos^2 t & 0 & 0 & -10 \end{bmatrix}, \quad f(x, t) = \begin{bmatrix} \varepsilon x_3^2 \\ \varepsilon x_4^2 \\ \varepsilon x_1^2 \\ \varepsilon x_2^2 \end{bmatrix}.$$

According to (2), $A(t)$ can be partitioned into as follows:

$$A_r = \begin{bmatrix} -10 & 0 \\ 0 & -8 \end{bmatrix}, \qquad A_{r\times m} = \begin{bmatrix} 0 & -\frac{1}{20}\cos t \\ \frac{1}{20}\sin t & \frac{1}{50}e^{-t} \end{bmatrix},$$

$$A_m = \begin{bmatrix} -6 & 0 \\ 0 & -10 \end{bmatrix}, \qquad A_{m\times r} = \begin{bmatrix} \frac{1}{60}e^{-t} & \frac{1}{40} \\ -\frac{1}{40}\cos^2 t & 0 \end{bmatrix}.$$

The eigenpolynomial of A_r can be obtained as

$$\begin{bmatrix} \lambda + 10 & 0 \\ 0 & \lambda + 8 \end{bmatrix} = 0,$$

and consequently, the eigenvalues of A_r can be obtained as $\lambda_1 = -10,\ \lambda_2 = -8.$ Make $\alpha = \min(\inf|\operatorname{Re}\lambda_1|, \inf|\operatorname{Re}\lambda_2|) = 8,$ and substitute it into (3), we have

$$B_r = \begin{bmatrix} -6 & 0 & 0 \\ 0 & -10-8+8 & 0 \\ 0 & 0 & -8+4 \end{bmatrix} = \begin{bmatrix} -6 & 0 & 0 \\ 0 & -10 & 0 \\ 0 & 0 & -4 \end{bmatrix},$$

and, one obtains $\det B_r = -240.$

By using (4), we have

$$\begin{aligned} |(p-\alpha/2)E_r - A_r| &= |(p-4)E_r - A_r| \\ &= \begin{bmatrix} p-4+10 & 0 \\ 0 & p-4+8 \end{bmatrix} = p^2 + 10p + 24 = 0, \end{aligned}$$

and, one obtains $\alpha_0 = 1,\ \alpha_1 = 10,\ \alpha_2 = 24.$

Therefore, we have the following results

$$\Delta_1 = \alpha_1 = 10, \qquad \Delta_2 = \begin{bmatrix} \alpha_1 & \alpha_3 \\ \alpha_0 & \alpha_2 \end{bmatrix} = \begin{bmatrix} 10 & 0 \\ 1 & 24 \end{bmatrix} = 240,$$

and substitute them into (6), one obtains

$$\begin{aligned} v_1 &= \frac{\Delta_1\Delta_2}{\det B_r} \begin{bmatrix} 0 & x_1^2 & 2x_1x_2 & x_2^2 \\ 1 & & & \\ 0 & & B_r & \\ 1 & & & \end{bmatrix} \\ &= \frac{\Delta_1\Delta_2}{\det B_r} \begin{bmatrix} 0 & x_1^2 & 2x_1x_2 & x_2^2 \\ 1 & -6 & 0 & 0 \\ 0 & 0 & -10 & 0 \\ 1 & 0 & 0 & -4 \end{bmatrix} = 400x_1^2 + 600x_2^2, \end{aligned}$$

$$v_1^* = \inf_{x_1^2+x_2^2=1} v_1 = 400, \quad \Delta = \sup(\Delta_1\Delta_2) = 2400, \quad b_r = \inf|\det B_r| = 240,$$

$$M_1 = \sup(|v_{ij}|,\ \ i,j = 1,2) = 600,$$

$$\varepsilon_1 < \frac{b_r}{3r^2M_1} = \frac{240}{3\cdot 4\cdot 600} = \frac{1}{30}, \quad m_1 = \frac{1}{40},$$

the eigenpolynomial of A_m can be obtained as

$$\begin{bmatrix} \mu+6 & 0 \\ 0 & \mu+10 \end{bmatrix} = 0,$$

and consequently, the eigenvalues of A_m can be obtained as $\mu_1 = -10,\ \mu_2 = -6.$ Make $\delta = \min(\inf|\operatorname{Re}\mu_1|,\ \inf|\operatorname{Re}\mu_2|) = 6,$ and substitute it into (3), we have

$$B_m = \begin{bmatrix} -6+\dfrac{6}{2} & 0 & 0 \\ 0 & -6-10+6 & 0 \\ 0 & 0 & -10+\dfrac{6}{2} \end{bmatrix} = \begin{bmatrix} -3 & 0 & 0 \\ 0 & -10 & 0 \\ 0 & 0 & -7 \end{bmatrix},$$

and, one obtains $\det B_m = -210$.

From (5), we have

$$|(q-\delta/2)E_m - A_m| = |(q-3)E_m - A_m| = \begin{bmatrix} q-3+6 & 0 \\ 0 & q-3+10 \end{bmatrix} = q^2 + 10q + 21 = 0,$$

and, one obtains $b_0 = 1,\ b_1 = 10,\ b_2 = 21$.

Therefore, we have the following results

$$\Delta_1^* = b_1 = 10, \qquad \Delta_2^* = \begin{bmatrix} b_1 & b_3 \\ b_0 & b_2 \end{bmatrix} = \begin{bmatrix} 10 & 0 \\ 1 & 21 \end{bmatrix} = 210,$$

and substitute them into (7), we have

$$v_2 = \frac{\Delta_1^*\Delta_2^*}{\det B_m}\begin{bmatrix} 0 & x_3^2 & 2x_3x_4 & x_4^2 \\ 1 & & & \\ 0 & & B_m & \\ 1 & & & \end{bmatrix} = \frac{\Delta_1^*\Delta_2^*}{\det B_m}\begin{bmatrix} 0 & x_3^2 & 2x_3x_4 & x_4^2 \\ 1 & -3 & 0 & 0 \\ 0 & 0 & -10 & 0 \\ 1 & 0 & 0 & -7 \end{bmatrix} = 700x_3^2 + 300x_4^2,$$

$$v_2^* = \inf_{x_3^2+x_4^2=1} v_2 = 300, \quad \Delta^* = \sup(\Delta_1^*\Delta_2^*) = 2100, \quad b_m = \inf|\det B_m| = 210,$$

$$M_2 = \sup(|v_{ij}|,\ \ i,j=3,4) = 700, \quad m_2 = \frac{1}{40},$$

$$\varepsilon_2 < \frac{b_m}{3(n-r)^2M_2} = \frac{210}{3\cdot 4\cdot 700} = \frac{1}{40},$$

$$\gamma = r(n-r)M_2\left(\frac{\Delta^*(n-r)M_2m_2^2}{b_m^2} + \frac{\Delta^*\varepsilon_2}{b_m}\right)\Big/ v_1^* = \frac{49}{24},$$

$$\beta = r(n-r)M_2\left(\frac{\Delta^*M_2m_2^2}{b_m^2} + \frac{\Delta^*\varepsilon_2}{b_m}\right)\Big/ v_2^* = \frac{35}{12}.$$

One can see that it satisfies the conditions (i) – (iv) of Theorem 3.1, that is, the zero solution of the system (1) is asymptotically stable, which shows that the proposed criterion is efficient for the stability of a class of nonlinear time-varying dynamic system.

4 Conclusions

In this paper, we have given a feasible method to construct Liapunov function of a dynamic system (1), and established some of sufficient conditions for stability of the system. It is shown that for any differentiable matrix $A(t)$, if there exist submatrices A_r and A_m in $A(t)$ such that their eigenvalues all have negative real parts, then it is always available to take $v = (v_1, v_2)^{\mathrm{T}}$ as a vector Liapunov function of the system $dx/dt = A(t)x + f(x,t)$, and based on this, the conditions to ensure stability of the system can be established. Also, the efficiency of the presented criterion has been confirmed by means of a numerical example.

Acknowledgements

The authors would like to thank Professor A.A. Martynyuk for his valuable comments and helpful suggestions for this paper.

References

[1] Bellman, R. Vector Liapunov functions. *SIAM J. Control* **A1** (1962) 32–34.
[2] Matrosov, V.M. On the theorem of stability of motion. *Prikl. Matematika i Mekhanika* **26** (1962) 992–1002. [Russian]
[3] Lakshmikantham, V., Matrosov, V.M. and Sivasundaram, S. *Vector Liapunov functions and Stability Analysis of Nonlinear Systems.* Kluwer Academic Publishers, The Netherlands, 1991.
[4] Bailey, F.N. The application of Liapunov's second method to interconnected systems. *SIAM J. Control* **A3** (1965) 443–462.
[5] Šiljak, D.D. *Large–Scale Dynamic System: Stability and Structure.* North-Holland Publishers, New York, 1978.
[6] Grujić, Lj.T., Martynyuk, A.A. and Ribbens-Pavella, M. *Large Scale Systems Stability under Structural and Singular Perturbations.* Springer-Verlag, 1987.
[7] Galperin, E.A. Some generalizations of Lyapunov's approach to stability and control. *Nonlinear Dynamics and Systems Theory* **2** (2002) 1–24.
[8] Gruyitch, Ly.T. Consistent Lyapunov methodology: non-differentiable nonlinear systems. *Nonlinear Dynamics and Systems Theory* **1** (2001) 1–22.
[9] Martynyuk, A.A. and Slyn'ko, V.I. Solution of the problem of constructing Liapunov matrix function for a class of large scale systems. *Nonlinear Dynamics and Systems Theory* **1** (2001) 193–204.
[10] Martynyuk, A.A. *Qualitative Methods in Nonlinear Dynamics: Novel Approach to Liapunov's Matrix Functions.* Marcel Dekker, Inc., New York, 2002.
[11] Jin, Y. Asymptotical stability of n-order nonlinear time-varying dynamic system. *J. Engin. Math.* **16** (1999) 85–90. [Chinese]
[12] Qin, Y., Wang, M. and Wang, L. *Stability Theory of Motion and Its Application.* Science Press, Beijing, 1981. [Chinese]
[13] Barbashin, E. A. *Liapunov Functions.* Nauka, Moscow, 1970. [Russian]
[14] Krasovskii, N.N. *Stability of Motion.* Stanford University Press, California, 1963.

Nonlinear Dynamics and Systems Theory, **4**(2) (2004) 231–240

Imaginary Axis Eigenvalues of a Delay System with Applications in Stability Analysis

Z. Zahreddine

[1] *Department of Basic Sciences, College of Arts & Sciences, University of Sharjah, Sharjah, P.O. Box 27272,*

Received: June 18, 2003; Revised: May 6, 2004

Abstract: We present a matrix method for determining the imaginary axis eigenvalues of a delay differential system. Both neutral and retarded delay systems are considered. We produce a second order polynomial matrix which is singular for all imaginary axis eigenvalues of the delay system leading to the recovery of eigenvectors associated with imaginary axis eigenvalues. The use of Kronecker products is emphasized in the proofs. Examples are given to illustrate the applicability of the new results in stability analysis.

Keywords: *Delay systems; stability analysis; Kronecker products; imaginary axis eigenvalues.*

Mathematics Subject Classification (2000): 34A25, 34C20; 34A09, 93D99.

1 Introduction

Consider a linear delay differential equation of the form

$$x'(t) + Ax'(t-h) = Bx(t) + Cx(t-h),$$

where A, B and $C \in \mathbf{R}^{n\times n}$, $\mathbf{R}$ being the set of real numbers. When $A = 0$, we get a retarded delay system, otherwise the system is neutral.

The purpose of this work is to present a matrix method for determining the imaginary axis eigenvalues of the above equation. Such eigenvalues occupy a special place in the theory of delay equations. They can be used to give the frequencies of oscillating solutions, and detect the onset of Hopf bifurcations. Although the idea of the approach is taken from the theory of quadratic functionals for delay equations [8], but the proofs will be quite direct, with strong emphasis on Kronecker products. In addition, we shall look at the matrix single delay case, and we propose a $2n^2 \times 2n^2$ matrix having spectrum containing all imaginary axis eigenvalues of the delay system. Our technique works equally well for both neutral and retarded delay systems. Therefore, we produce a polynomial matrix which is second order in s, and is singular for all values of s which are imaginary axis eigenvalues of the delay system, and in so doing, we can often directly recover the eigenvectors associated with imaginary axis eigenvalues.

Cooke and Grossman [4] made use of imaginary axis eigenvalues in their paper on stability switching for retarded systems. Also, Marshall [7] gave a polynomial elimination method for finding imaginary axis eigenvalues.

Imaginary axis eigenvalues were studied by the author in stability contexts in [10], where such eigenvalues represented singularities arising in the extended Routh array [9], which generalizes the well-known and historic Routh array to the complex domain. In Section 2, we introduce the notations and basic definitions. The main results are given in Section 3. Examples illustrating the applicability of the new results in stability analysis will be given in Section 4.

2 Notations and Basic Definitions

In this section we introduce the basic ideas and the terminology that we shall be using in the remaining sections. The ideas that we present here, were primarily motivated by the quadratic energy functionals pioneered by Repin [8], and later promoted by Infante and Castelan [3, 5, 6]. In the following, we will be converting matrix ordinary differential equations to vector form and visa versa. In order to do this, we will be making use of the elementary transformation $\Phi\colon \mathbf{C}^{n\times n} \to \mathbf{C}^{n^2}$, $\mathbf{C}$ being the set of complex numbers, which transforms elements $E = [\mathbf{e}_1, \ldots, \mathbf{e}_n]^{\mathrm{T}}$ of $\mathbf{C}^{n\times n}$ into $\Phi(E) = [\mathbf{e}_1^{\mathrm{T}}, \ldots, \mathbf{e}_n^{\mathrm{T}}]^{\mathrm{T}}$.

For any two complex matrices M and N, we recall the Kronecker product $M \otimes N$ and we note the identity $\Phi(MPN) = (M \otimes N^{\mathrm{T}})\Phi(P)$. We shall use this identity to conveniently move between matrix equations and vector equations. On several occasions in this paper, we shall be using certain basic facts about Kronecker products, and for that we refer the reader to Brewer [1, 2].

We now introduce the ordinary differential equation which motivates our work. If A, B and C are as defined above, we consider the system of ordinary differential equations:

$$\begin{aligned} X'(t) + AY'(t) &= BX(t) + CY(t), \\ X'(t)A^{\mathrm{T}} + Y'(t) &= -X(t)C^{\mathrm{T}} - Y(t)B^{\mathrm{T}}. \end{aligned} \tag{1}$$

Let $\mathbf{C}_1$ denote the vector space $\mathbf{C}_1 = \mathbf{C}^{n\times n} \times \mathbf{C}^{n\times n}$, and Ψ the operator on $\mathbf{C}_1$ defined by

$$\Psi \begin{bmatrix} Q \\ R \end{bmatrix} = \begin{bmatrix} Q + AR \\ QA^{\mathrm{T}} + R \end{bmatrix}$$

for $Q, R \in \mathbf{C}^{n\times n}$. Also, we let Ω be given by

$$\Omega \begin{bmatrix} Q \\ R \end{bmatrix} = \begin{bmatrix} BQ + CR \\ -QC^{\mathrm{T}} - RB^{\mathrm{T}} \end{bmatrix}.$$

With

$$Z(t) = \begin{bmatrix} X(t) \\ Y(t) \end{bmatrix}$$

we write the matrix differential equation (1) as $\Psi Z'(t) = \Omega Z(t)$.

In order to write equation (1) in vector coordinates, let $x = \Phi(X)$, $y = \Phi(Y)$, $z = [x,\, y]^{\mathrm{T}}$ and consider the matrices

$$A_0 = \begin{bmatrix} I \otimes I & A \otimes I \\ I \otimes A & I \otimes I \end{bmatrix}, \qquad B_0 = \begin{bmatrix} B \otimes I & C \otimes I \\ -I \otimes C & -I \otimes B \end{bmatrix}.$$

In this way, (1) can be written as the following vector differential equation:

$$A_0 z'(t) = B_0 z(t). \tag{2}$$

Suppose now that $\mathbf{Z} = (\mathbf{X}, \mathbf{Y}) = (X_0 \mathbf{e}^{st},\, Y_0 \mathbf{e}^{st})$ is a matrix solution of the differential equation (1). When differentiating with respect to t, we get

$$\begin{gathered} (sI - B)\mathbf{X} + (sA - C)\mathbf{Y} = 0, \\ \mathbf{X}(sA^{\mathrm{T}} + C^{\mathrm{T}}) + \mathbf{Y}(sI + B^{\mathrm{T}}) = 0. \end{gathered} \tag{3}$$

For every complex number s, we define $\Gamma = \Gamma(s)$ to be the operator $\Gamma = s\Psi - \Omega$ taking $\mathbf{C}_1$ into $\mathbf{C}_1$, so that

$$\Gamma \begin{bmatrix} Q \\ R \end{bmatrix} = \begin{bmatrix} (sI - B)Q + (sA - C)R \\ Q(sA^{\mathrm{T}} + C^{\mathrm{T}}) + R(sI + B^{\mathrm{T}}) \end{bmatrix} \tag{4}$$

for $Q, R \in \mathbf{C}^{n \times n}$.

Therefore (3) can be written as $\Gamma \mathbf{Z} = 0$. With $\mathbf{z} = \Phi(\mathbf{Z})$, we have

$$(sA_0 - B_0)\mathbf{z} = 0.$$

In order to investigate the behavior of Γ, we try to solve

$$\Gamma \begin{bmatrix} Q \\ R \end{bmatrix} = \begin{bmatrix} Q_0 \\ R_0 \end{bmatrix} \tag{5}$$

for Q and R.

By combining (4) and (5), we get

$$\begin{bmatrix} (sI - B)Q + (sA - C)R \\ Q(sA^{\mathrm{T}} + C^{\mathrm{T}}) + R(sI + B^{\mathrm{T}}) \end{bmatrix} = \begin{bmatrix} Q_0 \\ R_0 \end{bmatrix}. \tag{6}$$

If in (6), we right multiply the upper equation by $sI + B^{\mathrm{T}}$, and left multiply the lower equation by $sA - C$, then subtract, we get

$$(sI - B)Q(sI + B^{\mathrm{T}}) - (sA - C)Q(sA^{\mathrm{T}} + C^{\mathrm{T}}) = Q_0(sI + B^{\mathrm{T}}) - (sA - C)R_0.$$

Similarly, if in (6), we right multiply the upper equation by $sA^{\mathrm{T}} + C^{\mathrm{T}}$, and left multiply the lower equation by $sI - B$, then subtract, we get

$$(sI - B)R(sI + B^{\mathrm{T}}) - (sA - C)R(sA^{\mathrm{T}} + C^{\mathrm{T}}) = (sI - B)R_0 - Q_0(sA^{\mathrm{T}} + C^{\mathrm{T}}).$$

The latter equation can better be expressed in concise operator language in the following way: For every complex s, let $\Gamma^+ = \Gamma^+(s)\colon\ \mathbf{C}_1 \to \mathbf{C}_1$ be the operator defined by

$$\Gamma^+ \begin{bmatrix} U \\ V \end{bmatrix} = \begin{bmatrix} U(sI + B^{\mathrm{T}}) - (sA - C)V \\ -U(sB^{\mathrm{T}} + C^{\mathrm{T}}) + (sI - B)V \end{bmatrix}$$

for $U, V \in \mathbf{C}^{n\times n}$, and let $\lambda = \lambda(s)$ be the operator on $\mathbf{C}^{n\times n}$ given by

$$\lambda W = (sI - B)W(sI + B^{\mathrm{T}}) - (sA - C)W(sA^{\mathrm{T}} + C^{\mathrm{T}})$$

for $W \in \mathbf{C}^{n\times n}$. It is clear that for each complex s, we have

$$\Gamma^+\Gamma \begin{bmatrix} Q \\ R \end{bmatrix} = \begin{bmatrix} \lambda Q \\ \lambda R \end{bmatrix}. \tag{7}$$

Again using the map Φ defined at the beginning of this section, we have natural associations of matrices with operators $\Gamma(s)$, $\Gamma^+(s)$, and $\lambda(s)$. With $q = \Phi(Q)$, $r = \Phi(R)$, $u = \Phi(U)$, $v = \Phi(V)$ we can write $H[\,q,\, r\,]^{\mathrm{T}}$ for $\Gamma[\,Q,\, R\,]^{\mathrm{T}}$ and $H^+[\,u,\, v\,]^{\mathrm{T}}$ for $\Gamma^+[\,U,\, V\,]^{\mathrm{T}}$, where

$$H = H(s) = \begin{bmatrix} (sI - B)\otimes I & (sA - C)\otimes I \\ I \otimes (sA + C) & I \otimes (sI + B) \end{bmatrix} = sA_0 - B_0,$$

$$H^+ = H^+(s) = \begin{bmatrix} I \otimes (sI + B) & -(sA - C)\otimes I \\ -I \otimes (sA + C) & (sI - B)\otimes I \end{bmatrix}.$$

Similarly, with $w = \Phi(W)$, we can write Λw for λW, where

$$\Lambda = \Lambda(s) = (sI - B)\otimes(sI + B) - (sA - C)\otimes(sA + C).$$

In particular, we note that (7) is written as $H^+H[\,q,\, r\,]^{\mathrm{T}} = [\,\Lambda q,\, \Lambda r\,]^{\mathrm{T}}$, i.e.

$$H^+H = \begin{bmatrix} \Lambda & 0 \\ 0 & \Lambda \end{bmatrix}.$$

It follows that the determinant of H is closely related to that of Λ, i.e., $|H^+H| = |\Lambda|^2$. The following theorem makes it evident that $H(s)$ and $H^+(s)$ have the same determinant.

Theorem 2.1 *For every complex s, we have $|H(s)| = |H^+(s)|$.*

Proof Write $H = \begin{bmatrix} \alpha & \beta \\ \chi & \delta \end{bmatrix}$, where $\alpha = a(s)\otimes I$, $\beta = b(s)\otimes I$, $\chi = I \otimes c(s)$, $\delta = I \otimes d(s)$, and $a(s) = sI - B$, $b(s) = sA - C$, $c(s) = sA + C$, $d(s) = sI + B$. With $m = n^2$ row interchanges, we get

$$|H| = (-1)^m \begin{vmatrix} \chi & \delta \\ \alpha & \beta \end{vmatrix}$$

and after the same number of column interchanges, we find that

$$|H| = \begin{vmatrix} \delta & \chi \\ \beta & \alpha \end{vmatrix}. \tag{8}$$

We consider two cases:

Case 1 If A is non-singular, then neither $|c(s)|$ nor $|d(s)|$ are uniformly zero. Consider following identity which holds for all but a finite number of complex s,

$$|H| = |\delta| \cdot |\alpha - \beta\delta^{-1}\chi| = |\delta| \cdot |\alpha\chi^{-1} - \beta\delta^{-1}| \cdot |\chi|. \tag{9}$$

If we use formula (8) in (9), we get the following identity which also holds for all but a finite number of complex s,

$$|H^+| = \begin{vmatrix} \delta & -\beta \\ -\chi & \alpha \end{vmatrix} = |\delta| \cdot |\alpha - \chi\delta^{-1}\beta| = |\delta| \cdot |\chi| \cdot |\chi^{-1}\alpha - \delta^{-1}\beta|. \tag{10}$$

Using the Kronecker product identities $(I \otimes M)(N \otimes I) = (N \otimes I)(I \otimes M)$ and $(N \otimes M)^{-1} = N^{-1} \otimes M^{-1}$, we see that $\alpha\chi^{-1} = \chi^{-1}\alpha$ and $\beta\delta^{-1} = \delta^{-1}\beta$ for all but a finite number of complex s, so that $|H(s)| = |H^+(s)|$ for all but a finite number of complex s as well. Since $|H(s)|$ and $|H^+(s)|$ are both polynomials, we conclude that $|H(s)| = |H^+(s)|$ for all $s \in \mathbf{C}$.

Case 2 If A is singular, let $A(\varepsilon) \to A$ as $\varepsilon \to 0$, with $A(\varepsilon)$ being non-singular for each nonzero ε in a neighborhood of zero. Define H_ε, H_ε^+ in the same way as H and H^+ with $A(\varepsilon)$ replacing A, we get $|H_\varepsilon(s)| = |H_\varepsilon^+(s)|$ for all $s \in \mathbf{C}$. By continuity of the determinant, we have $|H(s)| = |H^+(s)|$ for all $s \in \mathbf{C}$, and the proof is complete.

Corollary 2.1 *For all $s \in \mathbf{C}$, we have $|H(s)|^2 = |\Lambda(s)|^2$.*

Proof This follows immediately from $|H^+(s)H(s)| = |\Lambda(s)|^2$ and $|H(s)| = |H^+(s)|$.

Corollary 2.1 is enough for our purposes, since it makes it clear that the matrices $H(s)$ and $\Lambda(s)$ are either both singular, or both non-singular. But, it must be noted that with some intricate argument involving Kronecker products, the matrices $H(s)$ and $\Lambda(s)$ themselves can be shown to have equal determinants for all complex s.

3 Main Results

In this section, we consider the delay equation introduced at the beginning of Section 1

$$x'(t) + Ax'(t-h) = Bx(t) + Cx(t-h) \tag{11}$$

and we show that all imaginary axis eigenvalues of this equation are zeros of $|\Lambda(s)|$, and hence also of $|H(s)|$, so that they are generalized eigenvalues of the matrix pair (B_0, A_0) of Section 2.

Theorem 3.1 *Let A, B and $C \in \mathbf{R}^{n\times n}$. Then all imaginary axis eigenvalues of the delay differential equation (11) are zeros of $|\Lambda(s)|$, and therefore also of $|sA_0 = B_0|$. If s is an imaginary axis eigenvalue of (11) with associated eigenvector v, then $\mathbf{v} = \Phi(vv^*)$, is contained in the kernel of the matrix $\Lambda(s)$.*

Proof If $s = iw$ is an imaginary axis eigenvalue of the system (11), then we have

$$|s(I + Ae^{-sh}) - B - Ce^{-sh}| = 0 = |sI - B + e^{-sh}(sB - C)|.$$

We know that for every associated eigenvector v of (11), we have

$$(sI - B)v = -e^{-sh}(sA - C)v. \tag{12}$$

By applying the conjugation and the transposition operations, we get

$$v^*(-sI - B^{\mathrm{T}}) = -e^{sh}v^*(-sA^{\mathrm{T}} - C^{\mathrm{T}}),$$

from which we conclude that

$$v^*(sI + B^{\mathrm{T}}) = -e^{sh}v^*(sA^{\mathrm{T}} + C^{\mathrm{T}}). \tag{13}$$

Multiplying the left-hand side of (12) by the left-hand side of (13), and similarly for the right-hand sides, we get

$$(sI - B)vv^*(sI + B^{\mathrm{T}}) = (sA - C)vv^*(sA^{\mathrm{T}} + C^{\mathrm{T}}).$$

Let $\mathbf{v} = \Phi(vv^*)$, where the map Φ is as defined in Section 2, then

$$((sI - B) \otimes (sI + B) - (sA - C) \otimes (sA + C))\mathbf{v} = 0,$$

or in other words

$$\Lambda(s)\mathbf{v} = 0,$$

from which it follows that $|\Lambda(s)| = 0$.

By Corollary 2.1, it follows immediately that $0 = |H(s)| = |sA_0 - B_0|$ and that completes the proof.

A immediate corollary of Theorem 3.1 is the following.

Corollary 3.1 *Let A, B and $C \in \mathbf{R}^{n\times n}$. If $s = iw$ is an imaginary axis eigenvalue of the delay differential equation (11), then the operators $\Gamma(s)$ and $\lambda(s)$ defined in Section 2 are both singular at s.*

An interesting situation arises when, for an imaginary axis eigenvalue s of the delay differential equation (11), the kernel of $\Lambda(s)$ has dimension 1. In this case, we can easily find an eigenvector of (11), associated with s, directly from $\ker(\Lambda(s))$.

Corollary 3.2 *Let s be an imaginary axis eigenvalue of the delay differential equation (11), and suppose that $\ker(\Lambda(s))$ has dimension 1. Let $\mathbf{x}$ be any eigenvector of $\Lambda(s)$, and let $v = [\alpha_1, \ldots, \alpha_n]^{\mathrm{T}}$ be any eigenvector of (11) associated with s. Let $V = vv^* = [V_{jk}]$, $\Phi(V) = \mathbf{v}$, $\Phi(X) = \mathbf{x}$ and $X = [X_{jk}]$. Then $X_{jk} = 0$ if and only if $V_{jk} = 0$. If $X_{jj} \neq 0$, then the complex vector having $\overline{X}_{jk}/\overline{X}_{jj}$ for the k-th entry is the eigenvector v/α_j of (11), having 1 for j-th entry.*

Proof Since $\mathbf{v}, \mathbf{x} \in \ker(\Lambda(s))$, we have $\mathbf{x} = a\mathbf{v}$ for some nonzero complex a. Therefore $X = aV$. Now $X_{jk} = aV_{jk} = a\alpha_j\overline{\alpha}_k$, and if $X_{jj} \neq 0$, we have $X_{jk}/X_{jj} = \alpha_k/\alpha_j$, and the proof is complete.

It is worthwhile to mention the following remark.

Remark 3.1 Whenever we have $|A_0| \neq 0$, the zeros of $|sA_0 - B_0|$ coincide with those of $|sI - A_0^{-1}B_0|$, so that the pure imaginary eigenvalues of the delay system (11) of

Theorem 3.1 are also eigenvalues of the matrix $A_0^{-1}B_0$. In fact, there is quite a simple criterion for the condition that A_0 is singular. By [1], it is known that $(I \otimes A)(A \otimes I) = A \otimes A$, therefore $|A_0| = |I \otimes I - (I \otimes A)(A \otimes I)| = |I \otimes I - A \otimes A|$. Since $\mathrm{Eig}\,(R \otimes S)$ is the set product of $\mathrm{Eig}(R)$ with $\mathrm{Eig}(S)$ for any square matrices R and S, then A_0 is singular if and only if $1 = \mu\delta$ for some μ, δ in $\mathrm{Eig}(A)$.

4 Examples

We now give some examples to verify the applicability of Theorem 3.1 in stability computation.

Example 4.1. The first stability interval of a neutral system

Consider the neutral delay equation

$$x'(t) + Ax'(t-h) = Bx(t) + Cx(t-h)$$

where

$$A = \begin{bmatrix} 0.75 & 0.25 \\ -0.25 & 0 \end{bmatrix}, \quad B = \begin{bmatrix} 1.5 & 0.25 \\ -0.25 & 2 \end{bmatrix} \quad \text{and} \quad C = \begin{bmatrix} -3.5 & -0.5 \\ 0.5 & -3 \end{bmatrix}.$$

First note that $\mathrm{Eig}(A) \approx \{0.655, 0.095\}$, and therefore A is an asymptotically stable discrete matrix. Note that with zero delay, we have $(I + A)x'(t) = (B + C)x(t)$, and since $I+A$ is invertible, we can write this as $x'(t) = (I+A)^{-1}(B+C)x(t)$. A MATLAB computation shows that the eigenvalues of $(I + A)^{-1}(B + C)$ are -1.000 and -1.1379, and we have asymptotic stability of the above neutral delay system with zero delay.

If we wish to determine the smallest h for which the system is not asymptotically stable, we first have to find all possible imaginary axis eigenvalues of the system. Therefore, we form the matrices

$$A_0 = \begin{bmatrix} I \otimes I & A \otimes I \\ I \otimes A & I \otimes I \end{bmatrix}, \quad B_0 = \begin{bmatrix} B \otimes I & C \otimes I \\ -I \otimes C & -I \otimes B \end{bmatrix}.$$

Since $1 \notin \mathrm{Eig}(A)\cdot\mathrm{Eig}(A)$, we could compute the eigenvalues of $A_0^{-1}B_0$. Using MATLAB, we can also obtain the zeros of $|sA_0 - B_0|$ by determining the generalized eigenvalues of the matrix pair (B_0, A_0) directly. We then find that $\mathrm{Eig}(B_0, A_0) \approx \{\pm 4.1654i, \pm 2.3834i, \pm 1.4524 \pm 2.4206i\}$. Let $\Omega = \{\pm 4.1654, \pm 2.3834\}$, and note that $i\Omega$ contains all possible imaginary axis eigenvalues of the system. Next, we note that for real w, the matrix $T = iwI - B + e^{-iwh}(iwA - C)$ is singular if and only if $z = e^{-iwh}$ is a unit magnitude generalized eigenvalue of the matrix pair $(B - iwI, iwA - C)$. Checking all numbers of Ω, we find from MATLAB that for $w = 4.1654$, we have $\mathrm{Eig}(B - iwI, iwA - C) = \{-0.3987 - 0.9171i, 0.5369 - 1.3327i\}$, and $z = -0.3987 - 0.9171i$ lies on the unit circle. With $w = -4.1654$ we get the set of conjugates for generalized eigenvalues, and $z = -0.3987 + 0.9171i$ lies on the unit circle. With $w = 2.3834$ the generalized eigenvalues of the associated matrix pair are $0.0485 - 0.7281i$, $0.6286 - 0.7778i$, and we again have the conjugates for generalized eigenvalues with $w = -2.3834$. We have magnitude one for $z = 0.6268 \pm 0.7778i$.

Now for $w = 4.1654$, $z = -0.3987 - 0.9171i$ the smallest value of h with $\varepsilon^{-iwh} = z$, is $h_1 = 0.4756$. With $w = 2.3834$, $z = 0.6286 - 0.7778i$, the smallest value of h with $e^{-iwh} = z$ is $h_2 = 0.3739$. For the other two values of w, we obtain by symmetry the same two values h_1 and h_2. Therefore we have imaginary axis eigenvalues for the delay equation under consideration with $h \approx 0.3739$, and for all smaller nonnegative values of h the system is asymptotically stable.

Example 4.2. Stability switching in a retarded system

Consider the scalar delay equation

$$x''(t) + x'(t) - x'(t-h) + 4x(t) - 2x(t-h) = 0$$

which has (11) as matrix counterpart with

$$A = 0, \quad B = \begin{bmatrix} 0 & 1 \\ -4 & -1 \end{bmatrix} \quad \text{and} \quad C = \begin{bmatrix} 0 & 0 \\ 2 & 1 \end{bmatrix}.$$

With zero delay, this system is a pure oscillator having eigenvalues $\pm i\sqrt{2}$. To determine the other imaginary axis eigenvalues, we note that A_0 here is the $2n^2 \times 2n^2$ identity matrix, $n = 2$, and we use MATLAB to find the eigenvalues of B_0. Then we find $\mathrm{Eig}(B_0) \approx \{\pm 2.4495i, \pm 1.4142i, \pm 0.5000 \pm 1.9365i\}$, and the set of imaginary axis eigenvalues of B_0 is $i\Omega$, where $\Omega \approx \{\pm 2.4495, \pm 1.4142\}$. Now with $T = iwI - B - e^{-iwh}C$, we know T is singular if and only if $z = e^{-iwh}$ is a generalized eigenvalue of the pair $(iwI - B, C)$.

Now, for any $w \in \Omega$, we let $B_w = iwI - B$, and we note that the generalized eigenvalues of the pair (B_w, C) are the solutions z of the equation $|B_w - zC| = 0$. Writing B_w and C in terms of their rows as

$$B_w = \begin{bmatrix} b_1 \\ b_2 \end{bmatrix}, \quad C = \begin{bmatrix} 0 \\ c \end{bmatrix},$$

we have

$$0 = |B_w - zC| = |B_w| - z \begin{vmatrix} b_1 \\ c \end{vmatrix}.$$

With $w = 2.4495$, we get $z = 0.2000 + 0.9798i$, which has unit magnitude. With $w = 1.4142$, we get $z = 1 + 0i$, and we again obtain conjugate eigenvalues with opposite values of w. With $w = w_1 = 2.4495$, the smallest h making $e^{-iwh} = z = 0.2000 + 0.9798i$ is given by $w_1 h = 2\pi - \arctan(0.9798/0.2000)$ i.e. $h \approx 2.006$. Adding positive integer multiples of $2\pi/w_1$ provides the other corresponding values of h for which the delay system has imaginary axis eigenvalues. Similarly, with $w = w_2 = 1.4142$, the smallest h making $e^{-iwh} = z = 1$ is zero, and adding natural multiples of $2\pi/w_2$ again provides the others. The conjugate frequencies $w = -w_1$, $w = -w_2$ give us the same values of h. The first few values of h are

$$h_0 = 0, \quad h_1 \approx 2.006, \quad h_2 \approx 4.443, \quad h_3 \approx 4.571, \quad h_4 \approx 7.136.$$

Example 4.3. Using matrix polynomials for finding imaginary axis eigenvalues of a delay system

We reconsider the above examples to show how one can determine imaginary axis eigenvalues using the matrix polynomial $\Lambda(s)$ defined in Section 2. For the system (11), we recall that $\Lambda(s) = (sI - B) \otimes (sI + B) - (sA - C) \otimes (sA + C)$. $\Lambda(s)$ can also be written as $\Lambda(s) = D_0 s^2 + D_1 s + D_2$ where

$$\begin{aligned}
D_0 &= I \otimes I - A \otimes A, \\
D_1 &= I \otimes B - B \otimes I + C \otimes A - A \otimes C, \\
D_2 &= C \otimes C - B \otimes B.
\end{aligned}$$

If $\Lambda(s) = D_0 s^2 + D_1 s + D_2$ is put in the context of Example 4.1, then D_0 is invertible, so that the problem becomes that of looking for the s-values where $D_0^{-1}\Lambda(s) = E_0 s^2 + E_1 s + E_2$ is singular, with $E_0 = I \otimes I = I_0$, $E_1 = D_0^{-1} D_1$, $E_2 = D_0^{-1} D_2$. Now, these are the eigenvalues of the matrix

$$F = \begin{bmatrix} 0 & I_0 \\ -E_2 & -E_1 \end{bmatrix}.$$

With MATLAB computation we find that $\mathrm{Eig}(F) \approx \{\pm 4.1654i, \pm 2.3834i, \pm 1.4524 \pm 2.4206i\}$, just as before.

If $\Lambda(s) = D_0 s^2 + D_1 s + D_2$ is put in the context of Example 4.2, where $A = 0$, we get $D_0 = I \otimes I = I_0$, $D_1 = I \otimes B - B \otimes I$. Here, the s-values making $\Lambda(s)$ singular are the eigenvalues of

$$F = \begin{bmatrix} 0 & I_0 \\ -D_2 & -D_1 \end{bmatrix},$$

and with MATLAB computation we get $\mathrm{Eig}(F) \approx \{\pm 2.4495i, \pm 1.4142i, \ \pm 0.5000 \pm 1.9365i\}$, as in Example 4.2.

Example 4.4

This example is designed to show the practical simplicity of finding associated eigenvectors using matrix polynomials. Again we return to Example 4.1 and we show how the kernel of $\Lambda(s)$ can be used to obtain eigenvectors associated with delay equation imaginary axis eigenvalues. From these eigenvectors we can immediately find the value of $z = e^{-sh}$. Beginning with $s = 4.1654i$, we have $\Lambda(s) = D_0 s^2 + D_1 s + D_2$, and with MATLAB computation we find that this matrix has exactly one zero eigenvalue, with associated eigenvector

$$\mathbf{x} \approx \begin{bmatrix} 0.8476 + 0.3654i \\ -0.1357 - 0.2295i \\ -0.2600 + 0.0588i \\ 0.0707 + 0.0305i \end{bmatrix}.$$

With $\Phi(X) = \mathbf{x}$, we have

$$X \approx \begin{bmatrix} 0.8476 + 0.3654i & -0.1357 - 0.2295i \\ -0.2600 + 0.0588i & 0.0707 + 0.0305i \end{bmatrix}.$$

Since $X_{11} \neq 0$, we know from Corollary 3.2 that the eigenvector $v = [\,1 \;\; \alpha_2\,]^{\mathrm{T}}$ associated with s is given by $\alpha_2 = \overline{X}_{12}/\overline{X}_{11} \approx -0.2335+0.1701i$. We now return to the characteristic equation $(sI-B)v = -z(sA-C)v$ of the delay system (11), with $z = e^{-sh}$. Evaluating at $s = 4.1654i$, we write $(sI-B)v = m = [\,m_1 \;\; m_2\,]^{\mathrm{T}}$ and $(sA-C)v = r = [\,r_1 \;\; r_2\,]^{\mathrm{T}}$. Then $z = -m_1/r_1 = -m_2/r_2 \approx -0.3987 - 0.9171i$, as before, and z has unit magnitude. Now, with the case $s = 2.3834i$, we obtain $v = [\,1 \;\; -3.9177 - 1.5938i\,]^{\mathrm{T}}$, $z = 0.6286 - 0.7778i$, $|z| = 1$, and z is as previously found. As usual, the values of z obtained from $s = -4.1654i$, $s = -2.3834i$ are conjugate to those obtained from the first two.

It is possible that an eigenvector v of the delay equation (11) simultaneously satisfies $(sI-B)v = 0 = (sA-C)v$ for its associated eigenvalue s. In this case, it is possible to use the generalized eigenvalue approach displayed in Examples 4.1 and 4.2 to find the value of $z = e^{-sh}$.

References

[1] Brewer, J.W. Kronecker products and matrix calculus in system theory. *IEEE Trans Circuits Syst.* **25** (1978) 772–781.

[2] Brewer, J.W. Correction to "Kronecker products and matrix calculus in system theory". *IEEE Trans. Circuits Syst.* **26** (1979) 360.

[3] Castelan, W.B. and Infante, E.F. A Liapunov functional for a matrix neutral difference-differential equation with one delay. *J. Math. Anal. Appl.* **71** (1979) 105–130.

[4] Cooke, K.L. and Groosman, Z. Discrete delay, distributed delay and stability switches. *J. Math. Anal. Appl.* **86** (1982) 592–627.

[5] Infante, E.F. Some results on the Liapunov stability of functional equations, Volterra and functional differential equations. Proc. Conf., Blacksburg/Va. 1981. *Lect. Notes Pure Appl. Math.* **81** (1982) 51–60.

[6] Infante, E.F. and Castelan, W.B. A Liapunov functional for a matrix difference-differential equation. *J. Differ. Eqns* **29** (1978) 439–451.

[7] Marshall, J.E. *Time-Delay Systems: Stability and Performance Criteria with Applications.* Ellis Horwood, New York, 1992.

[8] Repin, I.M. Quadratic Liapunov functionals for systems with delay. *PMM, J. Appl. Math. Mech.* **29** (1965) 669 – 672; transl. from *Prikl. Mat. Mekh.* **29** (1965) 564 – 566.

[9] Zahreddine, Z. An extension of the Routh array for the asymptotic stability of a system of differential equations with complex coefficients. *Appl. Anal.* **49** (1993) 61–72.

[10] Zahreddine, Z. Wide sense stability of complex systems of differential equations of arbitrary dimension. *Chinese Annals of Math.* **15B**(2) (1994) 193–204.

Nonlinear Dynamics and Systems Theory, **4**(2) (2004) 241–242

Corrigendum

Set Differential Equations and Monotone Flows

V. Lakshmikantham and A.S. Vatsala

Nonlinear Dynamics and Systems Theory, **3**(2) (2003) 151–161.

Remark 3.1

(1) In Theorem 3.1, if $G(t,Y) \equiv 0$, then we get a result when F is nondecreasing.

(2) In (1) above, suppose that F is not nondecreasing but $\widetilde{F}(t,X) = F(t,X) + MX$ is nondecreasing in X for each $t \in J$, for some $M > 0$. Then one can consider the IVP $D_H U + MU = \widetilde{F}(t,U)$, $U(0) = U_0$, to obtain the same conclusion as in (1). To see this, use the transformation $\widetilde{U} = Ue^{Mt}$. Assuming that $D_H\widetilde{U}$ exists, we have

$$D_H\widetilde{U} = [D_H U + MU]e^{Mt} = \widetilde{F}(t, \widetilde{U}e^{-Mt})e^{Mt} \equiv F_0(t,\widetilde{U}).$$

Thus the IVP is

$$D_H\widetilde{U} = F_0(t,\widetilde{U}), \quad \widetilde{U}(0) = U_0. \tag{3.17}$$

Then $\widetilde{V} = Ve^{Mt}$ is a lower solution and $\widetilde{W} = We^{Mt}$ is an upper solution for (3.17) and now we have the same conclusion as in (1).

(3) If $F(t,X) = 0$ in Theorem 3.1, then we obtain the result for G nonincreasing.

(4) If in (3) above, G is not monotone but there exists two functions MU and $\widetilde{G}(t,U)$ such that the Hukuhara difference $G(t,U) = MU + \widetilde{G}(t,U)$ exists and $\widetilde{G}(t,U)$ is nonincreasing in U for each $t \in J$. Then setting $U = \widetilde{U}e^{Mt}$, we obtain

$$D_H\widetilde{U} = G_0(t,\widetilde{U}), \quad \widetilde{U}(0) = U_0, \tag{3.18}$$

where $G_0(t,\widetilde{U}) = \widetilde{G}(t,\widetilde{U}e^{Mt})e^{-Mt}$. In this case, we need to assume that (3.18) has coupled lower and upper solutions to get the same conclusion as in (3).

(5) Suppose that in Theorem 3.1, $G(t,Y)$ is nonincreasing in Y and $F(t,X)$ is not monotone but $\widetilde{F}(t,X) = F(t,X) + MX$, $M > 0$ is nondecreasing in X. Then we consider the IVP

$$D_H U + MU = \widetilde{F}(t,U) + G(t,U), \quad U(0) = U_0. \tag{3.19}$$

The transformation in (2) yields the conclusion by Theorem 3.1 in this case as well.

(6) If in Theorem 3.1, F is nondecreasing and G is not monotone then we suppose that there exists two functions MU and $\widetilde{G}(t,U)$ as in (4) and consider the IVP

$$D_H\widetilde{U} = F_0(t,\widetilde{U}) + G_0(t,\widetilde{U}), \quad U(0) = U_0, \tag{3.20}$$

where $F_0(t,\widetilde{U}) = F(t,\widetilde{U}e^{Mt})e^{-Mt}$ and $G_0(t,\widetilde{U}) = \widetilde{G}(t,\widetilde{U}e^{Mt})e^{-Mt}$.

(7) If both F and G are not monotone in Theorem 3.1, then suppose that there are functions $\widetilde{F}(t,U)$, $\widetilde{G}(t,U)$ and MU for some constant $M > 0$ such that the Hukuhara difference $F(t,U) + G(t,U) = \widetilde{F}(t,U) + \widetilde{G}(t,U) + MU$ exists and $\widetilde{F}(t,U)$ is nondecreasing in U and $\widetilde{G}(t,U)$ is nonincreasing in U. Now the transformation $U = \widetilde{U}e^{Mt}$ gives,

$$D_H\widetilde{U} = F_0(t,\widetilde{U}) + G_0(t,\widetilde{U}), \quad U(0) = U_0, \tag{3.20*}$$

where $F_0(t,\widetilde{U}) = \widetilde{F}(t,\widetilde{U}e^{Mt})e^{-Mt}$, $G_0(t,\widetilde{U}) = \widetilde{G}(t,\widetilde{U}e^{Mt})e^{-Mt}$. Assuming that (3.20*) has coupled lower and upper solutions of type I, one gets the same conclusion by Theorem 3.1.

Also note that assumption (A2) in Theorem 3.1 is modified as follows:

(A2) F, $G \in C[J \times K_c(\mathbb{R}^n), K_c(\mathbb{R}^n)]$, $F(t,X)$ is nondecreasing in X and $G(t,Y)$ is nonincreasing in Y, for each $t \geq 0$, and F, G map bounded sets to bounded sets in $K_c(\mathbb{R}^n)$.

NONLINEAR DYNAMICS AND SYSTEMS THEORY

An International Journal of Research and Surveys

INSTRUCTIONS FOR CONTRIBUTORS

(1) General. The Journal will publish original carefully refereed papers, brief notes and reviews on a wide range of nonlinear dynamics and systems theory problems. Contributions will be considered for publication in ND&ST if they have not been published previously. Before preparing your submission, it is essential that you consult our style guide; please visit our website: http://www.sciencearea.com.ua

(2) Manuscript and Correspondence. Contributions are welcome from all countries and should be written in English. Two copies of the manuscript, double spaced one column format, and the electronic version by AMSTEX, TEX or LATEX program (on diskette) should be sent directly to

Professor A.A. Martynyuk
Institute of Mechanics,
Nesterov str.3, 03057, MSP 680
Kiev-57, Ukraine
(e-mail: anmart@stability.kiev.ua).

or to one of the Editors or to a member of the Editorial Board.

The title of the article must include: author(s) name, name of institution, department, address, FAX, and e-mail; an Abstract of 50-100 words should not include any formulas and citations; key words, and AMS subject classifications number(s). The size for regular paper 10-14 pages, survey (up to 24 pages), short papers, letter to the editor and book reviews (2-3 pages).

(3) Tables, Graphs and Illustrations. All figures must be suitable for reproduction without being retouched or redrawn and must include a title. Line drawings should include all relevant details and should be drawn in black ink on plain white drawing paper. In addition to a hard copy of the artwork, it is necessary to attach a PC diskette with files of the artwork (preferably in PCX format).

(4) References. Each entry must be cited in the text by author(s) and number or by number alone. All references should be listed in their alphabetic order. Use please the following style:

Journal: [1] Poincaré, H. Title of the article. *Title of the Journal* **Vol.1**(No.1) (year) pages. [Language].

Book: [2] Liapunov, A.M. *Title of the book.* Name of the Publishers, Town, year.

Proceeding: [3] Bellman, R. Title of the article. In: *Title of the book.* (Eds.). Name of the Publishers, Town, year, pages. [Language].

(5) Proofs and Reprints. Proofs sent to authors should be returned to the Editor with corrections within three days after receipt. Acceptance of the paper entitles the author to 10 free reprints.

(6) Editorial Policy. Every paper is reviewed by the regional editor, and/or a referee, and it may be returned for revision or rejected if considered unsuitable for publication.

(7) Copyright Assignment. When a paper is accepted for publication, author(s) will be requested to sign a form assigning copyright to Informath Publishing Group. Failure to do it promptly may delay the publication.

NONLINEAR DYNAMICS AND SYSTEMS THEORY
An International Journal of Research and Surveys

Volume 4 Number 2 2004

CONTENTS

Robust Control for a Class of Dynamical Systems with Uncertainties 125
Xinkai Chen and Guisheng Zhai

A Modified *LQ*-Optimal Control Problem for Causal Functional Differential Equations 139
C. Corduneanu

Adaptive Calculation of Lyapunov Exponents from Time Series Observations of Chaotic Time Varying Dynamical Systems 145
A. Khaki-Sedigh, M. Ataei, B. Lohmann and C. Lucas

A Nonlinear Model of Composite Delaminated Beam with Piezoelectric Actuator, with Account of Nonpenetration Constraint for the Delamination Crack Faces 161
V.Y. Perel and A.N. Palazotto

Robust Active Control for Structural Systems with Structured Uncertainties 195
Sheng-Guo Wang, H.Y. Yeh and P.N. Roschke

A Criterion for Stability of Nonlinear Time-Varying Dynamic System 217
Yongmao Wang, Yan Shi and Hirofumi Sasaki

Imaginary Axis Eigenvalues of a Delay System with Applications in Stability Analysis 231
Z. Zahreddine

CORRIGENDUM

Set Differential Equations and Monotone Flows 241
V. Lakshmikantham and A.S. Vatsala

 ISSN 1562-8353 Printed in Ukraine
To receive contents pages by e-mail, visit our Website at: **http://www.sciencearea.com.ua**